The Physics of MRI

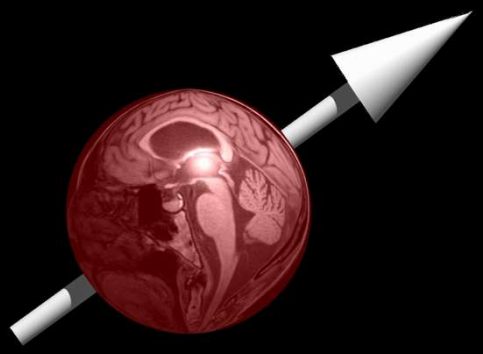

Martin Graves
mjg40@cam.ac.uk

UNIVERSITY OF CAMBRIDGE

Cambridge University Hospitals NHS
NHS Foundation Trust

On-line Resource

www.cantab.net/users/martin.graves

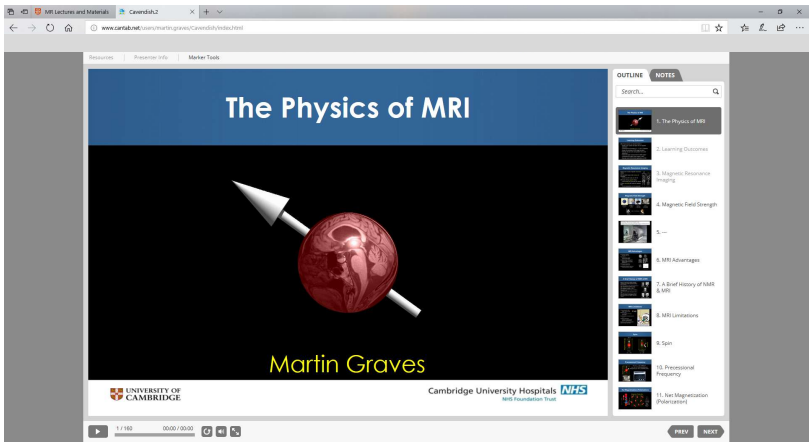

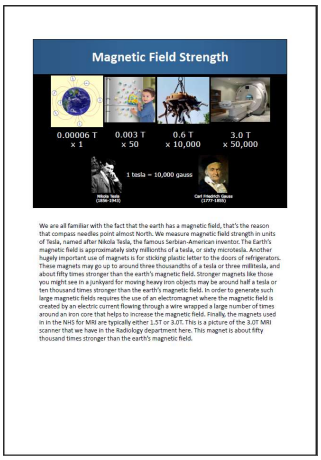

Suggested Reading

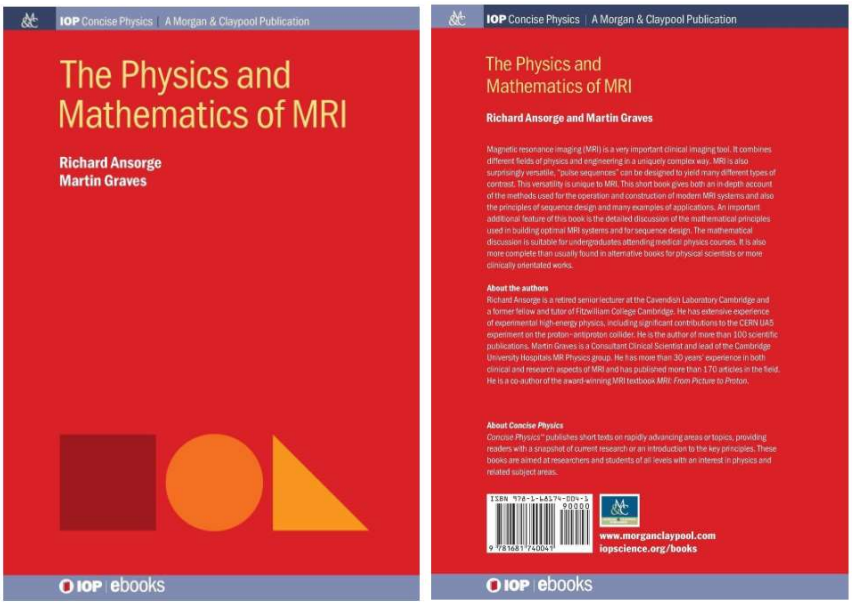

http://iopscience.iop.org/book/978-1-6817-4068-3

Learning Outcomes

- After these lectures you should be able to:
  - Explain how nuclear spin gives rise to magnetic resonance
  - Understand the principles of T_1, T_2 and T_2^* relaxation
  - Explain the principles of MR image formation
  - Describe the spin echo and gradient echo pulse sequences
  - Outline the basic components of an MRI system
  - Understand the safety issues related to MRI
  - Describe some advanced applications of MRI

Magnetic Resonance Imaging

- Based upon nuclear magnetic resonance (NMR)
- MRI primarily looks at the nucleus of hydrogen
  - Human body 60% water and 16% fat
- MRI uses strong magnetic fields
  - Protons behave as microscopic bar magnets
- Protons resonate with external magnetic field
  - The net magnetisation can be manipulated

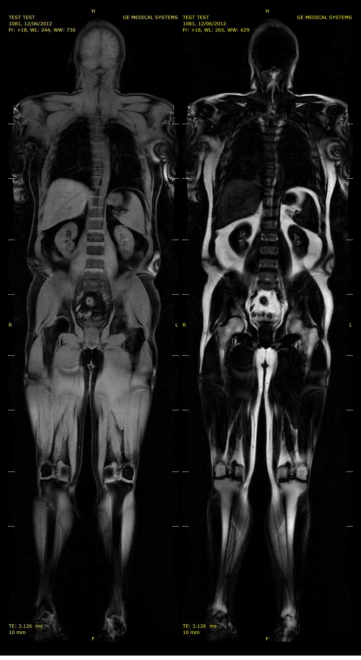

A typical adult is approximately 60% water, 16% fat, 18% proteins and 6% other elements. The majority of clinical MRI utilises the nucleus of hydrogen, i.e. a single proton, although other NMR active nuclei can be imaged in certain rare circumstances. Protons have a magnetic moment which can interact with the magnetic fields of the MRI systems to create images. The hydrogen protons can be considered to precess at a specific frequency and they can interact with a matching, i.e. resonant, external alternating magnetic field.

Clinical Applications

- Neurology – stroke, multiple sclerosis, tumours
- Oncology – diagnosis, staging, treatment response
- Musculoskeletal – trauma, degeneration
- Cardiovascular – heart and blood vessel morphology and function
- Infectious diseases and inflammation
- Congenital/anatomical defects

Example Clinical Applications

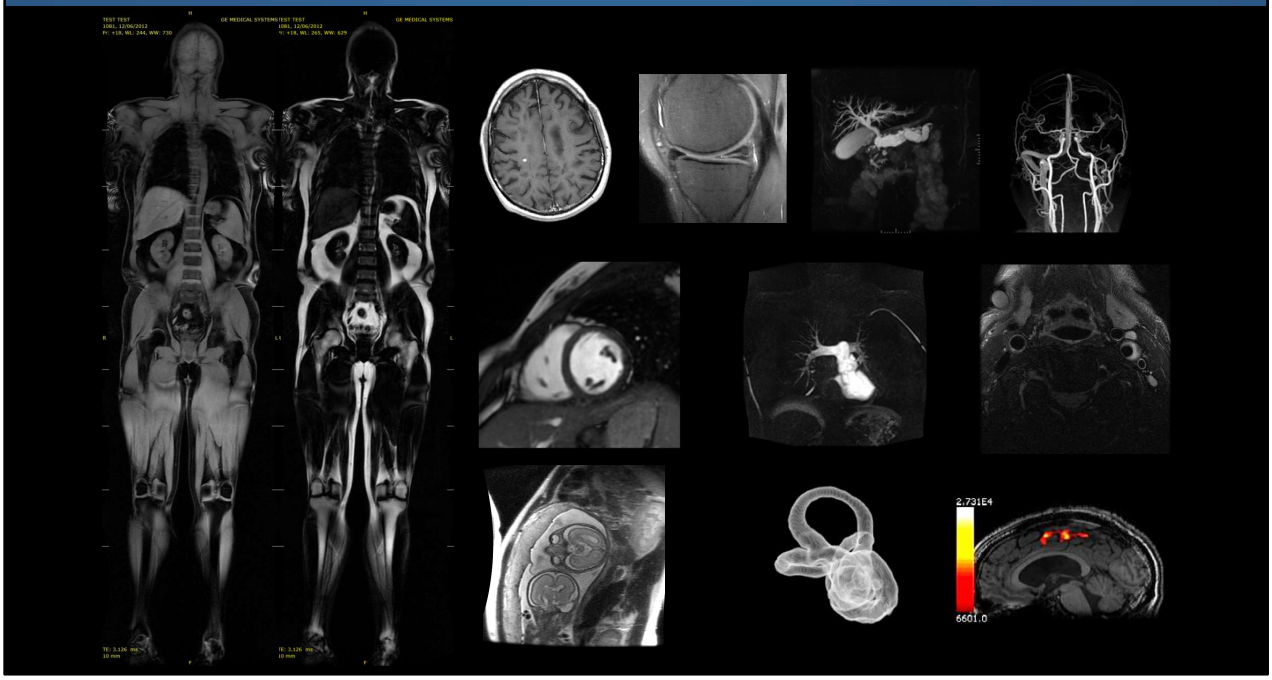

Magnetic Field Strength

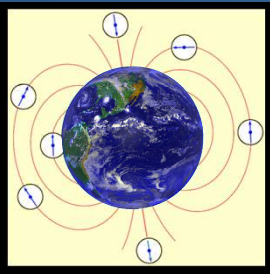

0.00006 T
x 1

0.003 T
x 50

0.6 T
x 10,000

3.0 T
x 50,000

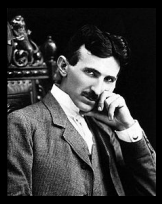

Nikola Tesla
(1856-1943)

1 tesla = 10,000 gauss

Carl Friedrich Gauss
(1777-1855)

We are all familiar with the fact that the earth has a magnetic field, that's the reason that compass needles point almost North. We measure magnetic field strength in units of Tesla, named after Nikola Tesla, the famous Serbian-American inventor. The Earth's magnetic field is approximately sixty millionths of a tesla, or sixty microtesla. Another hugely important use of magnets is for sticking plastic letter to the doors of refrigerators. These magnets may go up to around three thousandths of a tesla or three millitesla, and about fifty times stronger than the earth's magnetic field. Stronger magnets like those you might see in a junkyard for moving heavy iron objects may be around half a tesla or ten thousand times stronger than the earth's magnetic field. In order to generate such large magnetic fields requires the use of an electromagnet where the magnetic field is created by an electric current flowing through a wire wrapped a large number of times around an iron core that helps to increase the magnetic field. Finally, the magnets used in in the NHS for MRI are typically either 1.5T or 3.0T. This is a picture of the 3.0T MRI scanner that we have in the Radiology department here. This magnet is about fifty thousand times stronger than the earth's magnetic field.

Wheelchair flies across hospital room

A hospital is facing a £20,000 bill to repair damage caused by a wheelchair which was flung across a room by powerful magnets in an MRI machine.

Fortunately, nobody was injured in this case but this wheelchair will have been attracted to the magnet at around 30 miles per hour. The field is generally never switched off in a superconducting magnet, which is why it cost £20,000 pounds to switch off the magnet, remove the wheelchair and power it up again, as well as repairing the damage to the covers surrounding the magnet.

MRI Advantages

- No ionising radiation
  - Magnetic fields only
- Multi-planar
  - Axial, coronal, sagittal, single/double oblique
- Multiple contrast mechanisms
  - Proton density, T_1, T_2, flow, diffusion, chemical exchange, spectroscopy …
- Good spatial resolution
  - Variable field-of-view
- Reasonable temporal resolution
  - Dynamic/functional imaging

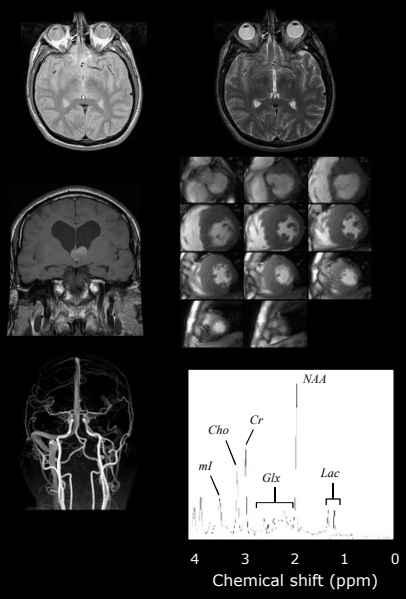

Unlike X-ray or nuclear medicine based imaging methods MRI does not utilise ionizing radiation. Instead it relies on magnetic fields for image formation. MRI is a tomographic imaging techniques that acquires data in multiple thin slices or sections. These sections can be acquired in any orientation, including oblique planes. MR images can reflect a number of different contrast mechanisms including proton density, T_1 and T_2 relaxation times and number of other microscopic and macroscopic phenomena. MRI is particularly noted for its excellent soft-tissue contrast. Spectroscopy can be used to investigate different tissue metabolites since the protons within these molecules exhibit small chemical shifts

A Brief History of NMR & MRI

- Based on the principle of Nuclear Magnetic Resonance discovered by Bloch and Purcell *simultaneously* in 1946 (awarded 1952 Nobel Prize in Physics)
- The initial concept for the medical application of NMR originated with Damadian in 1971
- NMR imaging of two tubes of water first demonstrated by Lauterbur in 1973
- Slice selection (and other things) invented by Mansfield in 1973
- First commercial system developed by EMI in 1975
- 2003 Nobel Prize for Physiology or Medicine award to Lauterbur and Mansfield for "their discoveries concerning magnetic resonance imaging"


Edward Purcell (1912-1997)


Felix Bloch (1901-1999)

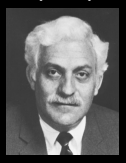
Raymond Damadian (1936-)


Peter Mansfield (1933-2017)


Paul Lauterbur (1929-2007)

In 1952 Edward Purcell (Harvard) and Felix Bloch (Stanford) jointly received the Nobel Prize for physics 'for their development of new methods for nuclear magnetic precision measurements and discoveries in connection therewith'. Of Purcell's discovery, the Boston Herald reported that 'it wouldn't revolutionize industry or help the housewife'. Bloch, a Swiss-born Jew and friend of quantum physicist Werner Heisenberg, quit his post in Leipzig in 1933 in disgust at the Nazi's expulsion of German Jews (as a Swiss citizen, Bloch himself was exempt). Bloch's subsequent career at Stanford was crammed with major contributions to physics and he has been called 'the father of solid state physics'. The 2003 Nobel Prize for Physiology or Medicine was awarded to Paul Lauterbur and Sir Peter Mansfield for 'for their discoveries concerning magnetic resonance imaging'. Paul Lauterbur is said to have been inspired to use field gradients to produce an image whilst eating a hamburger. His seminal paper 'Image Formation by Induced Local Interactions. Examples Employing Nuclear Magnetic Resonance' (*Nature* **242**, March 16, 1973) was originally rejected. 30 years later, Nature placed this work in a book of the 21 most influential scientific papers of the 20th century. Raymond Damadian and his colleagues at the State University of New York, starved of mainstream research funding, went so far as to design and build their own superconducting magnet operating in their Brooklyn laboratory and the first human body image by NMR is attributed to them. There is some dispute about who actually is the founder of modern **M**agnetic **R**esonance **I**maging (MRI), but one thing is certain, Damadian coined the first MR acronym, namely FONAR (**F**ield f**O**cused **N**uclear m**A**gnetic **R**esonance).

MRI Limitations

- Strong magnetic field
  - Safety, acoustic noise
- Relatively slow
  - c.f. ultrasound, CT, X-ray angiography
- Cannot directly visualise calcium
  - c.f. CT
- Complex technology
  - Expensive, requires skilled operators (Radiographers)
- Subjects can feel claustrophobic (bore diameter 60/70cm)

"OK, Mrs. Dunn. We'll slide you in there, scan your brain, and see if we can find out why you've been having these spells of claustrophobia."

MRI has a number of limitations compared to other medical imaging techniques. Since it utilises magnetic field there are lethal safety concerns regarding the presence of ferromagnetic objects near MRI systems. Whilst not necessarily dangerous, the gradients used for spatial localisation can generate quite high acoustic noise levels. A typical MRI examination will comprises a number of imaging series, each having a different contrast mechanism and/or orientation. Whilst we can acquire some MRI images in under a second, most clinical imaging series take several minutes to acquire the data. A complete MRI examination can take anything from around 15 minutes to an hour depending upon the complexity of the investigation. Standard MRI sequences cannot visualise cortical bone , hence X-ray computerised tomography (CT) is still the method of choice for trauma imaging due to its speed and ability to visualise bone. The wide range of imaging parameters makes MRI a complex, expensive technology that requires skilled operators (Radiographers). The majority of MRI systems are based on superconducting magnet technology, with a 60-70cm patient aperture.

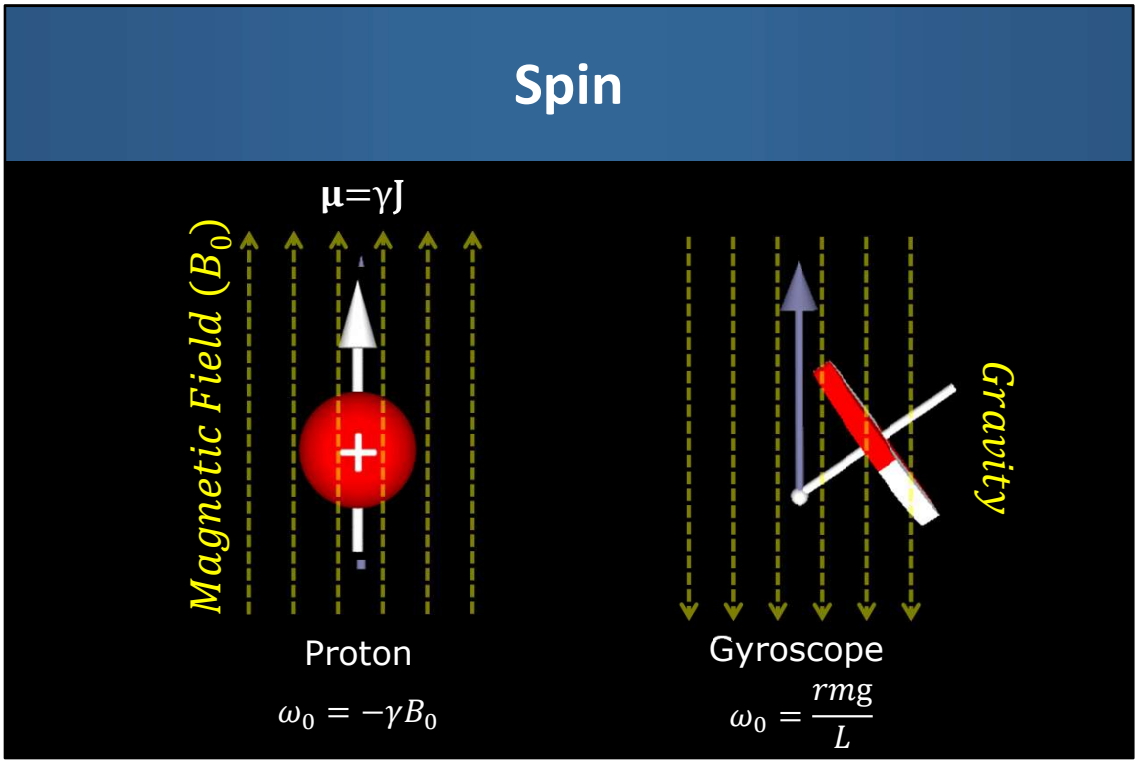

For the purposes of our discussion we will take a fanciful (and relativistically inadequate) representation of the proton as a spinning ball of charge. Due to the combination of a charge and spin we can consider that the proton behaves as a tiny bar magnet, i.e. it has a nuclear magnetic moment **μ**. The ratio of the magnetic moment **μ** to the angular momentum, **J**, is called the gyromagnetic ratio, γ. When placed in a static magnetic field (B_0) we can consider that it makes an angle with respect to the direction of B_0. It therefore experiences a torque and precesses about B_0 at a characteristic frequency $\omega_0 = -\gamma B_0$. The minus sign which will get quietly dropped in future just means that ω_0 defines a clockwise rotation about B_0.The proton precession is analogous to the precession of a gyroscope in the Earths gravitational field. Where r is the distance from the pivot, m is the mass, g is the acceleration due to gravity and L is the angular momentum.

Precessional Frequency

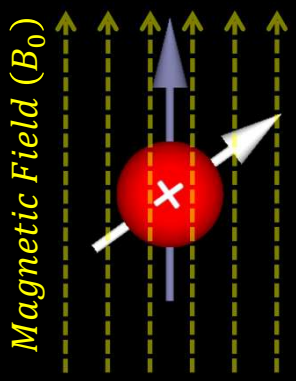

For ^1H $\gamma = 42.57$MHz/T
i.e., at 3.0T the precessional frequency of ^1H is 128 MHz (RF)

As we have seen the precessional frequency is dependent upon the strength of the magnetic field, and in our 3T magnet the protons in the body will precess at a frequency of 128MHz, i.e. in the radiofrequency part of the electromagnetic spectrum and a much lower frequency than those associated with X-rays for example. This is one of the reasons why MRI is actually a very safe imaging modality, unlike X-rays that involve the patient receiving a small dose of radiation.

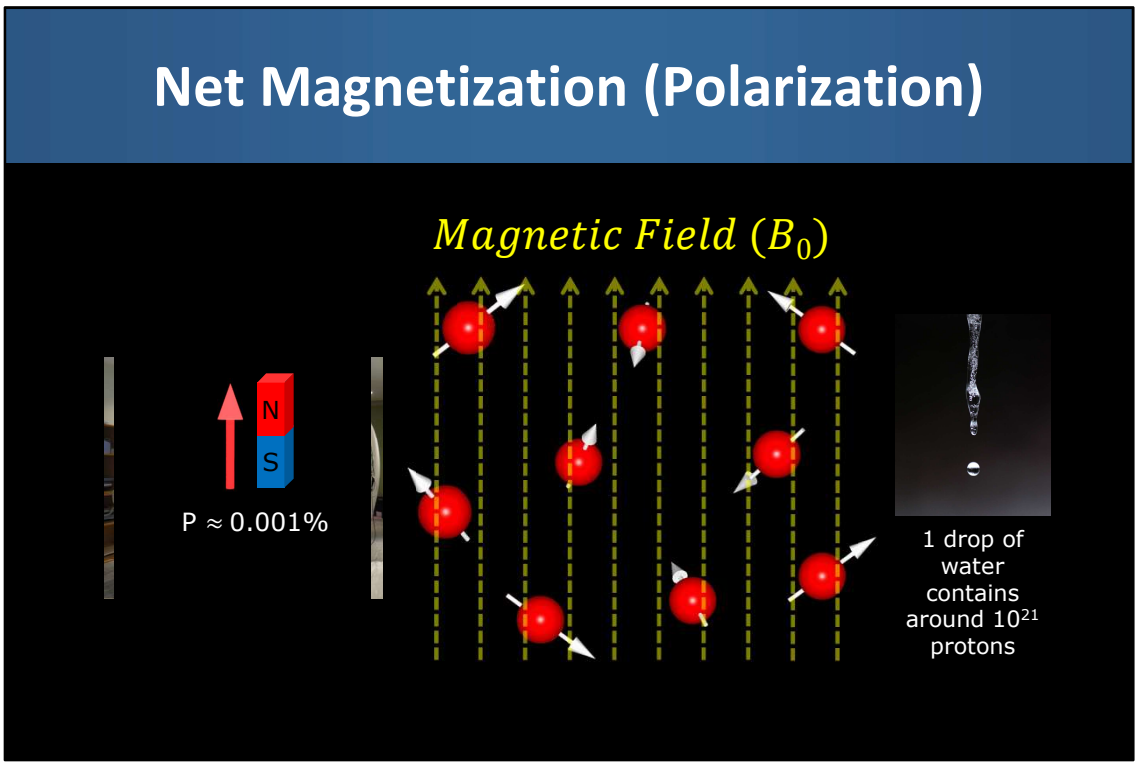

In addition to the individual protons precessing around the direction of the main magnetic field we can see that eventually just over half of the protons end up pointing in the same direction as the magnetic field and just under half end up pointing in the opposite direction. The ones pointing up appear like a large bar magnet pointing in the same direction as the magnetic field, whilst the one pointing down appear as a slightly smaller bar magnet pointing in the other direction. Since they are in opposite directions they subtract from each other, leaving a small, but measurable magnetisation pointing in the same direction as the magnetic field, this is known as the nuclear polarisation. Even so this net magnetisation is a very small percentage, fortunately there are a very large number of protons in the human body.

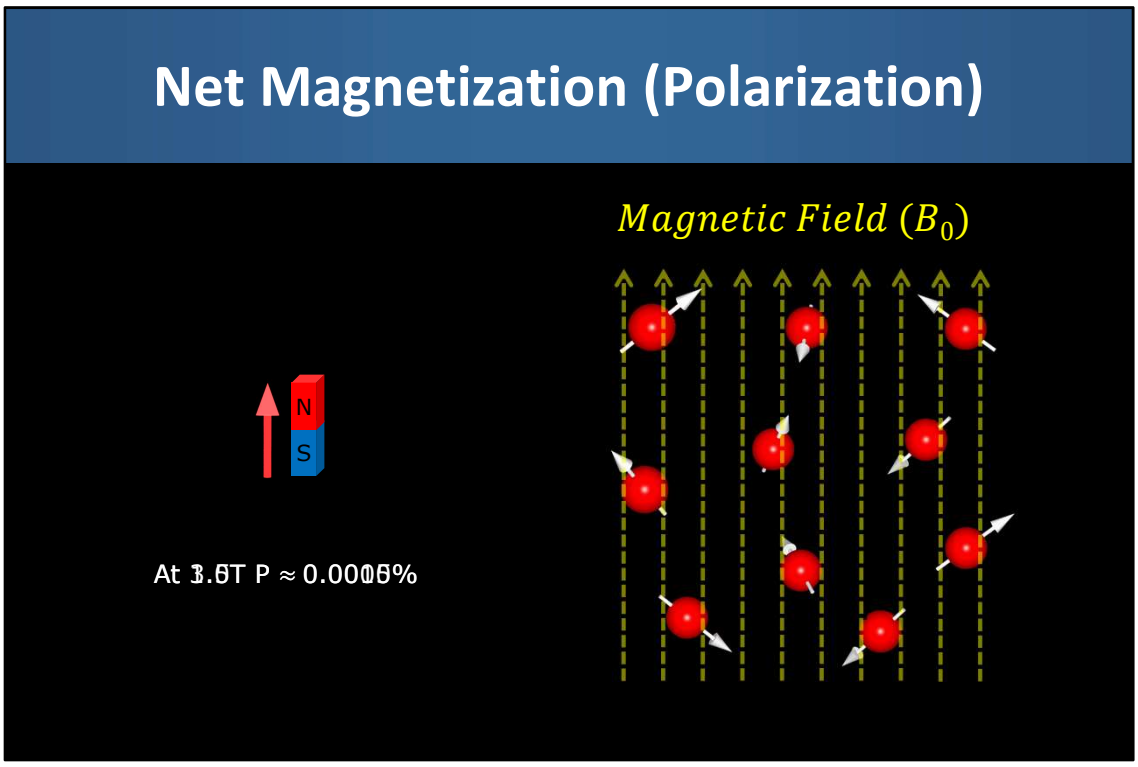

In addition to the individual protons precessing around the direction of the main magnetic field we can see that eventually just over half of the protons end up pointing in the same direction as the magnetic field and just under half end up pointing in the opposite direction. The ones pointing up appear like a large bar magnet pointing in the same direction as the magnetic field, whilst the one pointing down appear as a slightly smaller bar magnet pointing in the other direction. Since they are in opposite directions they subtract from each other, leaving a small, but measurable magnetisation pointing in the same direction as the magnetic field, this is known as the nuclear polarisation. Even so this net magnetisation is a very small percentage, fortunately there are a very large number of protons in the human body.

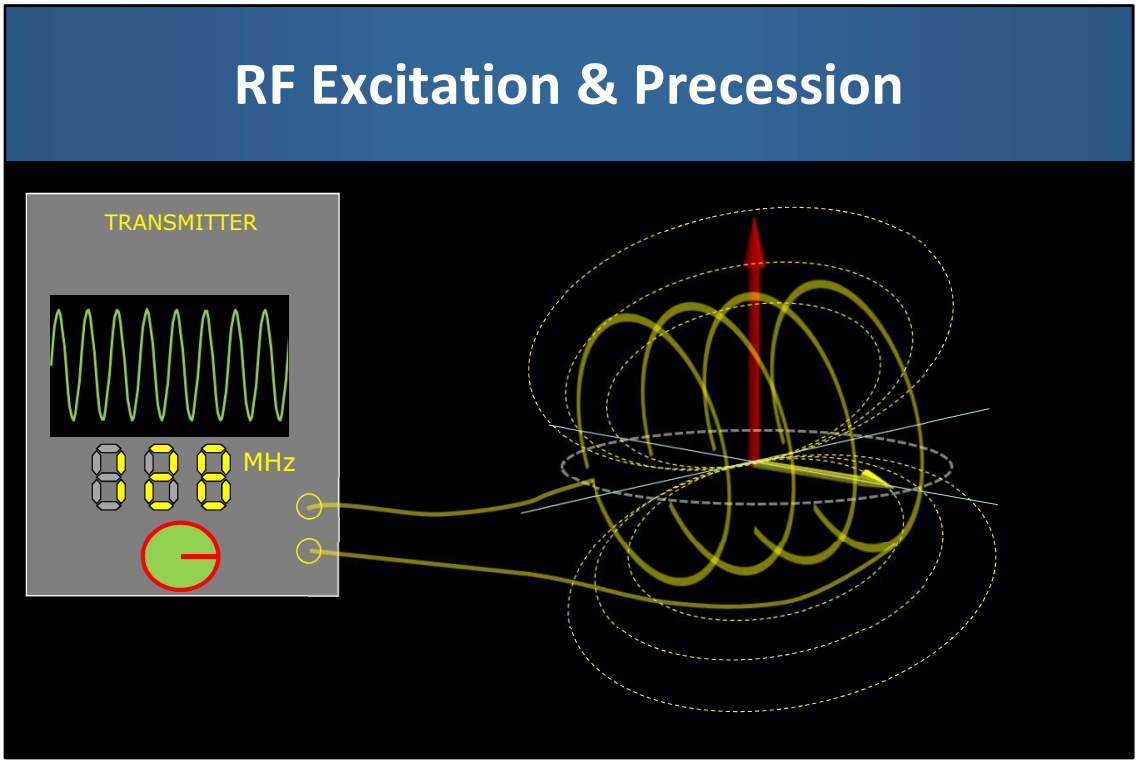

Since the net magnetisation **M** (red arrow) is pointing in the same direction as B_0 it is necessary to perturb the system away from equilibrium and then study how it returns back to equilibrium. We will denote the z-direction as the direction of the net magnetisation at equilibrium. We can perturb **M** away from z by applying a second (weaker) magnetic field, called B_1, at right angles to B_0. We can create this alternating B_1 field (yellow arrow) by applying an alternating current to a coil, creating an alternating magnetic field inside the coil at right angles to B_0. If B_1 is alternating at the same frequency as the natural precessional frequency, i.e. is resonant with ω_0 (in this case at 3T we use 128MHz) then in the laboratory frame of reference **M** will spiral down for as long as B_1 is applied. We often require that the magnetisation be tipped 90° away from z and into the transverse (x,y) plane.

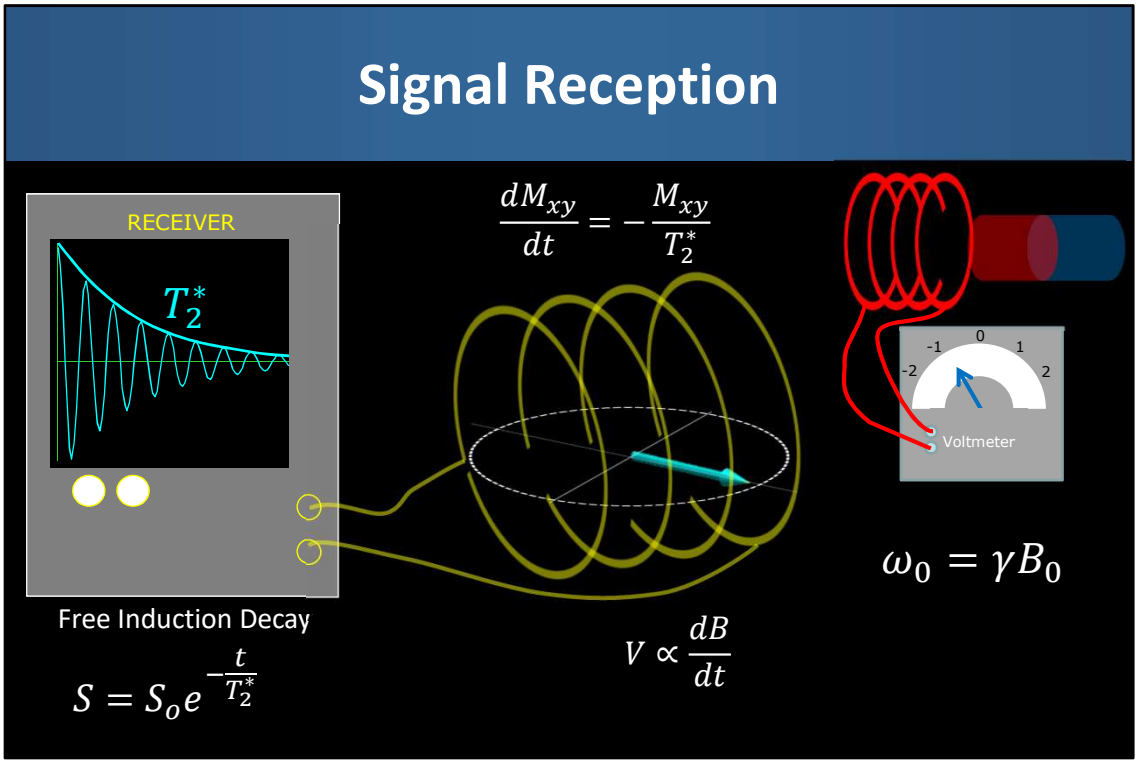

Once **M** has been tipped through 90°, if we turn off B_1 then **M** will continue to precess in the transverse plane. This (weak) precessing, i.e. alternating magnetisation will then induce an emf in the same coil that was originally used to create the B_1 field. For various reasons **M** will decay in amplitude whilst precessing. The induced emf can be seen on the oscilloscope as a exponentially decaying sinusoid. This is known as a free induction decay (FID) and is the most basic NMR signal. The time constant of the decay is characterised by a value known as T_2^*. In the laboratory frame we can see some nuclei precessing faster (yellow) and some precessing slower (white) than the nominal Larmor frequency. The cyan arrow represents the net magnetisation so it decreases in amplitude as the nuclei dephase with respect to each other in the transverse plane. The induced voltage is known as the free induction decay (FID)

Principles of NMR

- Protons possess an intrinsic angular momentum **J** and are positively charged
- A moving charge generates a magnetic field
- Hence we can consider a proton to behave like a bar magnets, i.e. it has a magnetic moment **μ**
- The magnetic moment **μ** is given by **μ**=γ**J**, where γ is the gyromagnetic ratio

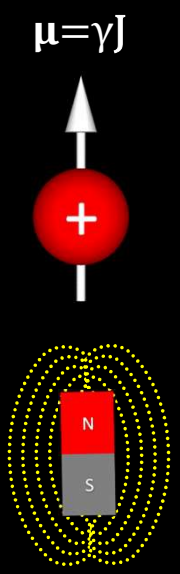

The physical basis of Nuclear Magnetic Resonance (NMR) centres around the concept of a nuclear "spin," its associated angular momentum and its magnetic moment. Spin is a purely quantum mechanical quantity with no classical analogy despite the simplified representation used here. For a hydrogen nucleus, i.e., a single proton (^{1}H) the spin angular momentum **J** and the magnetic moment **μ** are related through the proportionality constant γ, known as the gyromagnetic ratio and is a fundamental constant of a nucleus

Nuclear Spin

- The magnitude and direction of J is characterized by the nuclear spin quantum number I
- Atoms with equal number of protons and neutrons have no spin
  - I=0, e.g., ^{12}C, ^{16}O
- If the number of neutrons **plus** the number of protons is odd then the nucleus has half-integer spin
  - $I=^{1}/_{2}$, e.g., ^{1}H, ^{19}F, ^{13}C, ^{31}P,^{15}N
  - $I=^{3}/_{2}$, e.g., ^{23}Na, ^{37}Cl
- If the number of neutrons **and** the number of protons are both odd then the nucleus has integer spin
  - I=1, e.g., ^{2}H, ^{14}N

We primarily deal with the nuclei of hydrogen, i.e., a single proton which has a spin quantum number of ½.

Nuclear Splitting in an External Magnetic Field (B_0)

- $\boldsymbol{\mu}=\gamma\mathbf{J} = \hbar\gamma\sqrt{I(I+1)}$
- $\mu_z = \gamma J_z = \hbar\gamma m_I$, where magnetic moment quantum number $m_I \in \{-I, \ldots, I-1, I\}$ for a total of $2I+1$ values
- For nuclei with $I = {}^1/_2$, e.g. ^{1}H there are two orientations with $m_I = {}^1/_2$ and $-{}^1/_2$
- *Zeeman observed spectral line splitting in an external magnetic field in 1896*

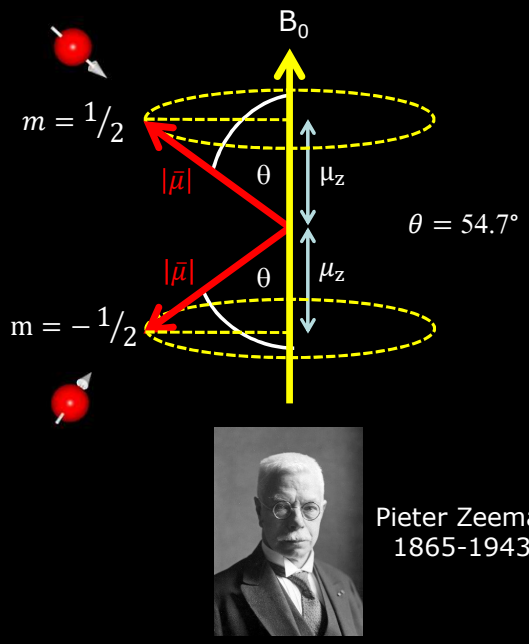

Pieter Zeeman
1865-1943

In 1896 Pieter Zeeman observed the splitting of optical spectral lines in an external magnetic field, which we will call B_0. Since then the splitting of energy levels proportional to an external magnetic field has been called the "Zeeman effect". We know from quantum mechanics that the angular momentum **J** is quantized. The total orbital angular momentum **J** is given by the nuclear spin quantum number l which is equal to ½ for protons. The vectors z projection is given by the reduced Planck's constant ($\hbar = \frac{h}{2\pi}$), where h = 6.63x10^{-34} J s times m_l and where m_l is the magnetic moment quantum number and has values of $-\mathrm{I} \leq m_I \leq I$

So for nuclei with $\mathrm{I} = \frac{1}{2}$

The angle of **J** is given by

$$|\bar{\mu}| = \hbar\gamma[\mathrm{I}(\mathrm{I}+1)]^{1/2}$$

$$\mu_z = \pm\frac{1}{2}\hbar\gamma$$

The angle is therefore $\cos^{-1}\left(\frac{\mu_z}{|\bar{\mu}|}\right) = \frac{{}^1/_2}{\sqrt{\left(\frac{1}{2}\left(\frac{1}{2}+1\right)\right)}} = \frac{{}^1/_2}{\sqrt{{}^3/_4}} = 0.544 = 54.7°$

Gyroscope Precession

- Torque $\boldsymbol{\tau} = \frac{d\mathbf{L}}{dt} = \mathbf{r} \times \mathbf{F}$
- $\boldsymbol{\tau} = \frac{d\mathbf{L}}{dt} = \mathbf{r} \times m\mathbf{g}$, since $\mathbf{F} = m\mathbf{g}$
- $d\theta = \frac{dL}{L} = \frac{rmg}{L}dt$
- $\omega_0 = \frac{d\theta}{dt} = \frac{rm}{L}$

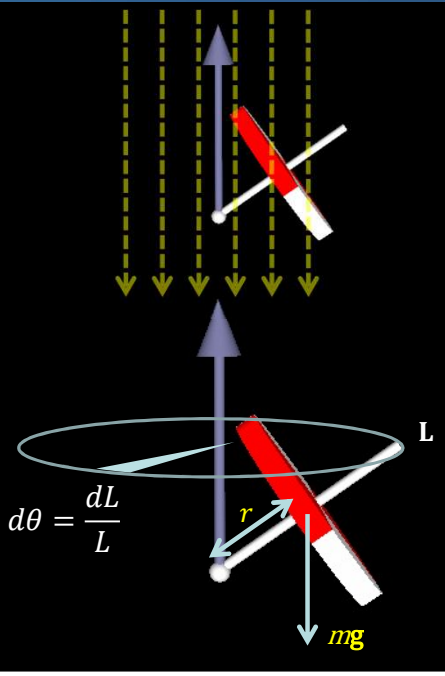

A gyroscope, under the influence of gravity, will precess about the vertical.

Classical Description of Nuclear Precession

- Torque $\boldsymbol{\tau} = \frac{d\mathbf{J}}{dt} = \boldsymbol{\mu} \times \mathbf{B}$
- $\boldsymbol{\tau} = \frac{d\mathbf{J}}{dt} = \gamma \mathbf{J} \times \mathbf{B}$, since $\boldsymbol{\mu} = \gamma \mathbf{J}$
- $d\theta = \frac{dJ}{J} = \gamma B_0 dt$
- $\omega_0 = \frac{d\theta}{dt} = -\gamma B_0$
- $f_0 = \frac{\gamma}{2\pi} B_0$

Joseph Larmor
1857-1942

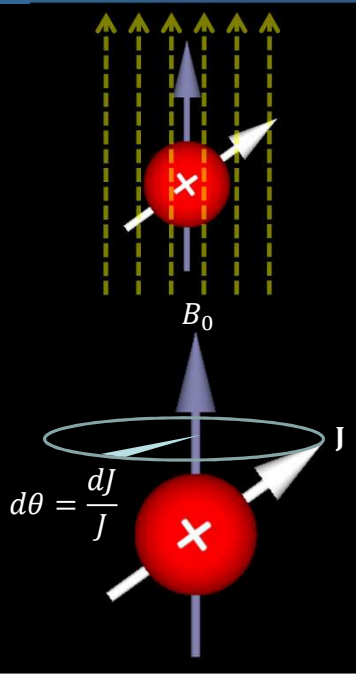

Similarly to the gyroscope the static magnetic field will cause our spinning nuclei to experience a torque $\boldsymbol{\tau}$ and hence precess around B_0. This precessional frequency is given by the Larmor equation $\omega = \gamma B_0$. Larmor worked in an era when the basic structure of the atom was still being elucidated and quantum mechanics had yet to be developed. His famous equation of 1897 had nothing to do with NMR, as this phenomenon was still several decades away from being discovered. Instead it arose from attempts to explain the Zeeman splitting observed one year previously. Larmor's theory was that Zeeman's spectral lines were produced by charged particles (electrons) moving in elliptical orbits. Larmor demonstrated mathematically that these electrons should precess around the direction of the applied magnetic field. He further calculated that the frequency of precession was directly proportional to the strength of the applied field times a constant. Larmor's constant was directly related to the particle's charge/mass ratio. In later years as more became known about atomic structure, Larmor's equation was found to apply to any particle with spin or angular momentum, taking the form we recognize today. The Larmor frequency is a signed quantity and is negative for nuclei with a positive gyromagnetic ratio. This means that for such spins the precession frequency is negative, as shown in the animation. Note that conventionally, the Larmor equation is written as $\omega_0 = \gamma B_0$, where ω_0 is the angular frequency of the protons precession, i.e., $\gamma = 2.67 \times 10^8$ radians s^{-1} T^{-1}. ($\omega = 2\pi f$). However, I find this number unmemorable and angular frequencies are not as intuitively understandable as regular (scalar) frequencies. I will therefore often refer to γ as 42 MHz T^{-1}, i.e. $\gamma/2\pi$.

Some NMR Active Nuclei

Nucleus	Unpaired Protons	Unpaired Neutrons	Net Spin	γ (MHz/T)	Natural Abundance (%)
^{1}H	1	0	1/2	42.58	99.98
^{13}C	0	1	1/2	10.71	1.1
^{14}N	1	1	1	3.08	99.6
^{19}F	1	0	1/2	40.08	100
^{23}Na	1	2	3/2	11.27	100
^{31}P	1	0	1/2	17.25	100

The neutron doesn't have charge but has a magnetic moment. This can be reconciled with the classical model if the neutron is considered as a proton orbited by a negatively charged pion. The neutron has spin $1/2\hbar$ but no net charge. The neutron is composed of three quarks and the magnetic moments of these elementary particles combine to give the neutron its magnetic moment. The gyromagnetic ratio γ dictates the precessional frequency of the nucleus, i.e. 42.57MHz/T. Therefore in a 3T MRI system the protons precess at approximately 128MHz.

Protons in a Magnetic Field

3.0T

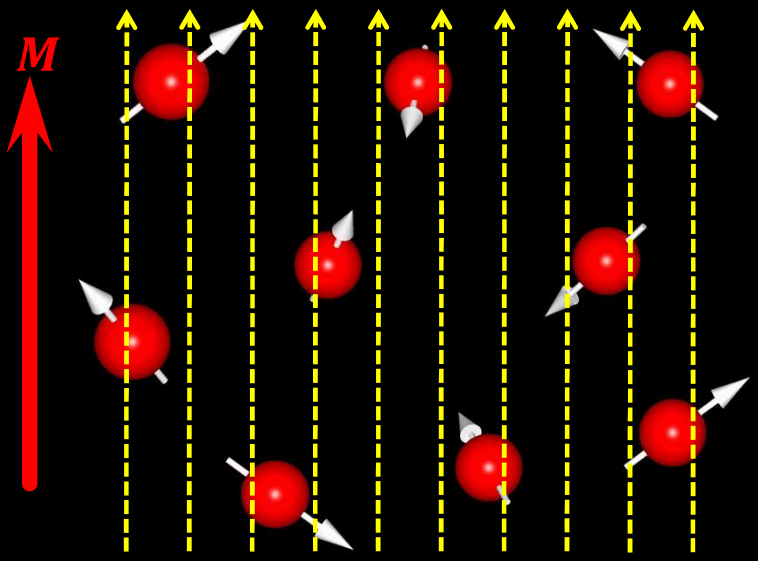

With no applied magnetic field, all nuclei (aka spins) are in the same energy state. Their magnetic moments are randomly oriented and do not form any coherent magnetization. However when the nuclei experience is placed in a static magnetic field (B_0) such as a 3.0T MRI system the nuclei split into two energy states, either aligned with “spin-up” or against “spin-down” the direction of B_0. The “spin-up” state is slightly preferred and thus has a lower energy level. This slight difference (0.001%) results in an overall net magnetisation (M) aligned in the same direction as B_0.

Energy Level Splitting

- The energy E of a magnetic moment $(\boldsymbol{\mu})$ in a magnetic field $\mathbf{B}$ is given by
  - $E = -\boldsymbol{\mu} \cdot \mathbf{B} = \hbar\gamma m_I \mathbf{B}$
- Selection rules only allow for transitions between $-I \leq m_I \leq I$ so for $I = {}^1/_2$
  - $\Delta E = ({}^1/_2 - - {}^1/_2)\gamma\hbar B_0 = \hbar\gamma B_0$
- From De Broglie's wave equation
  - $\Delta E = \hbar\omega$
- $\hbar\gamma B_0 = \hbar\omega_0$

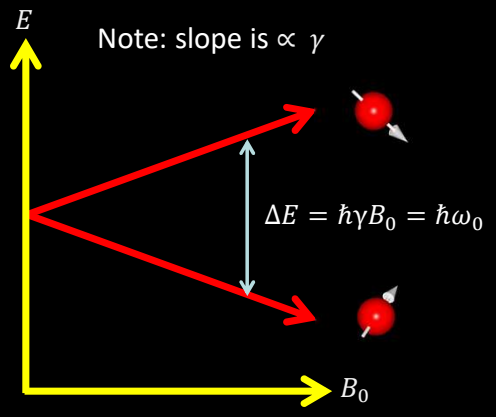

From a QM perspective the energy difference between the two orientations in a static magnetic field of B_0 is given by ΔE= γ$\hbar B_0$, and is exactly equivalent to the classical Larmor equation.

Nuclear Polarisation

$$P = \frac{N_\uparrow - N_\downarrow}{N_\uparrow + N_\downarrow} \approx \frac{1}{2}\frac{\gamma\hbar B_0}{k_b T} \approx 10\text{x}10^{-6}$$ (At 310K and 3.0T)

$$\frac{N_\downarrow}{N_\uparrow} = e^{-\frac{\Delta E}{k_b T}}$$

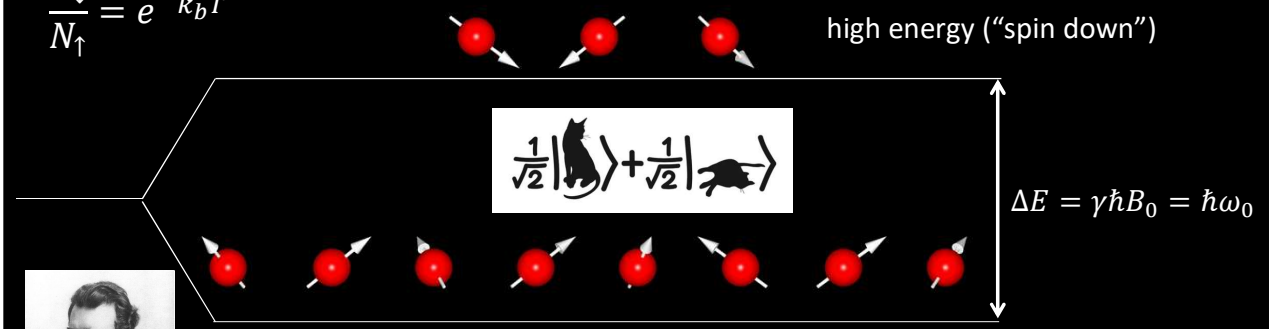

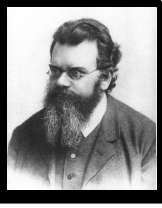

Ludwig Eduard Boltzmann
1844-1906

The population distribution, known as the polarisation (P), of the nuclei between the two states are characterised by the Boltzmann distribution which describes the distribution of energy among classical (distinguishable) particles. Where k_b is Boltzmann's constant (1.38x10^{-23} J/K)and T is the absolute temperature (human body temperature is normally about 310K). If we inject energy into this system at a angular frequency of ω_0, we can induce transitions between the two energy states. A spin-up nuclei can absorb energy and transition to a spin down state and a spin-down nuclei can give up energy and transition to spin-up. The excitation must be at this specific frequency in order to "resonate" with the nuclei – this frequency selectivity is the origin of the term resonance in nuclear magnetic resonance. The cartoon of Schrodinger's cat is to remind you that the spin and magnetic moment exist in all directions simultaneously, but their average behaviour is non-zero in only one of the directions. Therefore these diagrams are an attempt to provide some additional insights into how NMR works but their limitations should be appreciated

Net Magnetisation

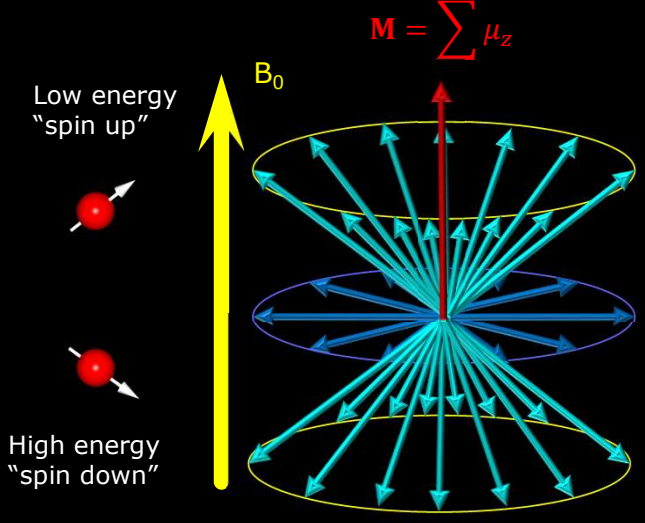

$$\langle \mu_x \rangle = \langle \mu_y \rangle = 0$$
$$\langle \mu_z \rangle = \frac{1}{2}\hbar\gamma$$

$$M_0 = \frac{\rho_0 \gamma^2 \hbar^2}{4k_b T} B_0$$

Water contains 6.67×10^{22} protons ml^{-1}. So at body temperature at 3.0T we get $M_0 \approx 0.02 \mu T ml^{-1}$. Assuming the human head has volume of 1500ml and is approximately 80% water we get $M_0 \approx 20 \mu T$

The spin (and associated magnetic moment and angular momentum) is probabilistic in nature (much in the same way that electrons surrounding the nucleus travel in probabilistic shells). Thus, each spin doesn't really align with B_0, but rather exists in a probabilistic cone and spin-up and spin-down implies that the cone faces up or down. The spin and magnetic moment exist in all directions simultaneously, but the average behaviour is non-zero in only one of the directions. Each spin contributes $\frac{1}{2}\hbar\gamma$ to the overall z-magnetisation of the sample. We cannot observe individual spins, only the ensemble average **M.**

MR Signal

- To create an MR signal we need to excite the spins out of equilibrium, i.e. we must tip the net magnetization away from the B_0 direction
- A transmit coil will create an orthogonal magnetic field (B_1), alternating at the Larmor frequency that will rotate the net magnetization into the transverse (x-y) plane (RF pulse)
- The precessing transverse magnetisation will induce a voltage in a receiver coil
- After the pulse the magnetization will return to thermal equilibrium by processes known as relaxation

The Bloch Equation

- The dynamics of nuclear magnetization are described phenomenologically by the Bloch equation

$$\frac{d\mathbf{M}}{dt} = \mathbf{M} \times \gamma\mathbf{B} - \frac{M_x i + M_y j}{T_2} - \frac{(M_z - M_0)k}{T_1} + D\nabla^2 M$$

Felix Bloch
1901-1999

- The last term accounts for the transfer of magnetisation by diffusion, with D being the molecular self-diffusion coefficient
- The transverse component will dephase in the x-y plane with a time constant T_2. This is known as "spin-spin", or "transverse" or "T_2" relaxation. This process only involves energy exchange
- The longitudinal component will regrow along the z-direction with a time constant T_1. This is known as "spin-lattice", or "longitudinal" or "T_1" relaxation. This process involve energy loss as heat to the surrounding macromolecules aka "lattice"

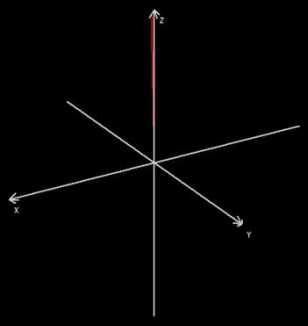

Motion in the Presence of an Applied Field

- Net nuclear magnetisation $\mathbf{M}$ will precess about $\mathbf{B}$ at a frequency $\omega_0 = \gamma B_o$ the motion is given by

$$\frac{d\mathbf{M}}{dt} = \mathbf{M} \times \gamma\mathbf{B}$$

- Define $\mathbf{M} = iM_x + jM_y + kM_z$ and expressing the cross product as the formal determinant

$$\frac{d\mathbf{M}}{dt} = \gamma\mathbf{M} \times \mathbf{B} = \gamma \det\begin{bmatrix} i & j & k \\ M_x & M_y & M_z \\ B_x & B_y & B_z \end{bmatrix}$$

- Using Sarrus's rule

$$\frac{d\mathbf{M}}{dt} = \gamma\left(i(M_yB_z - M_zB_y) + j(M_zB_x - M_xB_z) + k(M_xB_y - M_yB_x)\right)$$

- In addition to the static field $\mathbf{B}_o$ we introduce an an additional oscillating magnetic field $\mathbf{B}_1$ that rotates in the x-y plane at frequency ω_{rot}

$$B_1(t) = iB_1(t)\cos(\omega_{rot}t) - jB_1(t)\sin\omega_{rot}t$$

$$B_x = B_1\cos(\omega_{rot}t)$$

$$B_y = -B_1\sin(\omega_{rot}t)$$

$$B_z = B_0$$

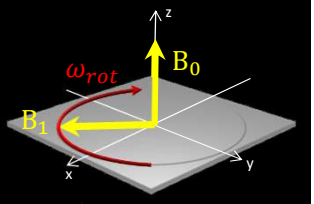

$$\frac{dM_x}{dt} = \gamma\left(M_yB_0 + M_zB_1\sin(\omega_{rot}t)\right)$$

$$\frac{dM_y}{dt} = \gamma(M_zB_1\cos(\omega_{rot}t) - M_xB_0)$$

$$\frac{dM_z}{dt} = \gamma(-M_xB_1\sin(\omega_{rot}t) - M_YB_1\cos(\omega_{rot}t))$$

Rotating Frame of Reference

- Lets define a rotating frame of reference with $\boldsymbol{\Omega}$ as the rotational angular velocity vector

$$\boldsymbol{\Omega} = -\omega_{rot} k$$

- With unit vectors in the rotating frame i', j', k' the net magnetisation $\mathbf{M}$ becomes

$$\mathbf{M} = i' M_x + j' M_y + k' M_z$$

- The total time derivative of $\mathbf{M}$ is

$$\frac{d\mathbf{M}}{dt} = \frac{dM_x}{dt} i' + M_x \frac{\partial i'}{\partial t} + \frac{dM_y}{dt} j' + M_y \frac{\partial j'}{\partial t} + \frac{dM_z}{dt} k' + M_z \frac{\partial k'}{\partial t}$$

- Note that $\frac{\partial u'}{\partial t} = \boldsymbol{\Omega} \times u'$ where u' represents each unit vector

$$\left(\frac{d\mathbf{M}}{dt}\right)_{lab} = \frac{\partial M}{\partial t} + \boldsymbol{\Omega} \times \left(M_x i' + M_y j' + M_z k'\right)$$

$$\left(\frac{d\mathbf{M}}{dt}\right)_{lab} = \left(\frac{\partial \mathbf{M}}{\partial t}\right)_{rot} + \boldsymbol{\Omega} \times \mathbf{M}$$

- Since we know the LHS is equal to $\mathbf{M} \times \gamma \mathbf{B}$

$$\mathbf{M} \times \gamma \mathbf{B} = \left(\frac{\partial \mathbf{M}}{\partial t}\right)_{rotating} + \boldsymbol{\Omega} \times \mathbf{M}$$

$$\left(\frac{\partial \mathbf{M}}{\partial t}\right)_{rot} = \mathbf{M} \times \gamma \mathbf{B} - \boldsymbol{\Omega} \times \mathbf{M}$$

$$\left(\frac{\partial \mathbf{M}}{\partial t}\right)_{rot} = \mathbf{M} \times \gamma \mathbf{B} + \gamma \mathbf{M} \times \frac{\boldsymbol{\Omega}}{\gamma}$$

$$\left(\frac{\partial \mathbf{M}}{\partial t}\right)_{rot} = \mathbf{M} \times \gamma \left(\mathbf{B} + \frac{\boldsymbol{\Omega}}{\gamma}\right)$$

$$\left(\frac{\partial \mathbf{M}}{\partial t}\right)_{rot} = \mathbf{M} \times \gamma \left(\mathbf{B} - \frac{\omega_{rot}}{\gamma}\right) = \mathbf{M} \times \gamma \mathbf{B}_{eff}$$

The term $\left(\mathbf{B} - \frac{\omega_{rot}}{\gamma}\right)$ is often known as the effective field

Behaviour of M in the presence of B_1

- If $\omega_{rot} = \omega_0 = \gamma \mathbf{B}_o$

$$\left(\frac{\partial \mathbf{M}}{\partial t}\right)_{rot} = \gamma \mathbf{M} \times \left(\mathbf{B}_o - \frac{\gamma B_0}{\gamma}\right) = 0$$

i.e. $\mathbf{M}$ is static in the rotating frame

- If we include $\mathbf{B}_1$, the effective $\mathbf{B}_{eff}$ field in a frame rotating at ω_{rot} is given by

$$\mathbf{B}_{eff} = \left(\mathbf{B}_0 - \frac{\omega_{rot}}{\gamma}\right) k' + \mathbf{B}_1 i'$$

$$\left(\frac{\partial \mathbf{M}}{\partial t}\right)_{rot} = \gamma \mathbf{M} \times \left(\mathbf{B}_o - \frac{\omega_{rot}}{\gamma} + \mathbf{B}_1\right)$$

- If $\omega_{rot} = \omega_0$ then $\mathbf{B}_1$ is static and $\mathbf{M}$ rotates about $\mathbf{B}_1$ at a frequency of $\omega_1 = \gamma B_1$

$$\left(\frac{\partial \mathbf{M}}{\partial t}\right)_{rot} = \gamma \mathbf{M} \times \mathbf{B}_1$$

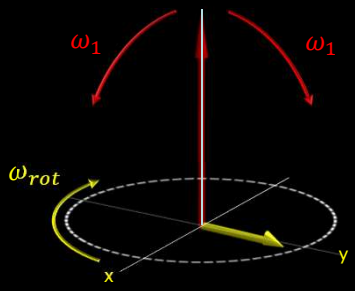

Laboratory frame

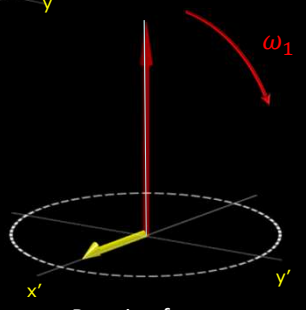

Rotating frame

Comparison of laboratory (fixed) and frame rotating at ω_{rot} behaviour. It is much easier to work in the rotating frame.

Behaviour of M in the presence of B_1

- If $\omega_{rot} = \omega_0 = \gamma \mathbf{B}_o$

$$\left(\frac{\partial \mathbf{M}}{\partial t}\right)_{rot} = \gamma \mathbf{M} \times \left(\mathbf{B}_o - \frac{\gamma B_0}{\gamma}\right) = 0$$

i.e. $\mathbf{M}$ is static in the rotating frame

- If we include $\mathbf{B}_1$, the effective $\mathbf{B}_{eff}$ field in a frame rotating at ω_{rot} is given by

$$\mathbf{B}_{eff} = \left(\mathbf{B}_0 - \frac{\omega_{rot}}{\gamma}\right) k' + \mathbf{B}_1 i'$$

$$\left(\frac{\partial \mathbf{M}}{\partial t}\right)_{rot} = \gamma \mathbf{M} \times \left(\mathbf{B}_o - \frac{\omega_{rot}}{\gamma} + \mathbf{B}_1\right)$$

- If $\omega_{rot} = \omega_0$ then $\mathbf{B}_1$ is static and $\mathbf{M}$ rotates about $\mathbf{B}_1$ at a frequency of $\omega_1 = \gamma B_1$

$$\left(\frac{\partial \mathbf{M}}{\partial t}\right)_{rot} = \gamma \mathbf{M} \times \mathbf{B}_1$$

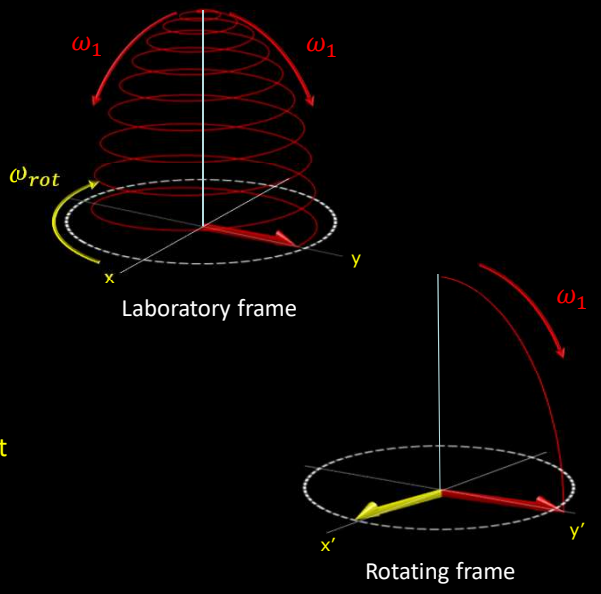

Static version of the previous slide

RF Excitation

- An alternating magnetic field of amplitude $\mathbf{B_1}$ (μT) applied for time t_{RF} at the Larmor frequency ω_0 will tip $\mathbf{M}$ by $\alpha = \omega_1 t = \gamma B_1 t_{RF}$

E.g. a rectangular (hard) RF pulse of 1ms duration with a B_1 of 5.87μT will flip the magnetization by 90°. Note that B_1 is considerably smaller than B_0

- RF pulses are the only way to rotate magnetization. Different flip angles are used for different applications
- In practice RF pulses will be shaped so more generally $\alpha = \gamma \int_0^{t_{RF}} B_1 dt$
- Note that MRI uses alternating magnetic fields in the RF part of the EM spectrum. It does not use radiowaves!

Excitation: Quantum Approach

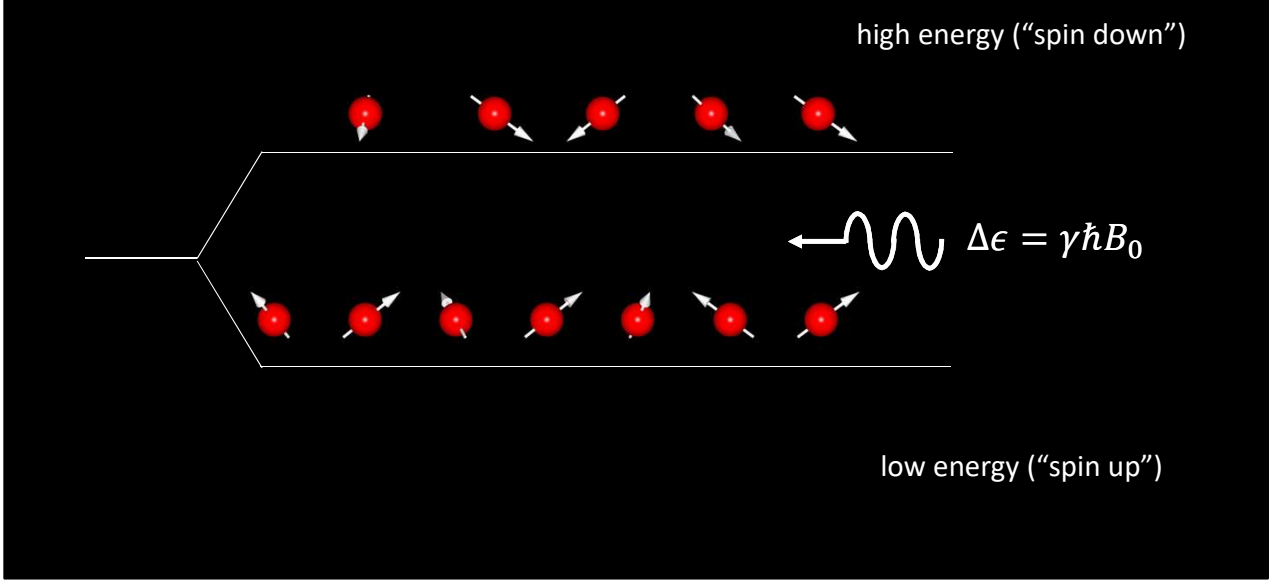

Proceeding extremely cautiously with our QM approach. When the population of protons is irradiated by an RF field, protons can flip between energy levels. Spin-up protons can absorb energy to jump into the spin-down position, while those in the spin-down state are stimulated into giving up an equal amount of energy to drop into the spin-up state, and there is an equal probability of each transition. Since in equilibrium there are more spin-up protons than spin-down, the net effect will be absorption of energy from the RF wave, causing the “temperature” of the spin system to rise. The protons’ temperature is considered separately from the temperature of the surrounding tissues, known as the lattice, which will eventually come into equilibrium with the spins. We will come back to this idea when we consider spin-lattice relaxation. Taking the simple idea of population difference and absorption of RF, it can be seen that the maximum absorption will be when all the spin-down protons have flipped into the spin-up position and vice versa. This is known as population inversion, and can be easily considered as a 180° pulse which flips the magnetization from *z* to -*z*. The definition of a 90° pulse can then be considered to be half that amount of energy, which is thought of as equalizing the populations leaving no magnetization along the *z* axis. Thus far the QM concepts seem to agree with our macroscopic observations, and they can be helpful up to this point.

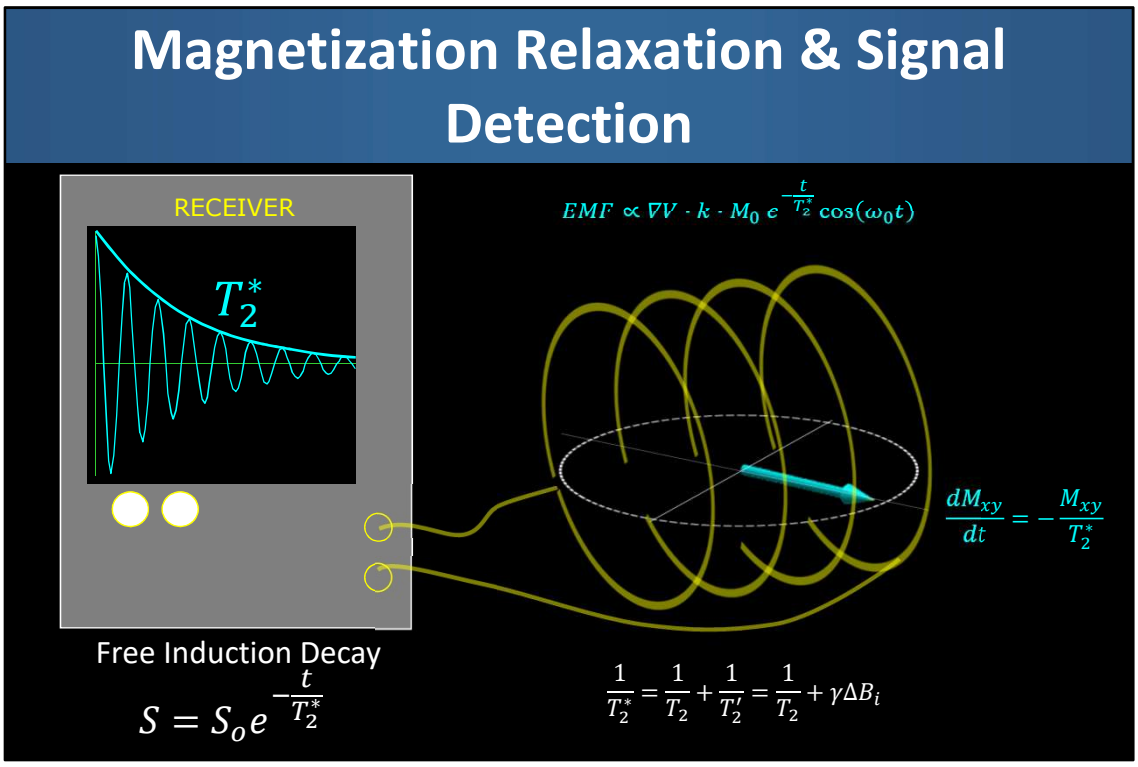

Relaxation is expressed in the Bloch equation. We have already met T_2 relaxation which is caused by the irreversible interaction of individual spins. This means that the individual nuclei that make up the net magnetisation will start to precess at different rates in the transverse plane due to spin-spin (T_2) interactions as well as other nonunifomities in the static magnetic field, either intrinsic to the magnet or due to magnetic susceptibilities within the body, these have a time constant given by T_2'. The overall relaxation time is the sum of these relaxivities, i.e., $\frac{1}{T_2^*} = \frac{1}{T_2} + \frac{1}{T_2'}$ In the laboratory frame we can see some nuclei precessing faster (yellow) and some precessing slower (white) than the nominal Larmor frequency. The cyan arrow represents the net magnetisation so it decreases in amplitude as the nuclei dephase with respect to each other in the transverse plane. The induced voltage is known as the free induction decay (FID)

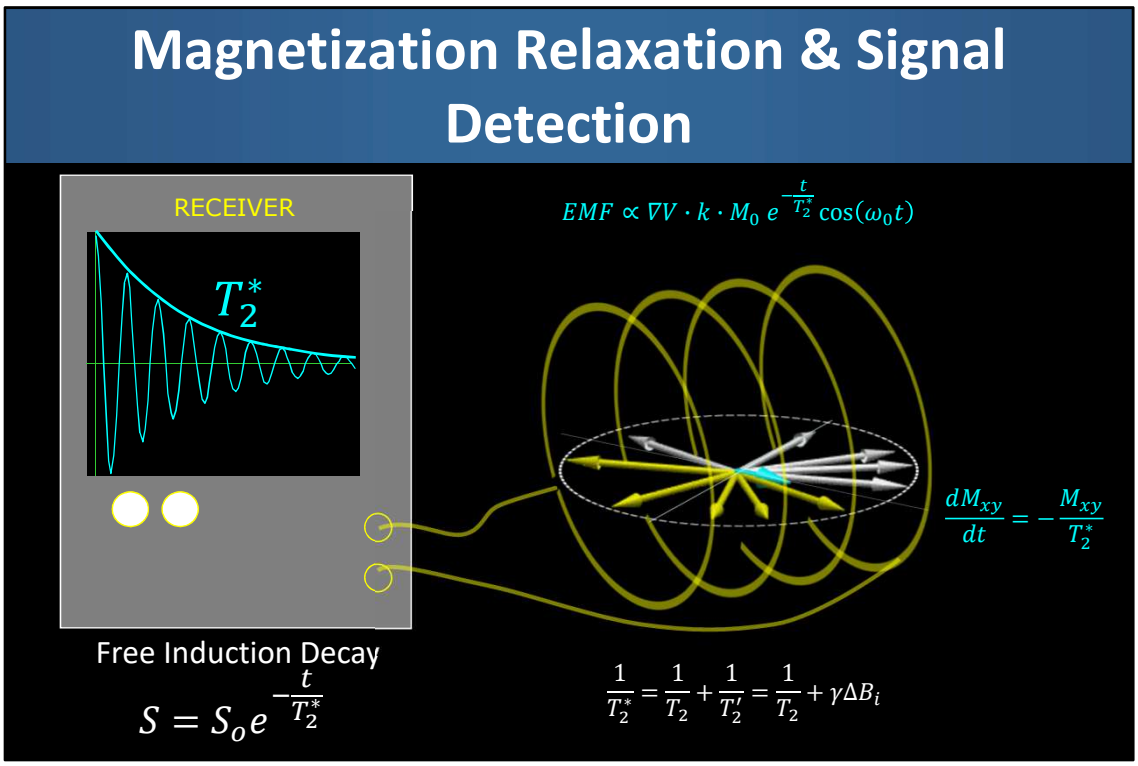

Static version of the previous slide showing near complete transverse dephasing.

Spin Echo

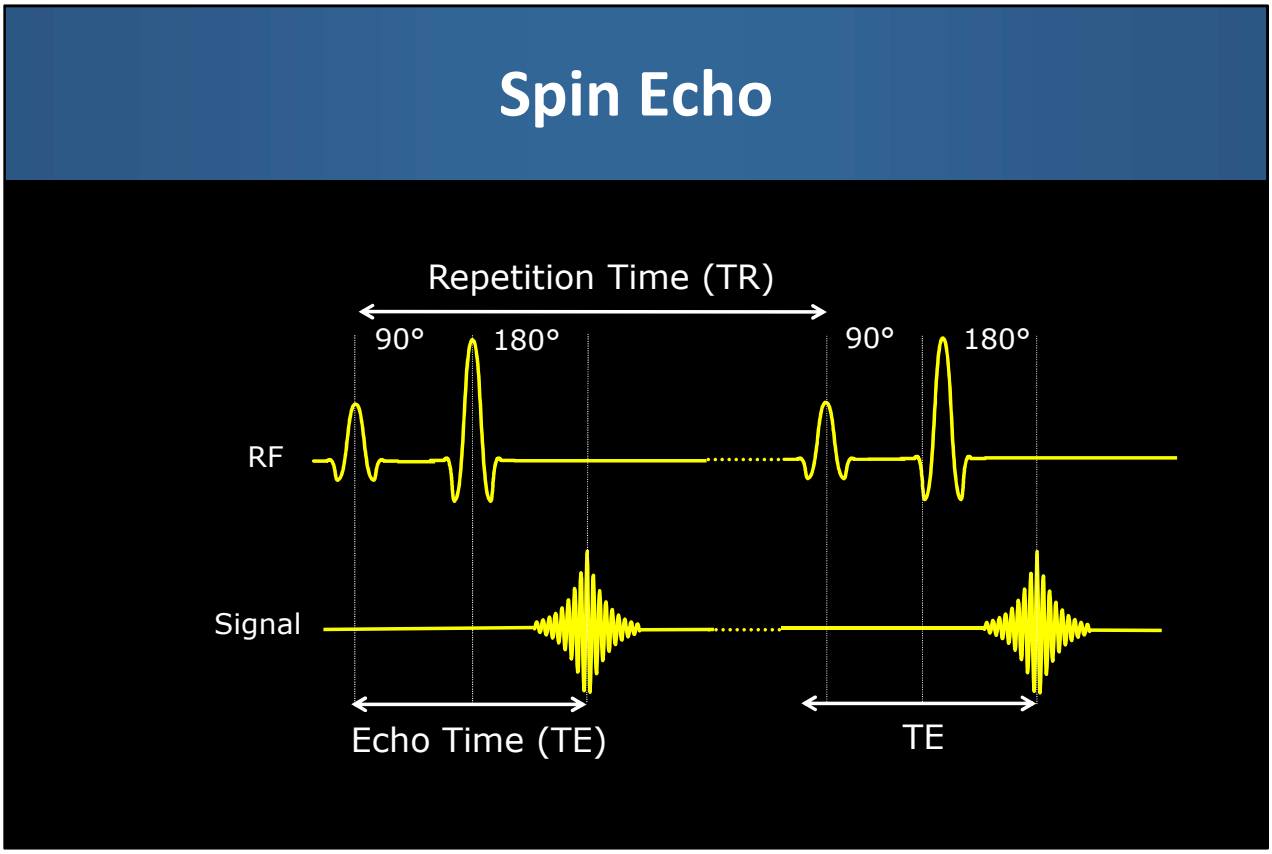

The spin echo uses a 180° "refocusing" pulse to eliminate the dephasing caused by ΔB_i. Following a 90° excitation pulse the transverse magnetisation dephases. At a time τ later a 180° pulse flips the magnetisation in the transverse plane. After a further time τ the magnetisation is refocused as a spin echo. The echo time TE = 2τ. Dephasing due to static T_2' effects are reversed, however T_2 related dephasing, which is irreversible, results in a reduced signal. Since different tissues have different T_2 values this will give rise to the desired T2-weighted image contrast. The longer TE the greater the T_2 signal differences. Note however, that as you increase TE the overall signal levels will decrease, i.e. contrast may improve but SNR will decrease. The spin echo is repeated with a repetition time (TR). T_1 recovery will occur during the TR period.

Spin Echo

T_2' is eliminated by using a spin-echo (90°-180°) pulse sequence

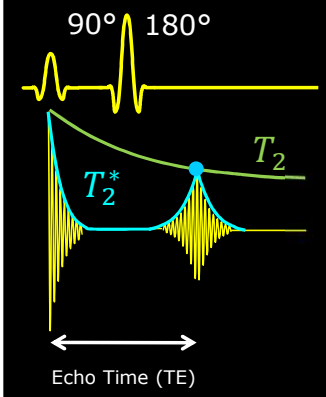

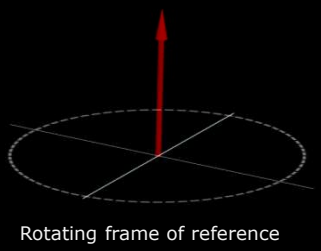

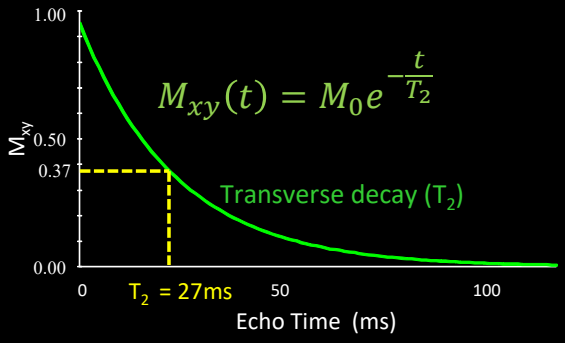

$$\frac{1}{T_2^*} = \frac{1}{T_2} + \cancel{\frac{1}{T_2'}} = \frac{1}{T_2} + \cancel{\gamma \Delta B_i}$$

Previously we showed the decay of the transverse magnetisation to be governed by T_2^* relaxation. In order to eliminate the often unwanted effects of T_2' we use a spin echo pulse sequence to eliminate the effects of static field non-uniformities and other magnetic susceptibility effects within the body. The spin echo sequences comprises a 90° pulse that tips the magnetisation into the transverse plane, followed by a 180° refocusing pulse. After the 90° pulse the magnetisation decays due to T_2^* relaxation. If after a certain time τ a 180° pulse is applied the disk of dephased magnetisation will undergo a 180° phase flip. Since the spins now have a reversed phase. If we wait for a further time τ the dephasing caused by the static magnetic field non-uniformities will be reversed, i.e. eliminated and an echo will be formed. Since spin-spin interactions are irreversible the echo will represent T_2 decay and hence the images will have T2-weighted contrast. Note that the time from the excitation pulse to the echo signal is called the echo time (TE) and TE = 2τ.

Transverse and Longitudinal Relaxation

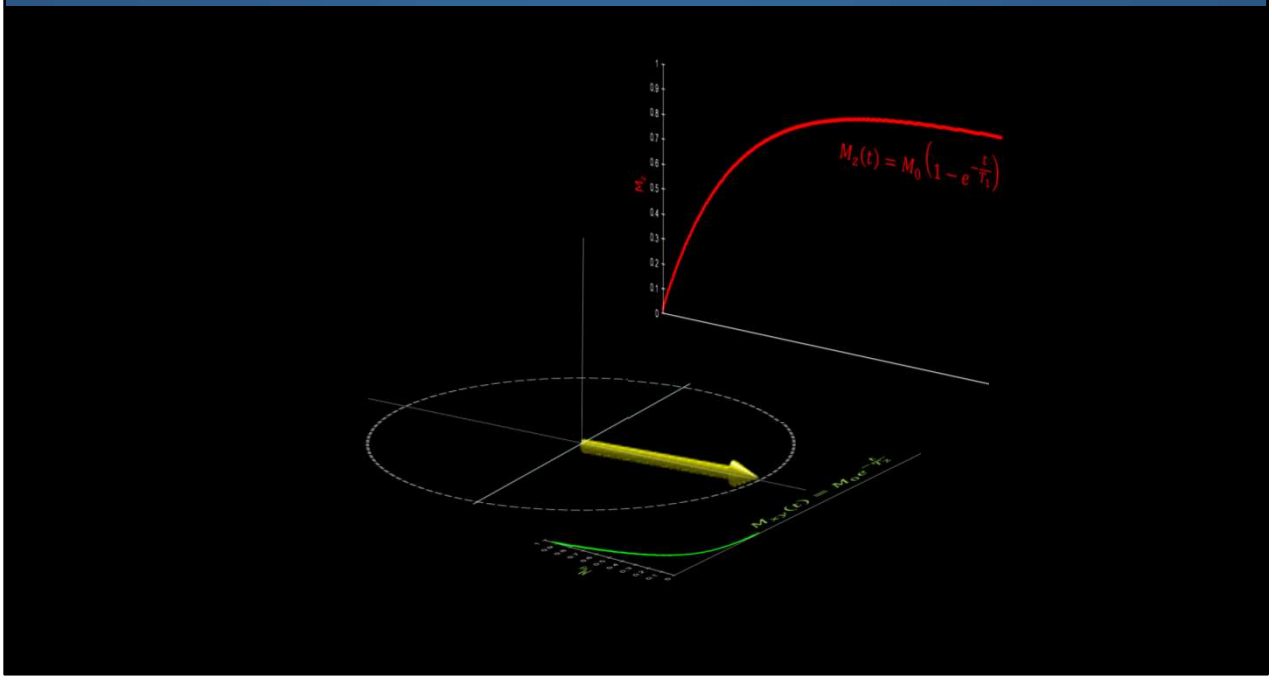

This figure shows the longitudinal magnetization recovery (red) and transverse magnetization decay (green) in the laboratory frame. In biological tissue T_2 is approximately an order of magnitude shorter than T_1, i.e. For brain white matter the T_1 is around 560ms and T_2 is around 90ms. Remember that M_0 is proportional to the proton density ρ.

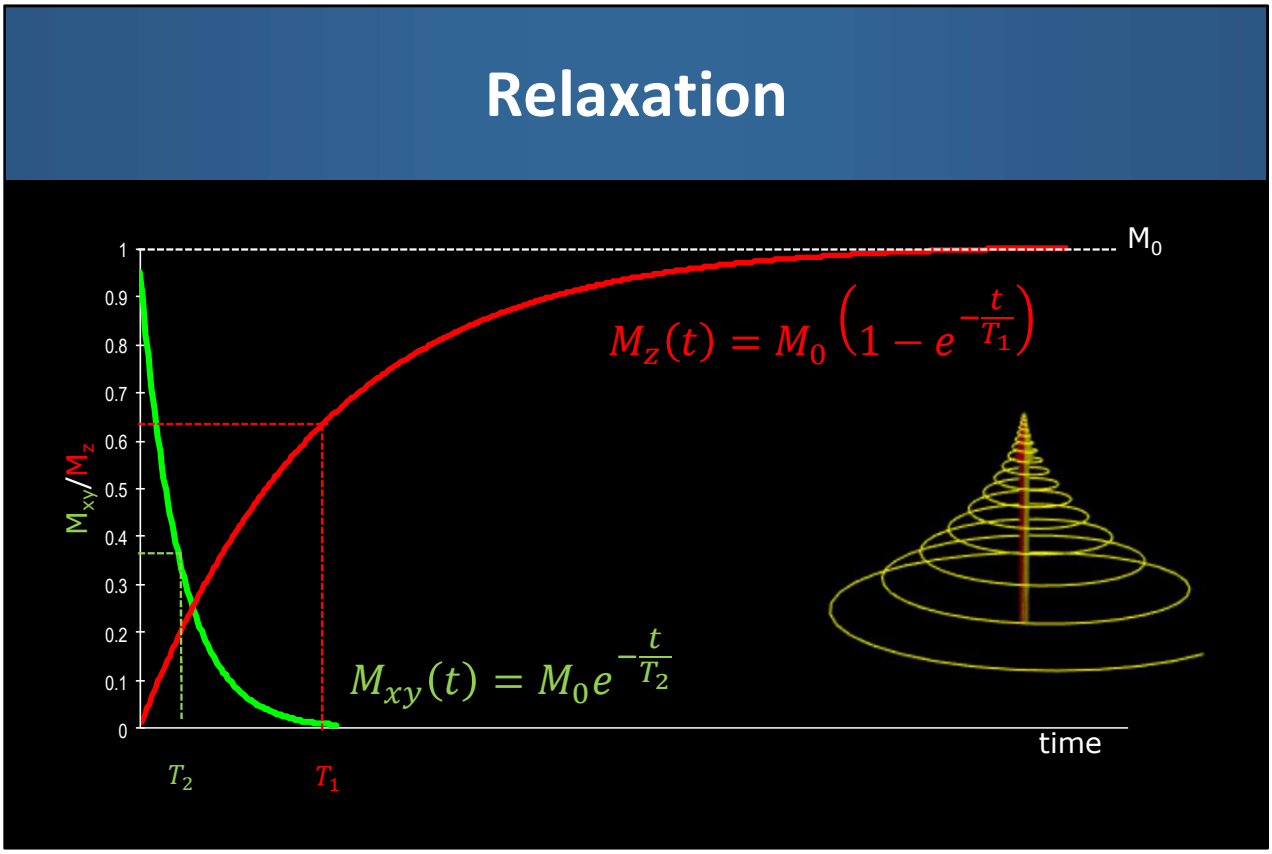

This figure shows the longitudinal magnetization recovery (red) and transverse magnetization decay (green).The T_1 is the time for 63% of the magnetisation to have recovered, whilst the T_2 is the time for 37% of the magnetisation to have decayed.

T_2 Relaxation Mechanism

Magnetic moments of neighbouring protons alter local magnetic field causing a loss of phase coherence (spin-spin relaxation)

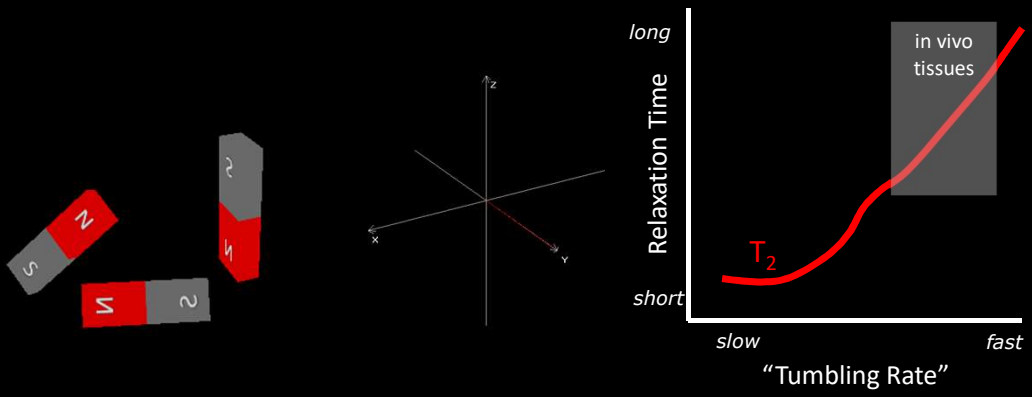

We know that T_2 relaxation arises from the exchange of energy between spins, hence the term 'spin-spin' relaxation. No energy is actually lost from the spin system but the decay of transverse magnetization arises from the loss of phase coherence between spins, which arises from magnetic field nonuniformities. These inhomogeneities may be either intrinsic or extrinsic, i.e. internal to the proton system or external in the scanner. Only the intrinsic inhomogeneities contribute to T_2. A description of molecular motions can also be used to describe the mechanism of T_2 relaxation. When molecules are tumbling very rapidly, i.e. we can consider them "free" and not "bound" to surrounding macromolecules then a particular spin dipole, i.e. bar magnet will see the local magnetic field as fluctuating very rapidly and effectively averaging out over a few milliseconds. This results in a relatively uniform local field and little dephasing, and is sometimes termed 'motional averaging'. Conversely a slowly tumbling molecule (bound protons close to large molecules) will see a relatively static magnetic field nonuniformity and will be more effectively dephased, i.e. will have a shorter T_2 with respect to other protons.

Measuring T_2 Relaxation

T_2 can be calculated from images acquired at different TEs but the TR needs to be maximised

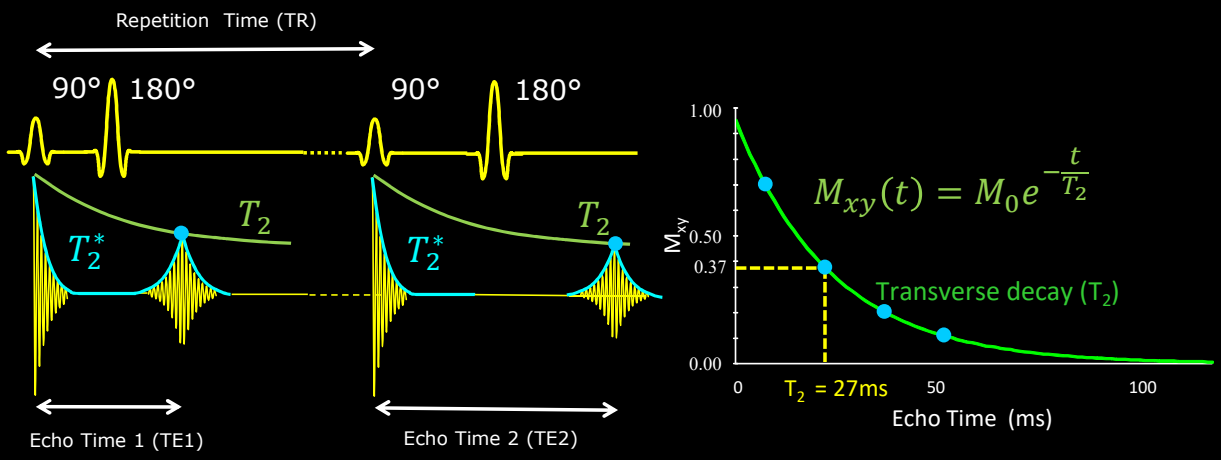

It would be possible to calculate the T_2 relaxation constant by acquiring signals with different TEs. However the TR needs to be kept as long as possible to minimise the T_1 effect on the measured signals. The blue circles show the echo amplitudes at different TEs from which the T_2 decay constant can be calculated.

T_1 Relaxation Mechanism

As molecules tumble/vibrate the protons are exposed to an alternating magnetic field that stimulates relaxation. Relaxation is dependent upon the tumbling rate.
Intramolecular and intermolecular dipole-dipole

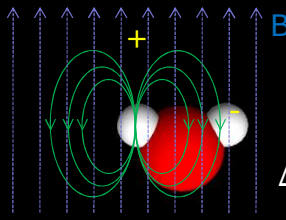

$$\Delta\epsilon = \gamma\hbar B_0$$

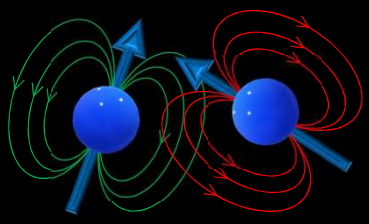

proton-proton
proton-electron

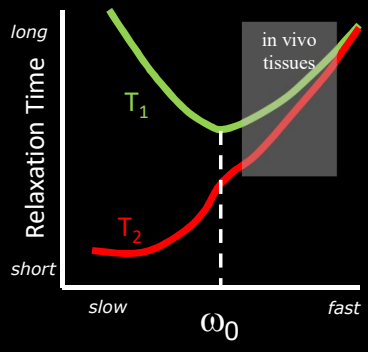

The alternating field comes from neighbouring protons or other nuclei or molecules, which have magnetic moments. In water the nearest adjacent nucleus will be the other hydrogen atom on the same molecule. Therefore, relaxation will primarily arise through the magnetic moment that one hydrogen nucleus 'sees' as it tumbles relative to the moment of the other hydrogen nucleus. This is often called an intra-molecular dipole-dipole interaction.

T_1 Relaxation: Quantum Approach

Quantum of energy (ΔE) stimulates move from high to low energy state, losing energy to surrounding lattice

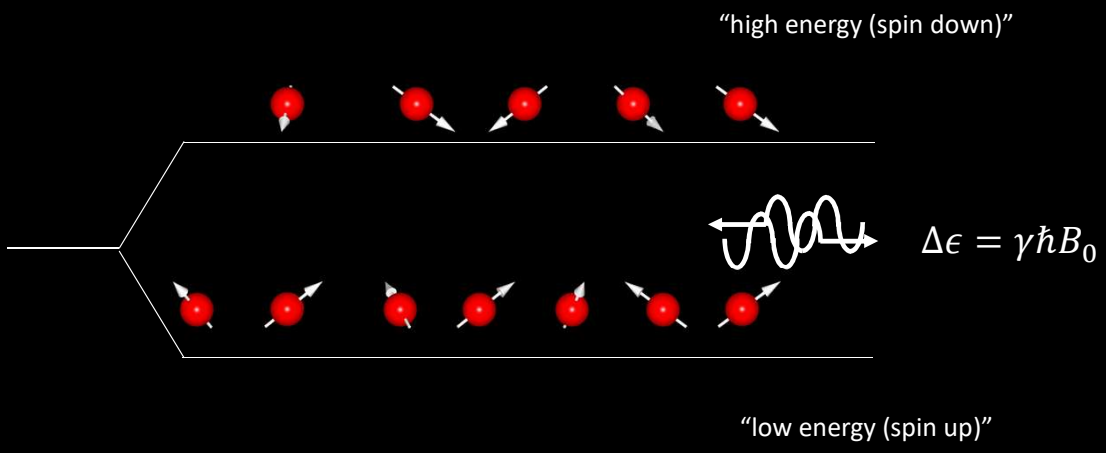

We know that an RF pulse on average promotes protons from the low energy state to the high energy state causing a net absorption of energy. T_1 relaxation is the loss of the extra energy from the spin system to the surrounding environment, or 'lattice' (hence 'spin-lattice' relaxation time). However, the high energy state is a stable position for the proton and it does not return to the lower state spontaneously but requires an external stimulating field. Since the external B_1 field has been switched off, where does this field come from?

Molecular Tumbling

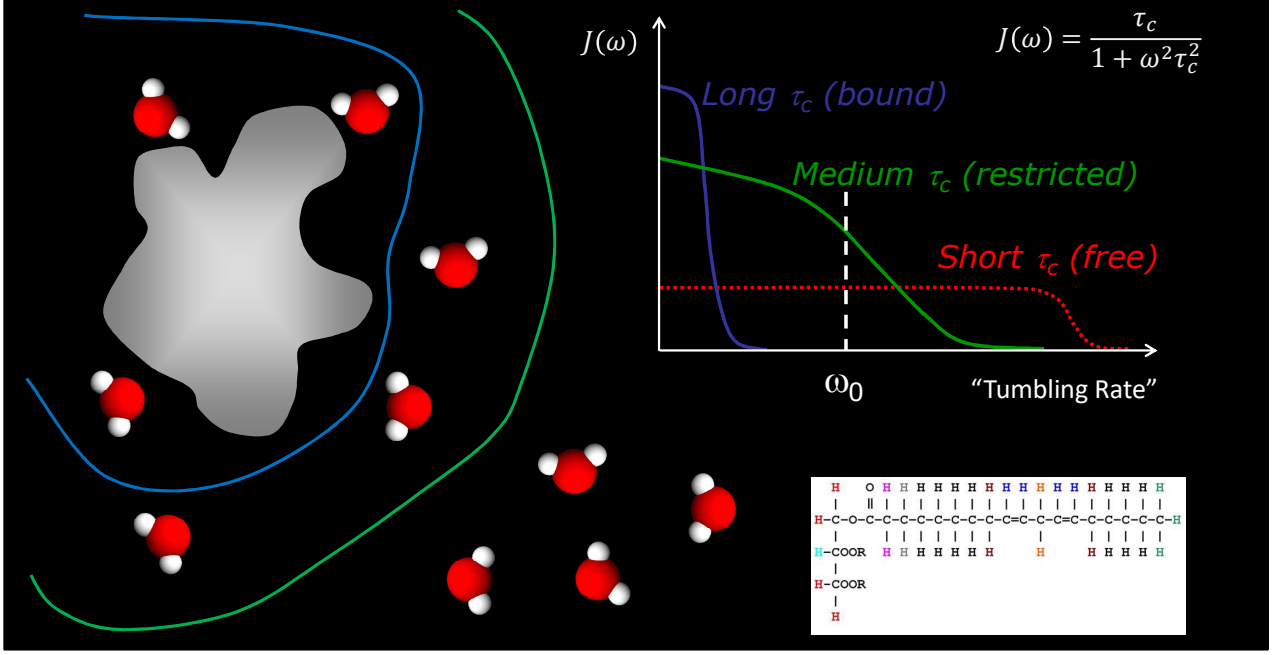

As mentioned in a previous slide T_1 relaxation will primarily arise through the magnetic moment that one hydrogen nucleus 'sees' as it tumbles relative to the moment of the other hydrogen nucleus. This is often called an intra-molecular dipole-dipole interaction. However nuclei have to tumble at the Larmor frequency to induce the transitions. In vivo water, with its small molecular size, tumbles much too rapidly in its free state to be effective at T_1 relaxation. T_1 values are longer for free water than for any other substance in the body (approximately 4000 ms at 1.5T). When the water is in a partially bound or in a restricted state, however, its tumbling may be slowed to a rate much closer to the Larmor frequency. Water molecules with restricted motion frequently occur in biological systems where their molecular motion is slowed by interaction with polar amide and hydroxyl groups on the surfaces of macromolecules. The T_1 value of "bound" or "structured" water is therefore much shorter than that of free water (typically about 400-800 ms at 1.5T). This is the type of water whose signal we primarily measure when imaging solid organs like the liver or brain. One way to characterize the motion of a molecule is by its *correlation time (τ_c)*, the time required to rotate by approximately 1 radian (~57°). As expected, smaller molecules rotate faster (and have smaller τ_c*'s)* than larger ones. The correlation time also decreases with increasing temperature (kinetic energy causes them to rotate faster). As a rule of thumb used by chemists, the rotational correlation time (in nanoseconds) of a molecule in aqueous solution at room temperature is about half its molecular weight (in kilodaltons).Because of random thermal fluctuations and collisions, otherwise identical molecules with the same correlation times (τ_c*)* will rotate at different angular velocities (ω). The probability of finding a molecule rotating at a given frequency is proportional to the ***spectral density function J(ω)***. For spherical molecules in solution the form of the spectral density is expressed by the equation above. For large molecule, like lipids, their tumbling rate is just right to result in efficient T_1 relaxation, hence why fat has the shortest natural T_1.

Measuring T_1 Relaxation

T_1 can be calculated from images acquired at different TRs but the TE needs to be minimised

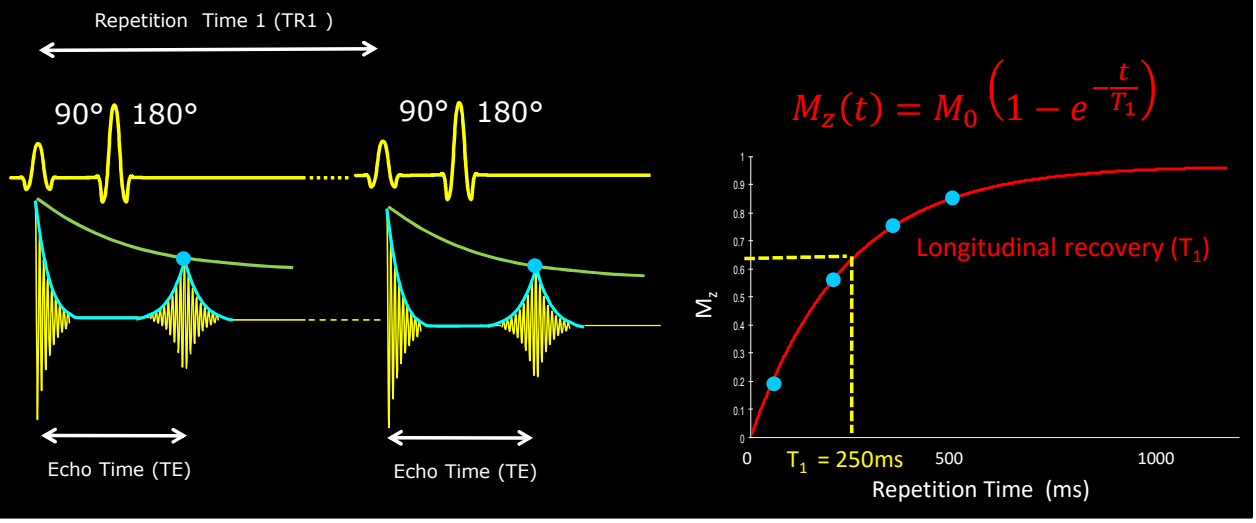

Following the echo signal the magnetisation recovers due to T_1 relaxation. It would be possible to calculate the T_1 relaxation constant by acquiring signals with different TRs. Since it is not possible to directly sample the longitudinal magnetisation it has to be tipped into the transverse plane. Therefore the TE needs to be kept as short as possible to minimise the T_2 effect on the measured signals. The blue circles how the transverse magnetisation at different TRs from which the T_1 relaxation time can be calculated.

Bloch Equations with Relaxation

- Following the RF excitation the transverse magnetisation decays to zero with a time constant T_2

$$\frac{dM_x(t)}{dt} = \gamma\left(M_y B_0 + M_z B_1 \sin(\omega_{rot} t)\right) - \frac{M_x}{T_2}$$

$$\frac{dM_y(t)}{dt} = \gamma(M_z B_1 \cos(\omega_{rot} t) - M_x B_0) - \frac{M_y}{T_2}$$

- And the longitudinal magnetisation returns to equilibrium with a time constant of T_1

$$\frac{dM_z(t)}{dt} = \gamma(-M_x B_1 \sin(\omega_{rot} t) - M_Y B_1 \cos(\omega_{rot} t)) - \frac{(M_z - M_0)}{T_1}$$

- Note that at equilibrium $M_z = M_o$

- Expressing the magnetisation in complex form $M_{xy} = M_x + iM_y$ then in the rotating frame of reference where $\omega_o = \omega_{rot}$ the equations simplify to

$$\frac{dM'_{xy}(t)}{dt} = -\frac{M'_{xy}}{T_2}$$

$$\frac{dM_z(t)}{dt} = -\frac{(M_z - M_0)}{T_1}$$

- These linear ordinary differential equations have the following solutions

$$M'_{xy}(t) = M_0 e^{-\frac{t}{T_2}}$$

$$M_z(t) = M_0\left(1 - e^{-\frac{t}{T_1}}\right)$$

Solving the Bloch equation which treats the relaxation as a first order process gives the behavior of the transverse and longitudinal magnetization

Spin Echo Contrast

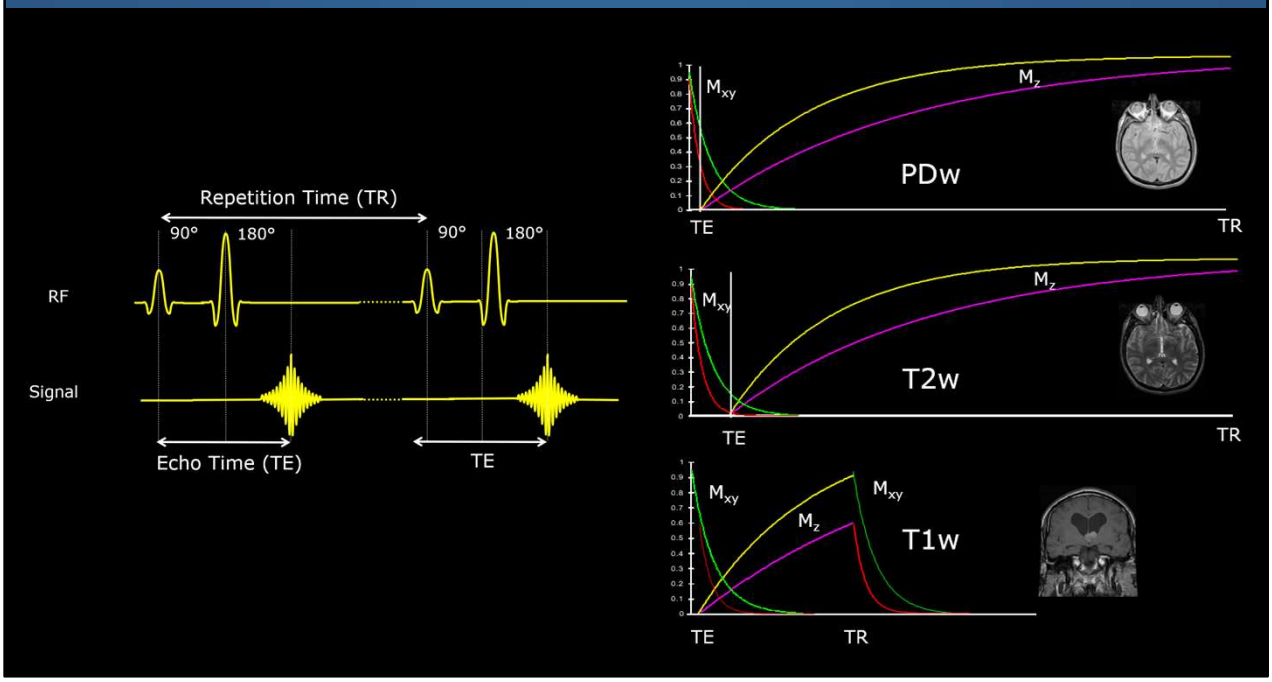

The contrast in a spin echo sequence is controlled by the TE and the TR. The TE controls the amount of T_2 dephasing, i.e. T2-weighting in the image, whilst the TR controls the amount of T_1 recovery, i.e. T1-weighting in the image. We describe images as “weighted” since it is extremely difficult to have either zero TE to eliminate T_2 or very long TR, .e.g. at least 5 times the longest T_1, to eliminate T_1. In any case the underlying proton density differences are always present. A proton density (PD) weighted image therefore has a long TR to reduce T_1 effects and a short TE to minimise T_2 effects. A T2-weighted images has a long TR to minimise T1 effects but a long TE to maximise T_2 contrast. A T1-weighted images has a short TR to maximise the differences in T_1 relaxation but a short TE to minimise T_2 effects. Of course it is not possible to directly observe the longitudinal recovery so the magnetisation has to be tipped into the transverse plane in order to detect the T_1 differences. The inevitable T_2 decay during the time required even for a minimum value of TE, due to the tiem required to play out the RF pulses, results in reduced T_1 contrast.

Spin Echo Contrast

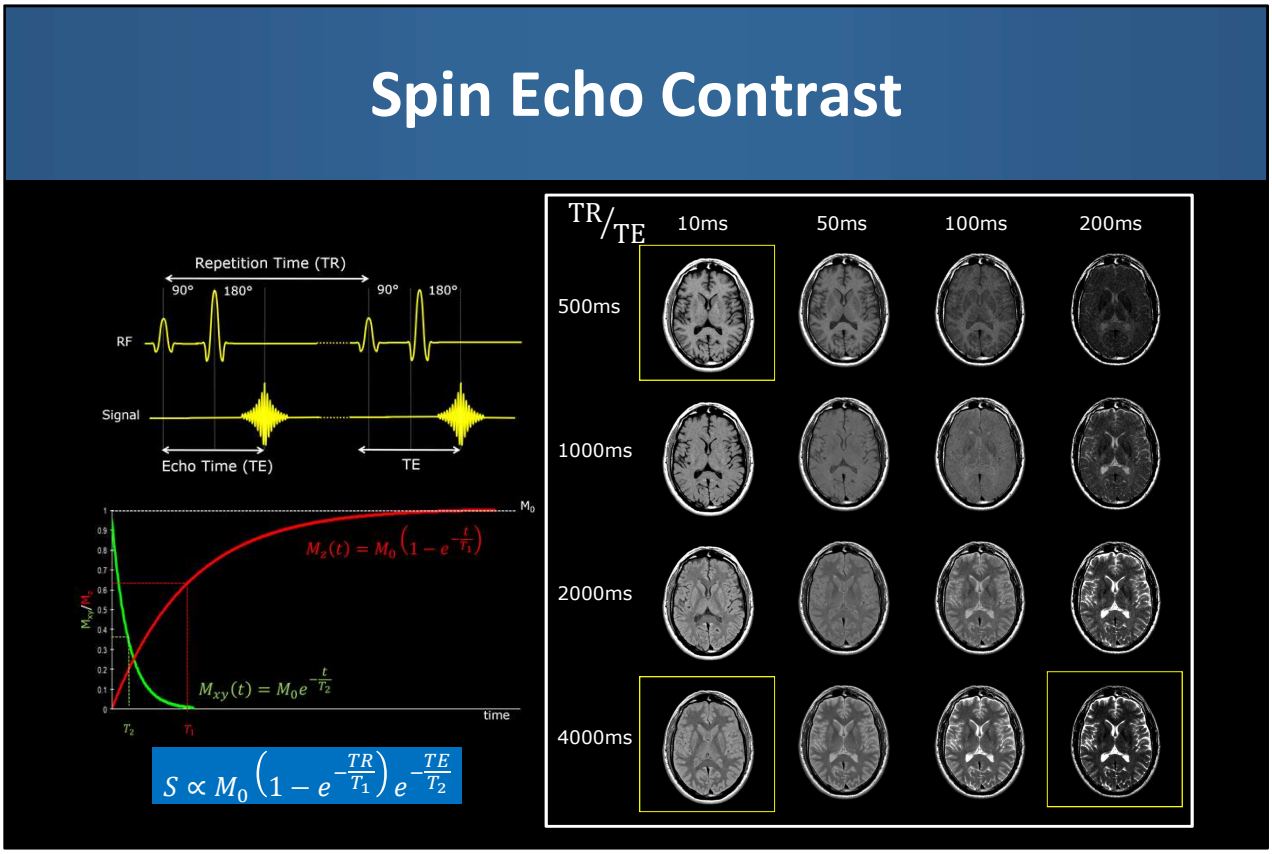

This slide shows the changes in contrast as TE and TR are varied. The main contrast weightings used clinically are T1w (top left hand corner), proton density (PDw) (bottom left hand corner) and T2w (bottom right hand corner)

Nuclear Magnetic Resonance Imaging

Paul Lauterbur (1929-2007) Peter Mansfield (1933-2017)

2003 Nobel Prize in Physiology or Medicine for "for their discoveries concerning magnetic resonance imaging"

How do we go from NMR to MRI in order to create images. We firstly we have to drop this pesky nuclear bit. With the obvious association of nuclear with radioactivity, of which we have seen there isn't any in relation to NMR, nuclear got dropped early on in the development of imaging to just leave Magnetic Resonance Imaging or MRI. Two of the leading lights in the field were Professor Paul Lauterbur from the State University of New York and Professor Sir Peter Mansfield from the University of Nottingham who were subsequently awarded the 2003 Nobel Prize in Physiology or Medicine for "for their discoveries concerning magnetic resonance imaging"

Imaging & Gradients

- The key to MRI imaging is the concept of a magnetic field gradient

$G_x = \frac{\partial B_z}{\partial x}, G_y = \frac{\partial B_z}{\partial y}, G_z = \frac{\partial B_z}{\partial z}$ superimposed on the main static magnetic field

- The gradient creates a spatially dependent variation of the Larmor frequency, e.g. in the x-direction $B(x) = B_0 + G_x x$
- Gradient amplitudes are typically measured in mT/m or G/cm (10mT/m = 1G/cm)

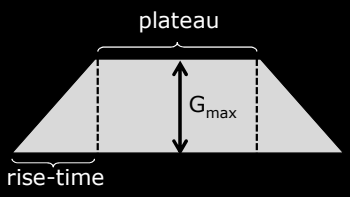

Paul Lauterbur
(1929-2007)

The crucial invention as far as imaging is concerned was made by Lauterbur who apparently had the idea whilst eating a hamburger. Lauterbur's great idea was to introduce a magnetic field gradient. He called his technique "zeugmatography" from the Greek ζεῦγμα "to join". The name didn't catch on!

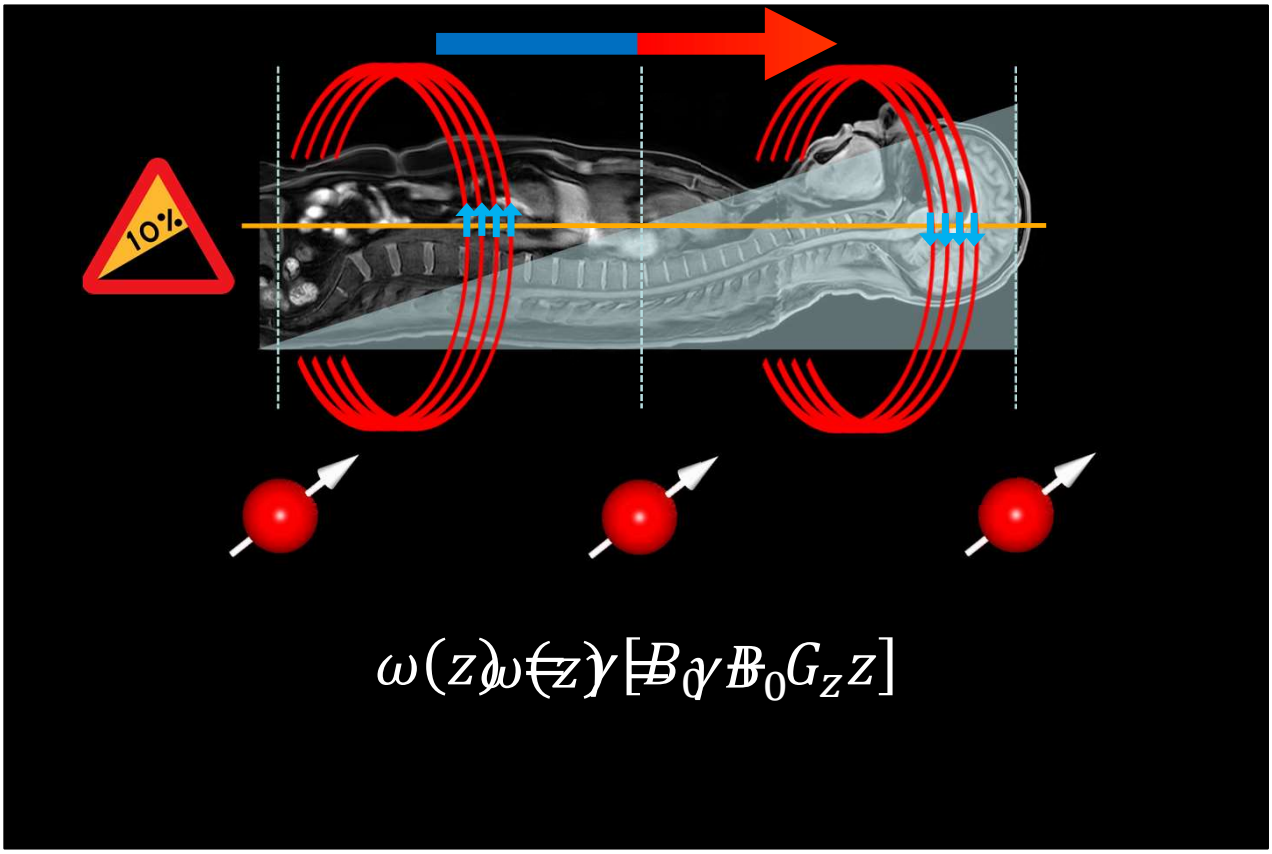

Here is our subject lying inside the magnet with the main magnetic field pointing from their feet to their head. At these three positions the main magnetic field is constant and the protons are all precessing at the same frequency. If we add yet more coils inside the MRI scanner then by passing current through these coils we can create a gradient, that is to say a slope in the magnetic field in addition to the main magnetic field. It is the switching on and off of this gradient that causes the characteristic knocking noise when imaging. These gradient coils physically flex, not by a lot, but enough to create the acoustic noise. You can see that when the gradient is applied there is now a difference in the precessional frequencies because the protons are now in slightly different magnetic fields due to the gradient.

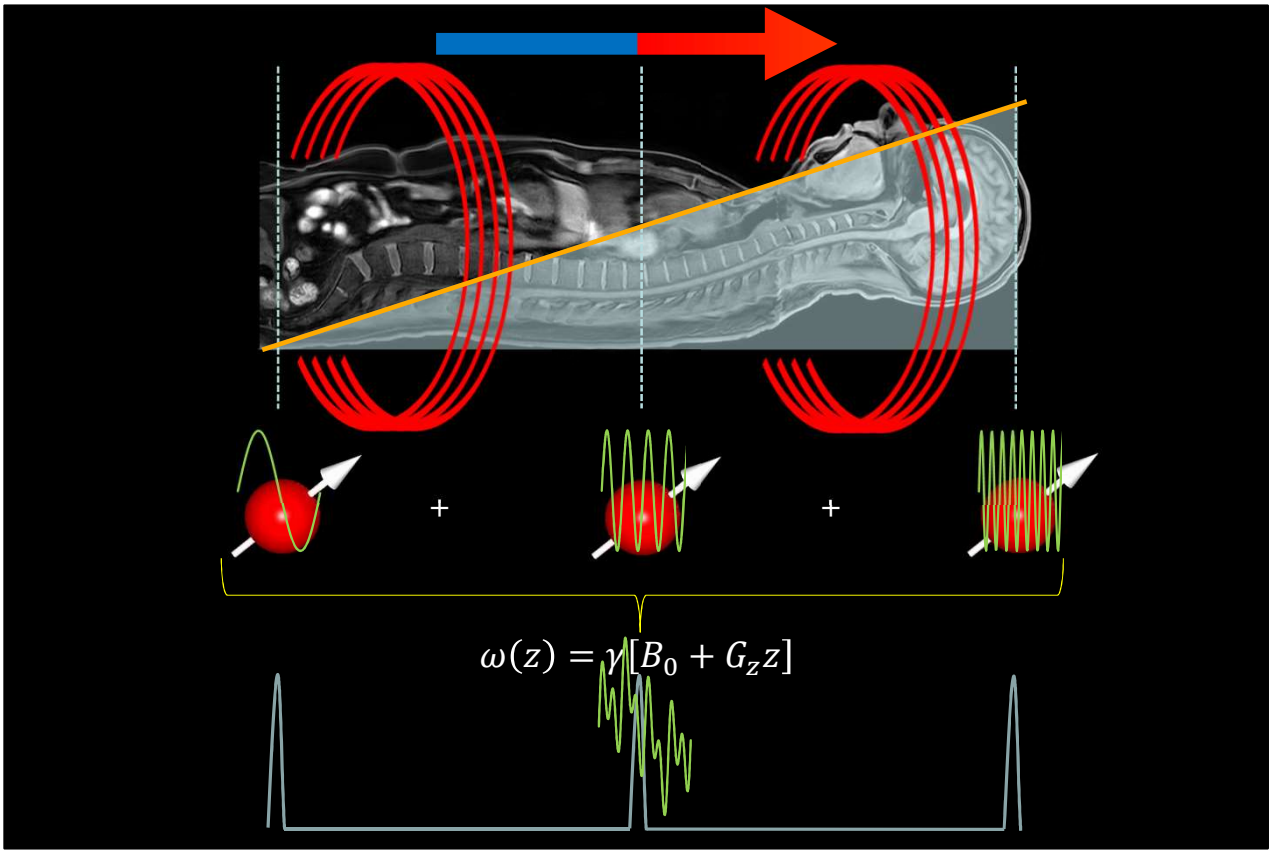

It may be easier to understand in term of musical notes. The proton on the left precesses at the lowest frequency, the proton in the middle at a slightly higher frequency whilst the proton on the right the right precesses at the highest frequency. Now the signal comes from all the protons so what we detect in this case is the sum of all three frequencies. How can we separate the individual notes from the sum? A Fourier transform can transform a time domain signal to the frequency domain. So we can see three peaks. The area under each peak would correspond to the weighted NMR signal at that position. If the gradient is accurately calibrated then we can go from frequency directly to spatial position

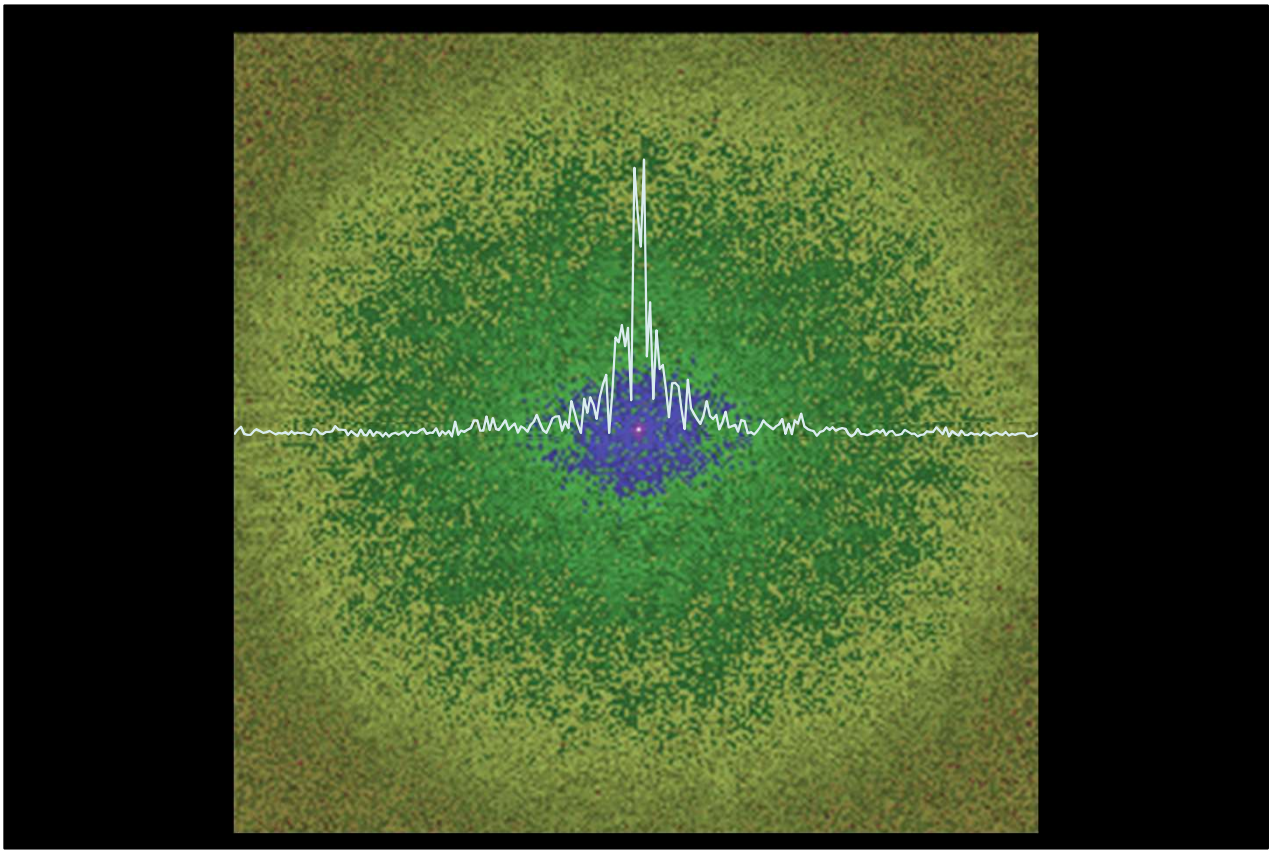

The real signal from a human subject looks like this and can be displayed as one line of a raw data image it looks like this. Now the complete MRI scan involves changing these gradients many hundreds of times and detecting the signals across the entire body. So the scanner acquires data like this. This is the raw data, sometimes called *k*-space.

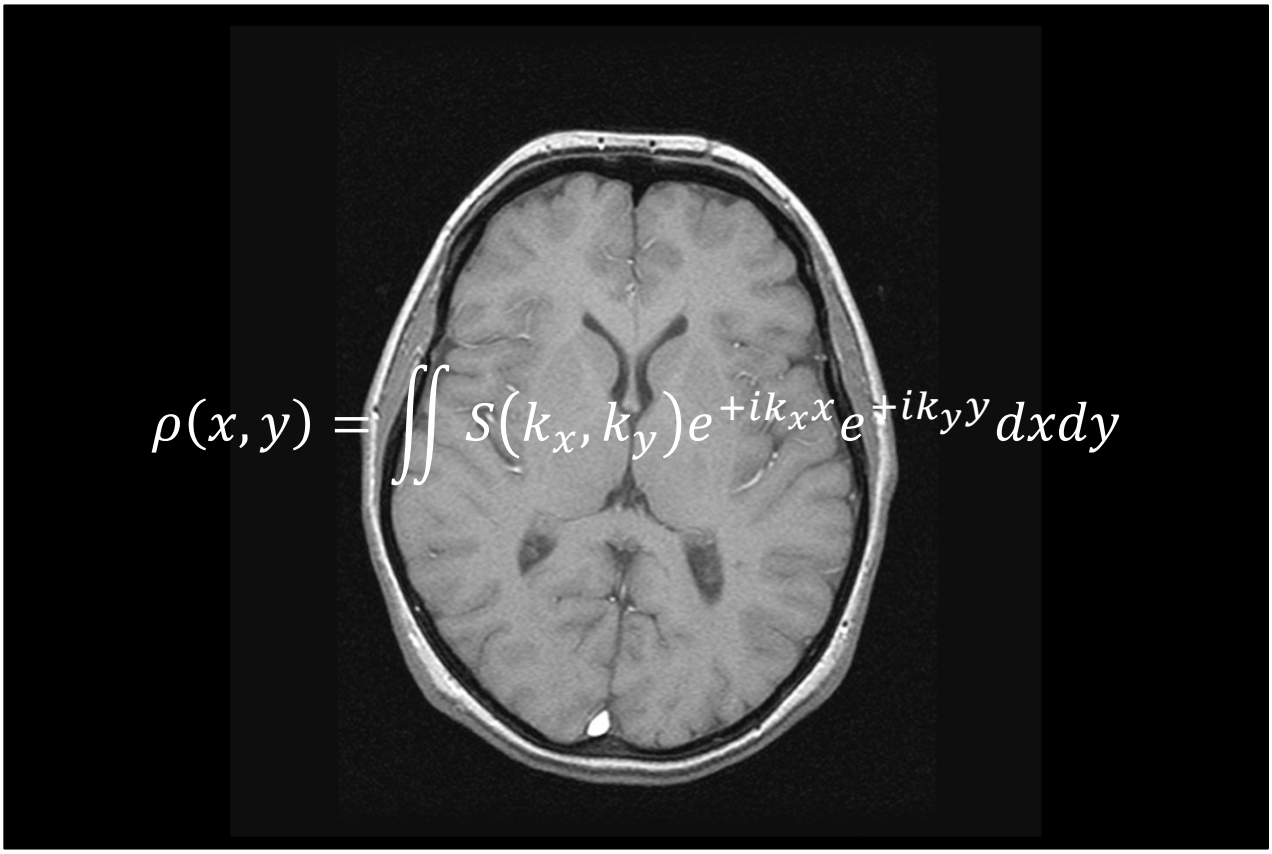

Simply performing an inverse 2D Fourier transform of this raw data reconstructs the image.

Slices

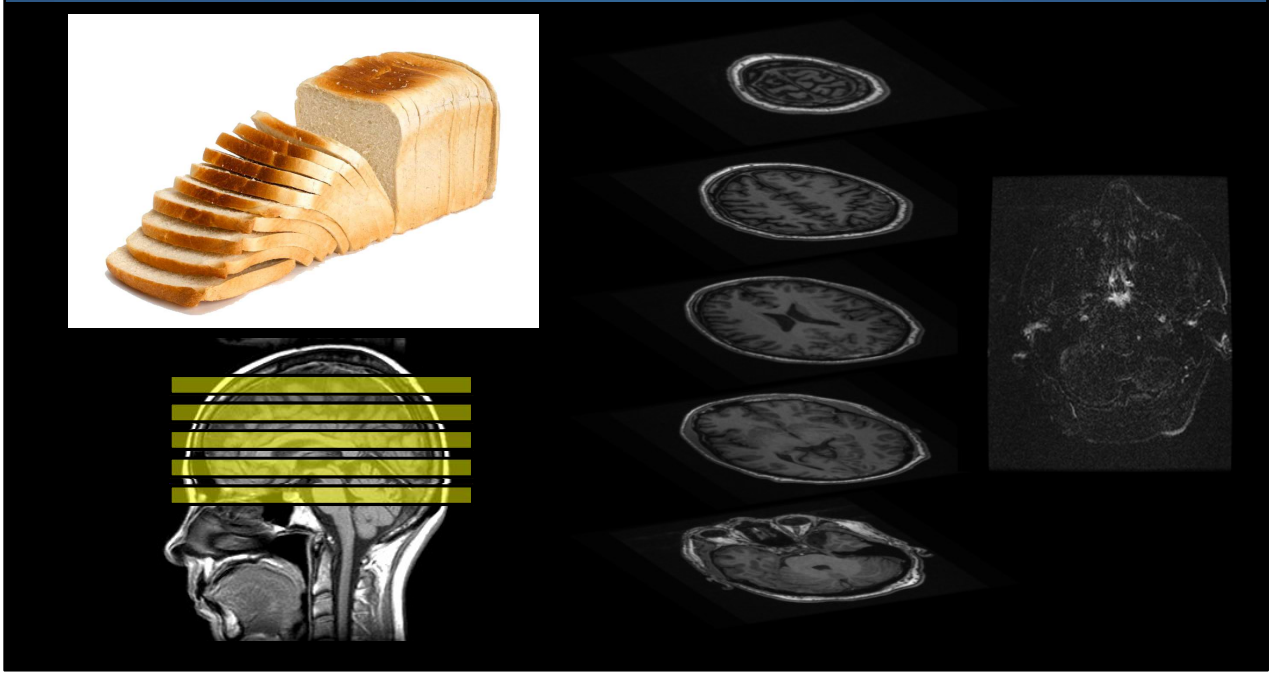

Images are usually acquired and displayed as “slices” or “sections” through the data volume. A brain MRI for examples would involve the acquisition of a number, typically 20-30 of relatively thin, e.g. 5mm slices throughout the brain.

Spatial Localisation

Spatial encoding of the MR signal is achieved through the use of magnetic field gradients

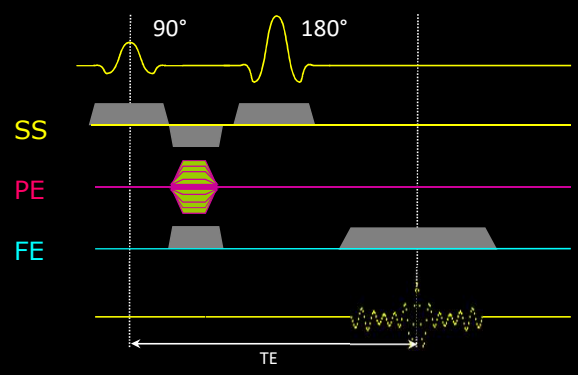

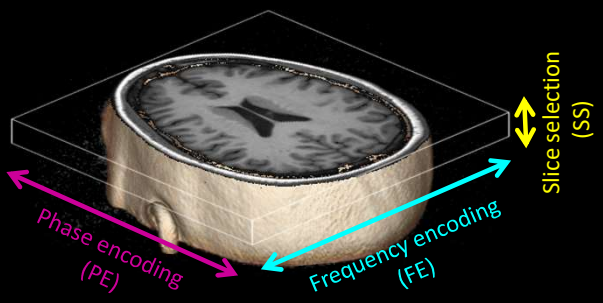

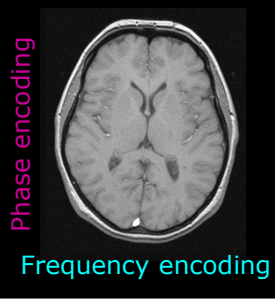

The acquisition of an MRI image involves the combination of RF pulses to tip the net magnetisation, various time delays to allow the desired contrast, e.g. T1w, to develop and gradient pulses to spatially encode the MR signal. The gradients are spatially-linear magnetic fields that are superimposed upon the static magnetic field. There are three orthogonal physical gradients in x, y and z but we will refer to them by the logical names of slice selection, phase encoding and frequency encoding. In this spin echo pulse sequence we can see these gradients represented as trapezoidal blocks. The trapezoidal shape means that it takes a finite time (ramp up) to switch on the gradient, it is then held on (the flat top), for a period of time before it ramps down.

Gradient Effects

Gradient pulses induce a change in Larmor frequency with amplitude/position, and phase accumulation with time

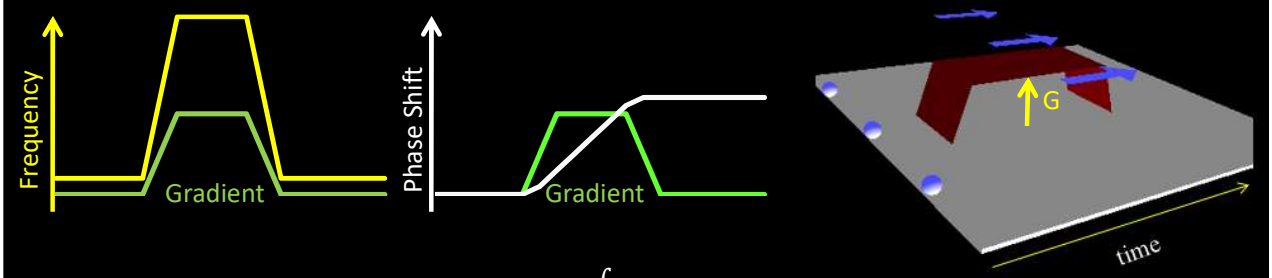

$$\omega(x) = \gamma[B_0 + G_x x]$$

$$\phi = \gamma \int \omega \, dt$$

A magnetic field gradient will not only cause a transient change in Larmor frequency but will also induce a (relative) phase shift in the transverse magnetisation proportional to the strength and duration, e.g. “area”, of the gradient pulse. The diagram shows three spins initially all precessing in phase (we will ignore spin dephasing/relaxation etc). The middle spin will then come under the influence of a magnetic field gradient pulse (in this case we assume the x-direction), whereas the others will not. Note how the spin precesses more rapidly due to the increased Larmor frequency. However at the end of the gradient pulse all three spins precess at the same frequency but the middle spin is 180° out of phase compared to the other two.

Gradient Effects

Gradient pulses induce a change in Larmor frequency with amplitude/position, and phase accumulation with time

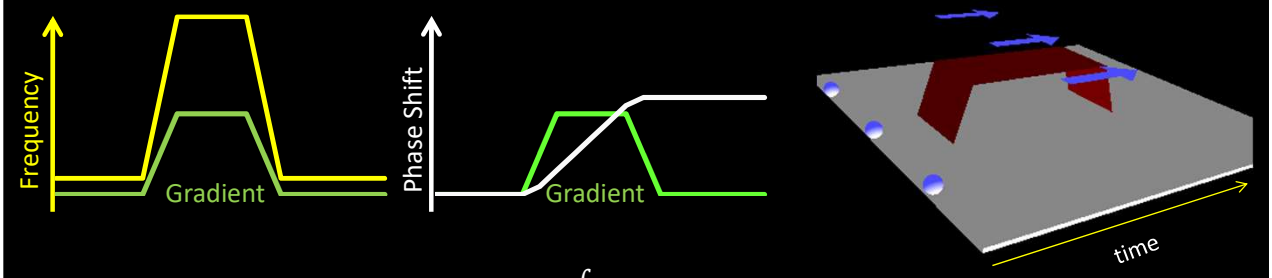

$$\omega(x) = \gamma[B_0 + G_x x]$$

$$\phi = \int \omega \, dt$$

$$\Delta\phi = \gamma \int_{t=0}^{t=T} G_x \, x \, dt$$

Defining $k_x = \gamma \int_{t=0}^{t=T} G_x(t) \, dt$, then $\Delta\phi = k_x \, x$

This phase shift can be represented in terms of a *k*-space with units of inverse distance

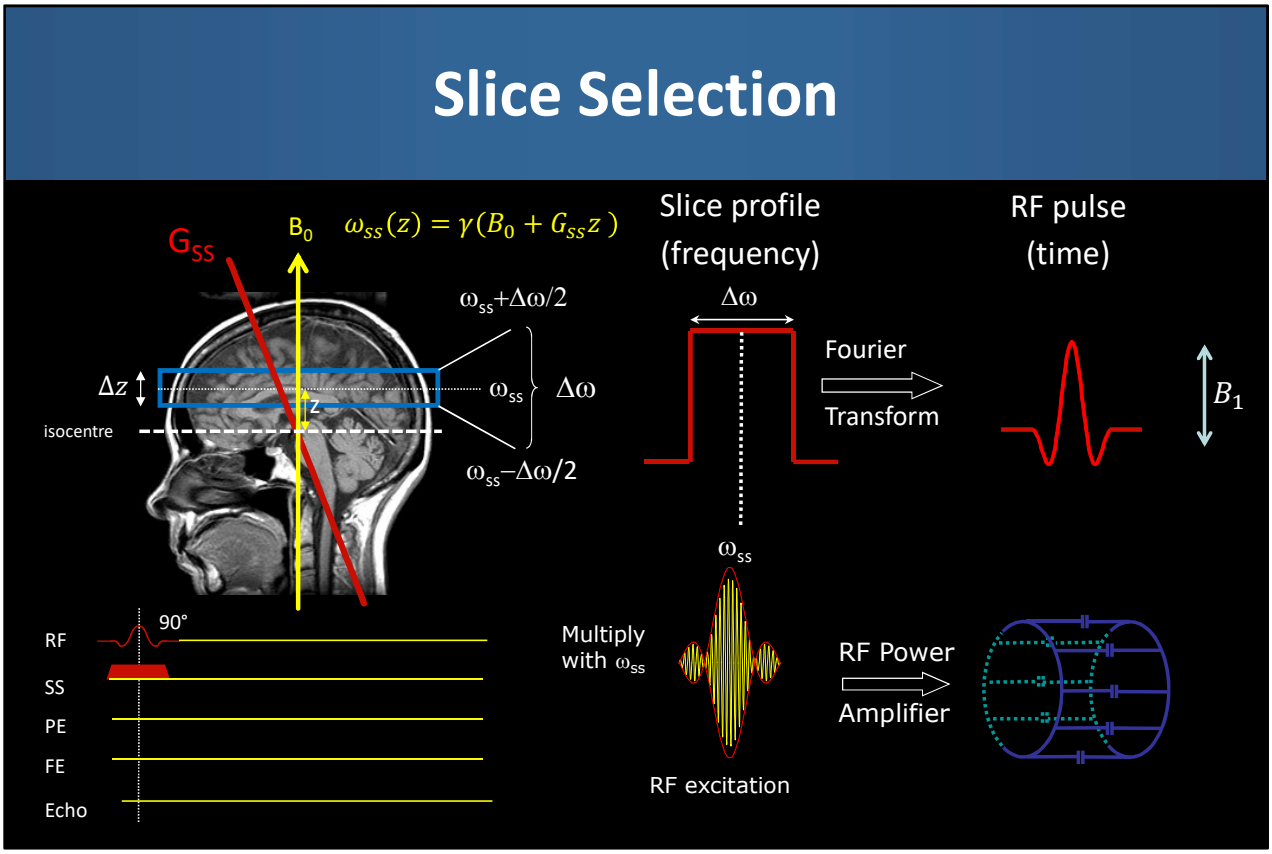

A slice through the body is selected by the application of an RF pulse together with a magnetic field gradient in the slice select direction. In this case an axial slice through the brain. We wish to only excite those spins at a particular physical offset (z) from the centre of the magnet known as the isocentre , i.e. the fulcrum of the gradients. We wish the slice to have a certain thickness (Δz), typically 5-10mm. From the Larmor equation we know that the spins within the slice will be precessing at $\omega_{ss} \pm \frac{\Delta\omega}{2}$, where $\omega_{ss}(z) = \frac{\gamma}{2\pi}(B_0 + G_{ss}z)$. The slice profile in the frequency domain will be a top hat function, which will be a sinc function ($sinc(x) = \frac{\sin(x)}{x}$) in the time-domain. The sinc envelope is used to amplitude modulate the transmit frequency ω_{ss}. If the amplitude and duration of the RF pulse are sufficient to nutate the magnetisation by 90° then all the spins that are resonant at $\omega_{ss} \pm \frac{\Delta\omega}{2}$ will be tipped into the transverse plane.

Slice Select Gradient Amplitude

3.2ms Hann windowed SINC (TBW = 8)

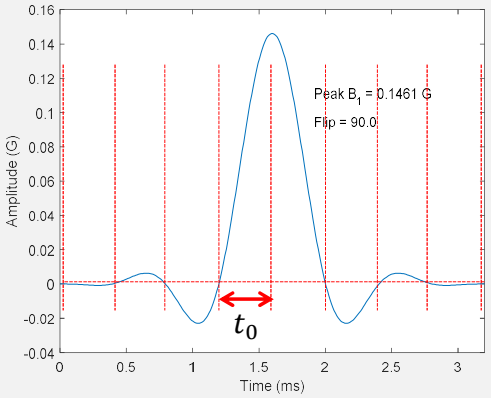

Time-Bandwidth Product (TBW) = no. of zero crossings

$$T\Delta f = N_L + N_R$$

$$\Delta f = \frac{N_L + N_R}{T}$$

$$\Delta f = \frac{1}{t_0}$$

Slice Profile

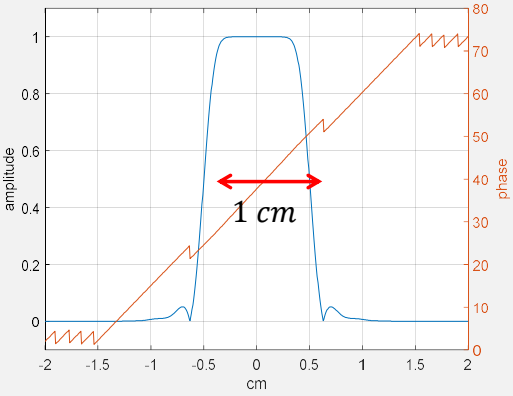

$$G_z = \frac{\Delta f}{\gamma\, \Delta z}$$

$$G_z = \frac{8/3.2ms}{4257 \cdot 1cm} = 0.59\ \mathrm{G/cm}$$

A sinc pulse with a TBW=4 and duration of T=3.2ms has four zero crossings with t_0= 0.8ms. This results in abandwidth of Δf=1250Hz, i.e. all spins within a bandwidth of $\omega_{ss} \pm \frac{1250}{2}$Hz will be tipped. A slice thickness of 5mm therefore requires a z-gradient amplitude of Gz = 5.87mT/m. Usually the RF bandwidth is fixed and the gradient amplitude is set by the operator defining the slice thickness. A very thin 2D slice prescription may be limited by the maximum gradient amplitude achievable. A thin slice will also have a relatively poor signal-to-noise ratio (SNR). Note the phase variation across the slice profile.

Slice Rephasing Gradient

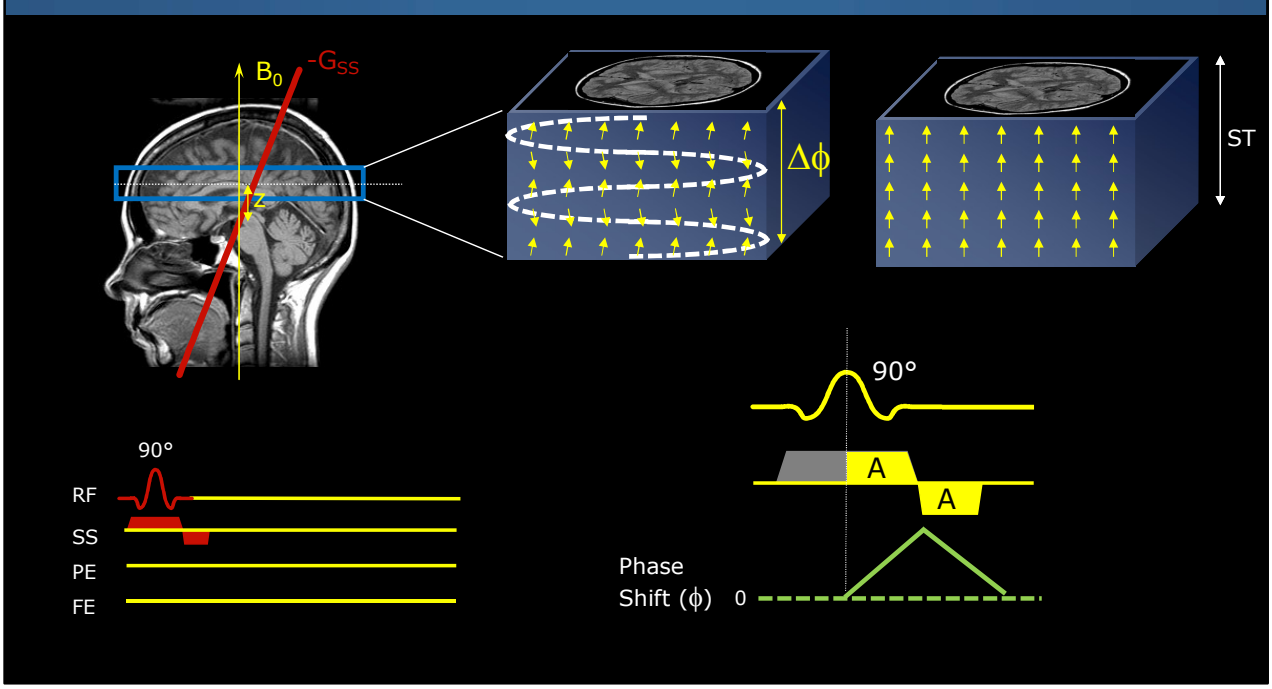

The phase shift across the slice can be reversed by the application of an opposite polarity pulse with an area equal to the area of the gradient from under the magnetic centre of the RF pulse to the end of the gradient. Without this rephasing gradient the signal across the slice would be totally dephased and you wouldn't see anything.

In-plane Spatial Localisation

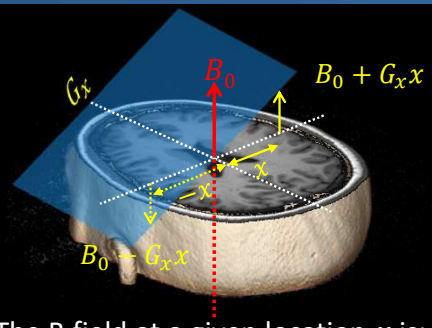

- The B field at a given location x is:
- $B(x) = B_0 + G_x x$
- $\omega(x) = \gamma[B_0 + G_x x]$
- In a reference frame precessing at ω_0
- $\omega(x) = \gamma G_x x$

- The solution of the Bloch equation in complex notation (ignoring T_2) is
- $M(x,t) = M_0(x)e^{-i\omega(x)t} = M_0(x)e^{-i\gamma G_x x t}$
- The spin density at location x is $\rho(x)$, in which case the signal S between x and dx is given by
- $S(x) = \int_x^{x+dx} \rho(x)e^{-i\gamma G_x x t} dx$

i.e., the signal is the Fourier transform of the spin density

- For a continuous 2D distribution $\rho(x,y)$
- $S(x,y) = \iint \rho(x,y)e^{-i\gamma G_x x t} e^{-i\gamma G_y y t}\, dx\, dy$

If we initially consider a gradient in the x-direction (left-right across the subjects head) then the gradient causes a spatially dependent change in the Larmor frequency which means that the MRI signal is the Fourier transform of the objects transverse magnetization.

k-space

- The spatial frequencies k_x and k_y can be defined as
- $k_x = \gamma \int G_x(t)\, dt$
- $k_y = \gamma \int G_y(t)\, dt$

- For simple constant amplitude gradients
- $k_x = \gamma G_x \mathrm{t}$ and $k_y = \gamma G_y \mathrm{t}$
- $S(k_x, k_y) = \iint \rho(x,y) e^{-ik_x x} e^{-ik_y y} dx dy$

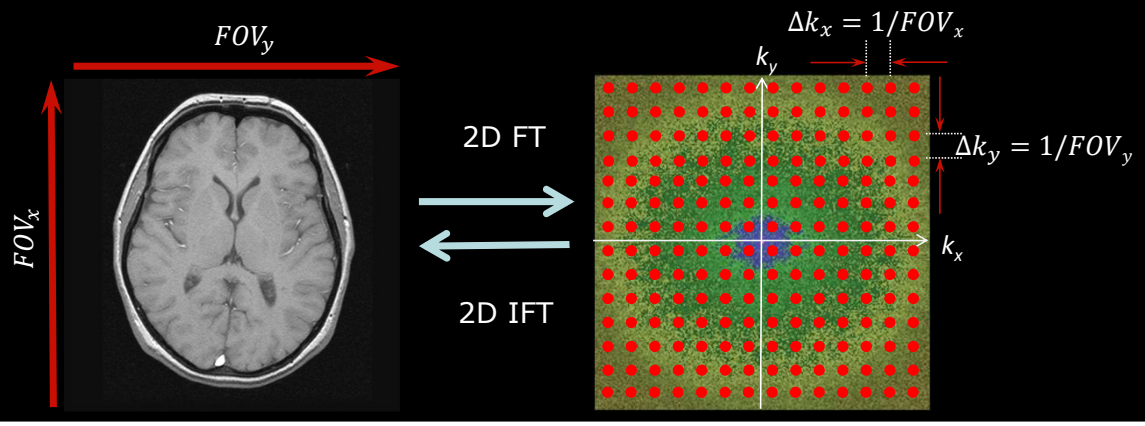

It is usual in MRI to define the *k*-space trajectory in terms of the areas of the gradient waveforms. This provides the basis of our 2D discrete sampling pattern. The raw data array shown on the right is often referred to as *k*-space. MR image reconstruction is a simple 2D inverse Fourier transformation. The reconstruction is generally performed using a fast Fourier transform, hence why image acquisition matrices are usually in powers of 2, e.g. 128, 256 or 512. It should be noted that MRI raw data is actually complex. The raw data is consists of multiple "lines" (k_y) of echo (k_x) data. I am assuming that $\gamma = \frac{\gamma}{2\pi}$

1D Projection

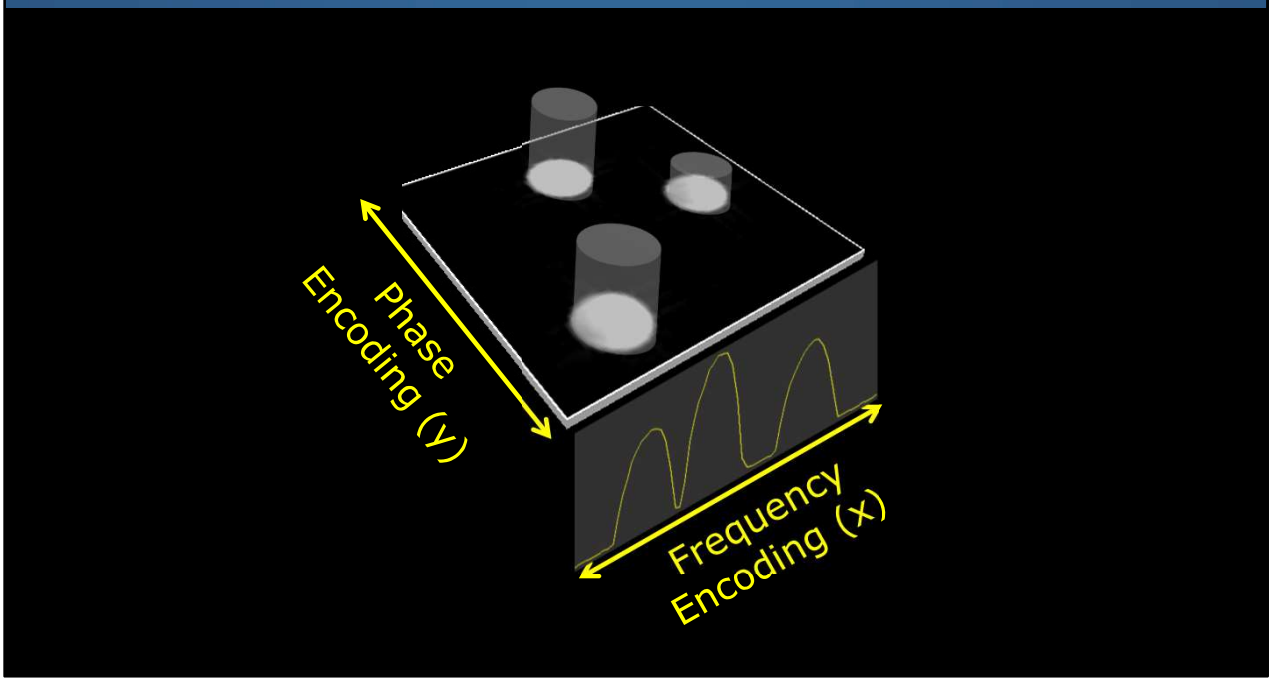

To explain the principles of MR imaging let us consider something slightly easier than a brain - three vials of water. Since the vials contain different volumes of water they contain are different proton densities represented by the different heights of the three peaks that represent a 1-dimensional projection through the data in the frequency encoding direction. We have no information as to their relative positions in the orthogonal phase-encoding direction.

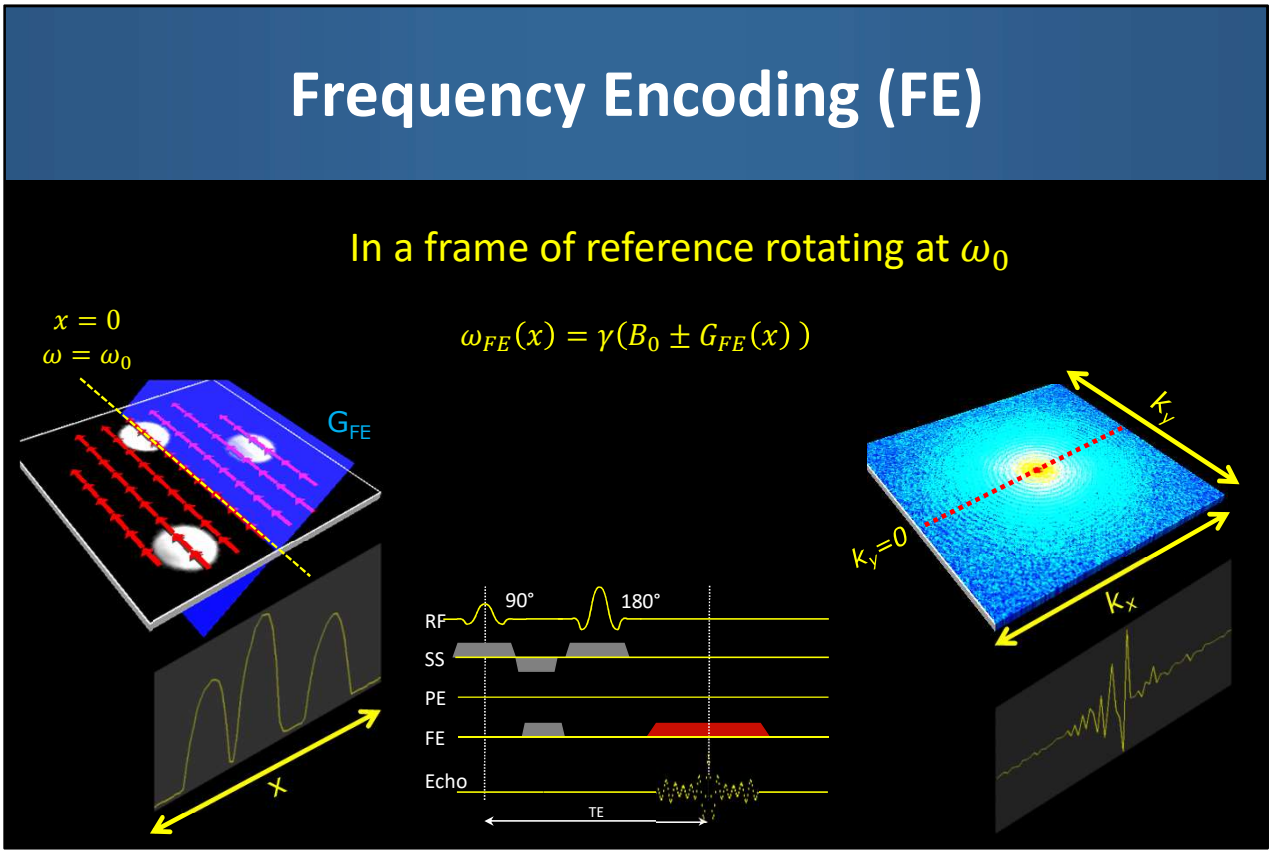

In the rotating frame of reference and ignoring any signal changes due to relaxation etc., the spins that have been tipped into the transverse plane by the RF pulse will all precess at ω_0. However if we apply the frequency encoding (FE) gradient, in this case along the x-axis, the spins will precess at different rates depending upon their position along the x-direction. Since we are in the rotating frame of reference at ω_0 the spins in the centre appear stationary whilst the spins on either side are precessing at different rates and in opposite senses. The spin echo that forms in the presence of this frequency encoding gradient represents a set of spatial (k_x) frequencies. This echo is the Fourier transform of the 1D projection. In our 2D *k*-space this single "line" of echo data will go through the centre. This is often known as the central slice theorem.

Frequency Encoding Gradient Amplitude

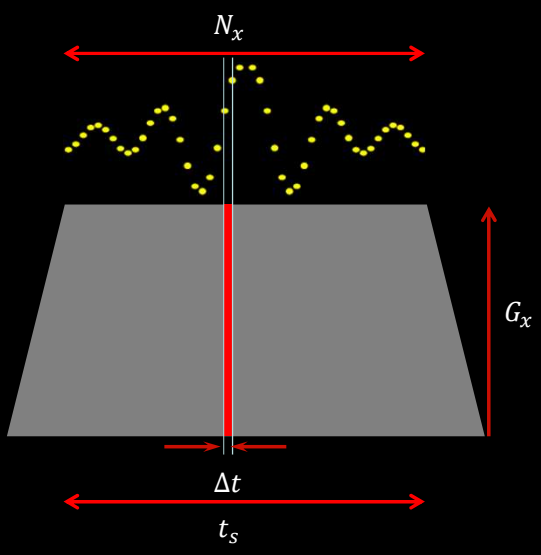

$$\Delta k_x = \gamma G_x \Delta t$$

$$FOV_x = \frac{1}{\Delta k_x}$$

$$t_s = N_x \Delta t$$

$$\Delta k_x = \gamma G_x \frac{t_s}{N_x}$$

$$Receiver\ bandwidth\ (RBW) = \frac{1}{\Delta t} = \frac{N_x}{t_s}$$

$$G_x = \frac{RBW}{\gamma\ FOV_x}$$

A typical receiver bandwidth is ±16kHz so RBW = 32kHz. If we acquire N_x= 256 samples then Δt= 0.03125ms and the total data acquisition time t_s= 8ms. For a 24cm field-of-view (FOV) the frequency encoding gradient amplitude required is Gx = 3.13mT/m. Very small fields-of-view may be limited by the available maximum gradient amplitude, assuming you have the available SNR.

Phase Encoding (PE)

A phase encoding gradient is used to induce a phase shift across the field-of-view in the y-direction to create a pseudo-spatial frequency (k_y)

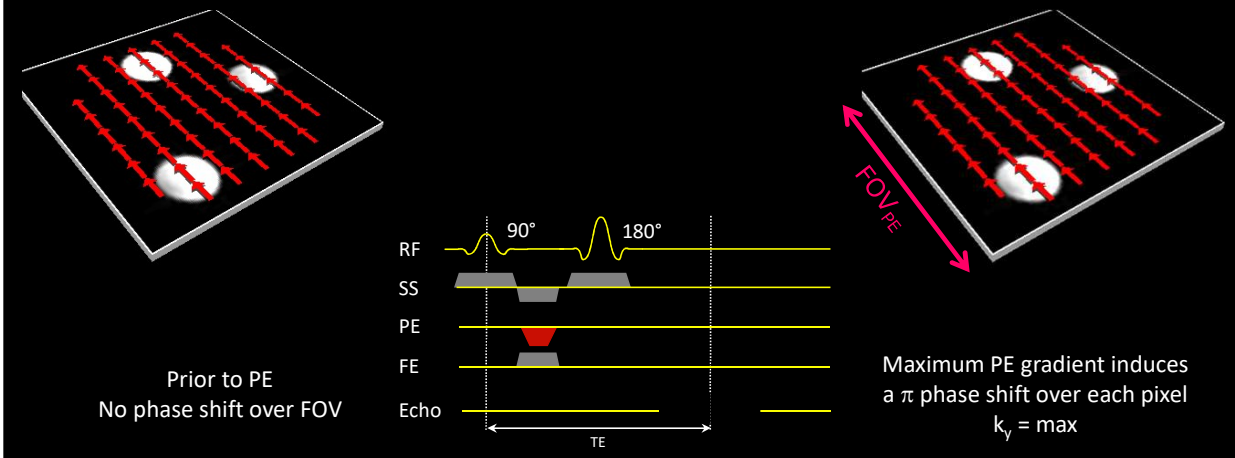

In order to encode other "lines" of *k*-space we induce "pseudo-frequencies" in the phase encoding or y-direction. The phase encoding (PE) gradient is applied prior to the frequency encoding gradient and introduces a phase "twist" into the spins along the y-direction. During imaging the spin echo pulse sequence is repeated k_y times with the phase encoding gradient being stepped through a number of values, from maximum negative to maximum positive. In this example the amplitude and duration of the PE gradient, i.e. the area, is such that a π phase shift is induced over each pixel. This is the maximum phase encoding step, i.e. k_y=max

Maximum Phase Encoding

The maximum PE gradient induces a π phase shift over each pixel

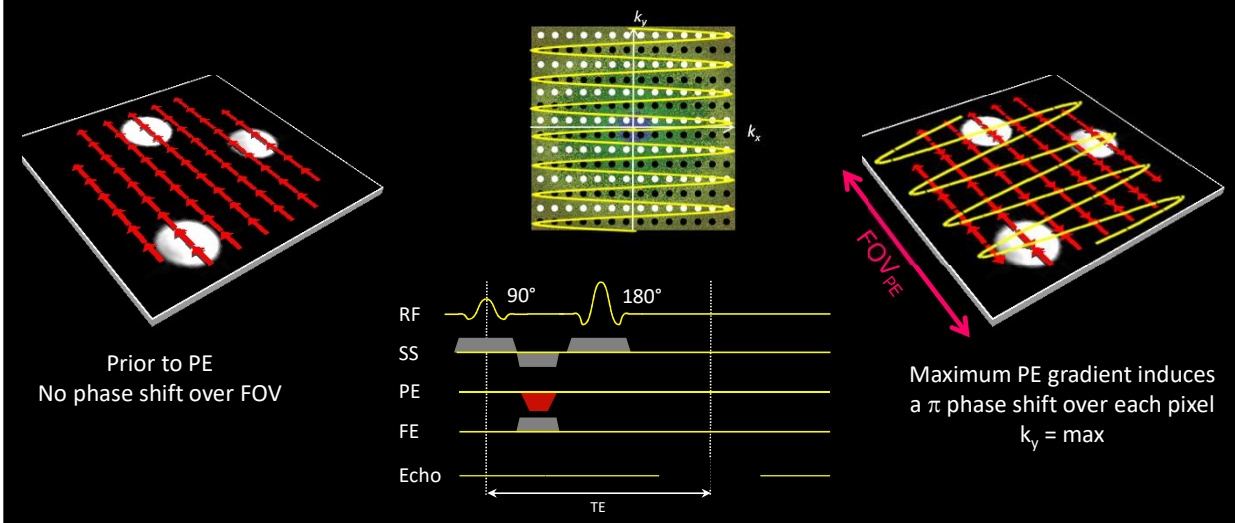

We can see that this maximum negative PE gradient has caused a π phase shift to be induced over each pixel. This represents the highest possible spatial frequency and hence the spatial resolution of the image in the y-direction.

Maximum Phase & Frequency Encoding

The phase encoded spins are then frequency encoded
(k_y = max)

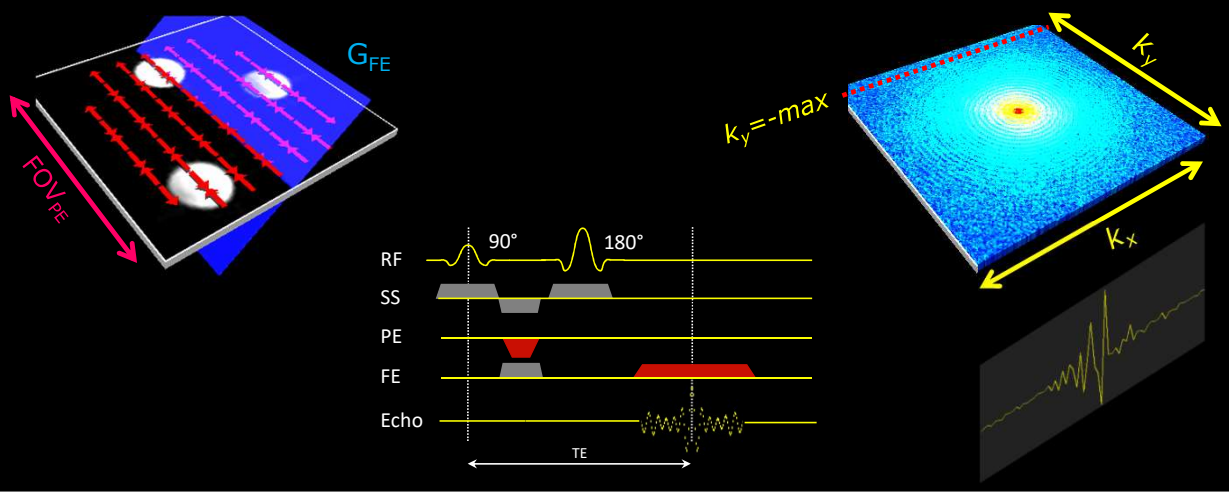

The y-direction phase shift induced by the PE gradient is retained during the formation of the echo in the presence of the FE gradient. In our 2D k-space this "line" of echo data will be assigned to the top of the raw data matrix , since it is acquired with maximum phase encoding, i.e. k_y=-max.

Minimum Phase Encoding

The minimum PE gradient induces a 2π phase shift over the FOV (k_y = min)

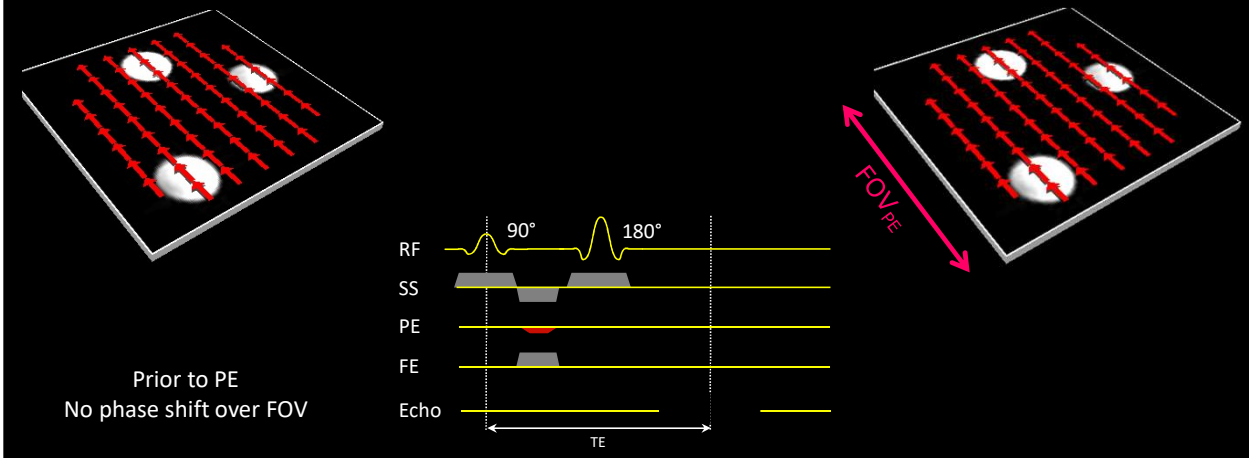

The phase encoding gradient is stepped k_y times equally, from the maximum negative value to the maximum positive value. In this example we consider the minimum negative value. We can see that this maximum negative PE gradient has caused a 2π phase shift to be induced over the entire field-of-view of the image in the y-direction. This represents the lowest possible spatial frequency. We do not actually acquire a line of data with zero amplitude PE gradient. If the y-resolution is 256 then we acquire ±128 equally spaced steps.

Minimum Phase & Frequency Encoding

The minimum PE gradient induces a 2π phase shift over the FOV
(k_y = min)

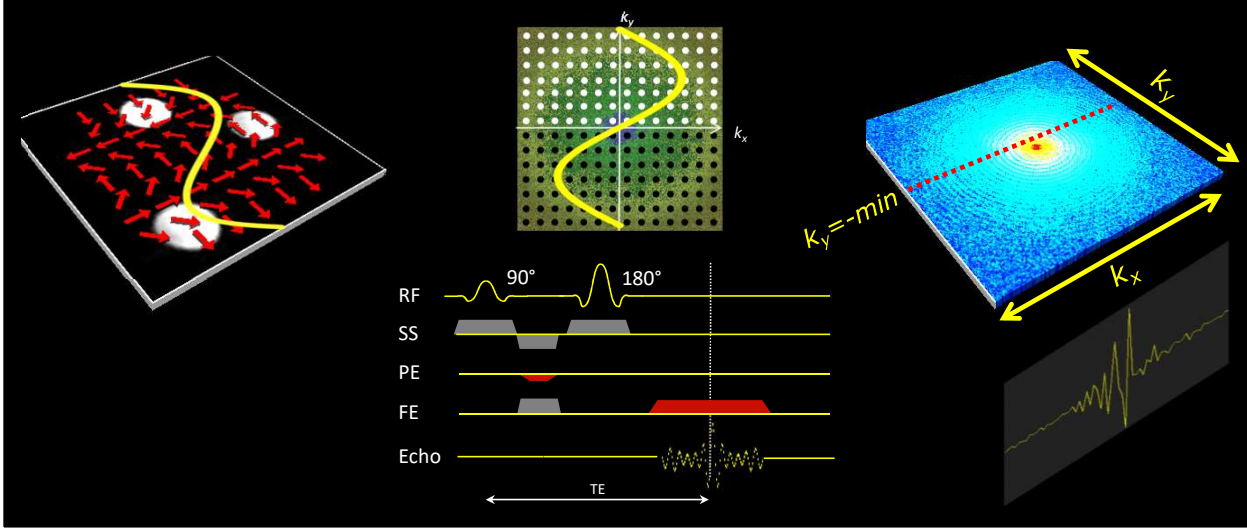

We can see that this minimum negative PE gradient has caused a 2π phase shift to be induced over each pixel. Following frequency encoding in our 2D k-space this "line" of echo data will be assigned nearest the centre of the raw data matrix , since it is acquired with minimum phase encoding, i.e. k_y=-min.

Phase Encode Gradient Area

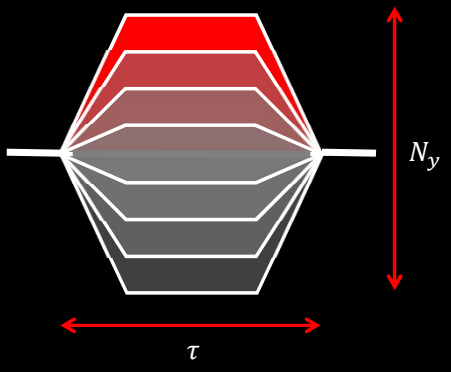

$$k_{y,max} = \gamma \int_0^{\tau} G_{y,max}\, dt$$

$$k_{y,max} = \frac{1}{2}(N_y - 1)\Delta k_y$$

$$FOV_y = \frac{1}{\Delta k_y}$$

$$A_{y,max} = \frac{(N_y - 1)}{\gamma\, FOV_y}$$

The phase encode gradient needs to be stepped through N_y steps. For each phase encoding the data is subsequently frequency encoded and the data placed in the corresponding part of k-space prior to 2D Fourier transformation

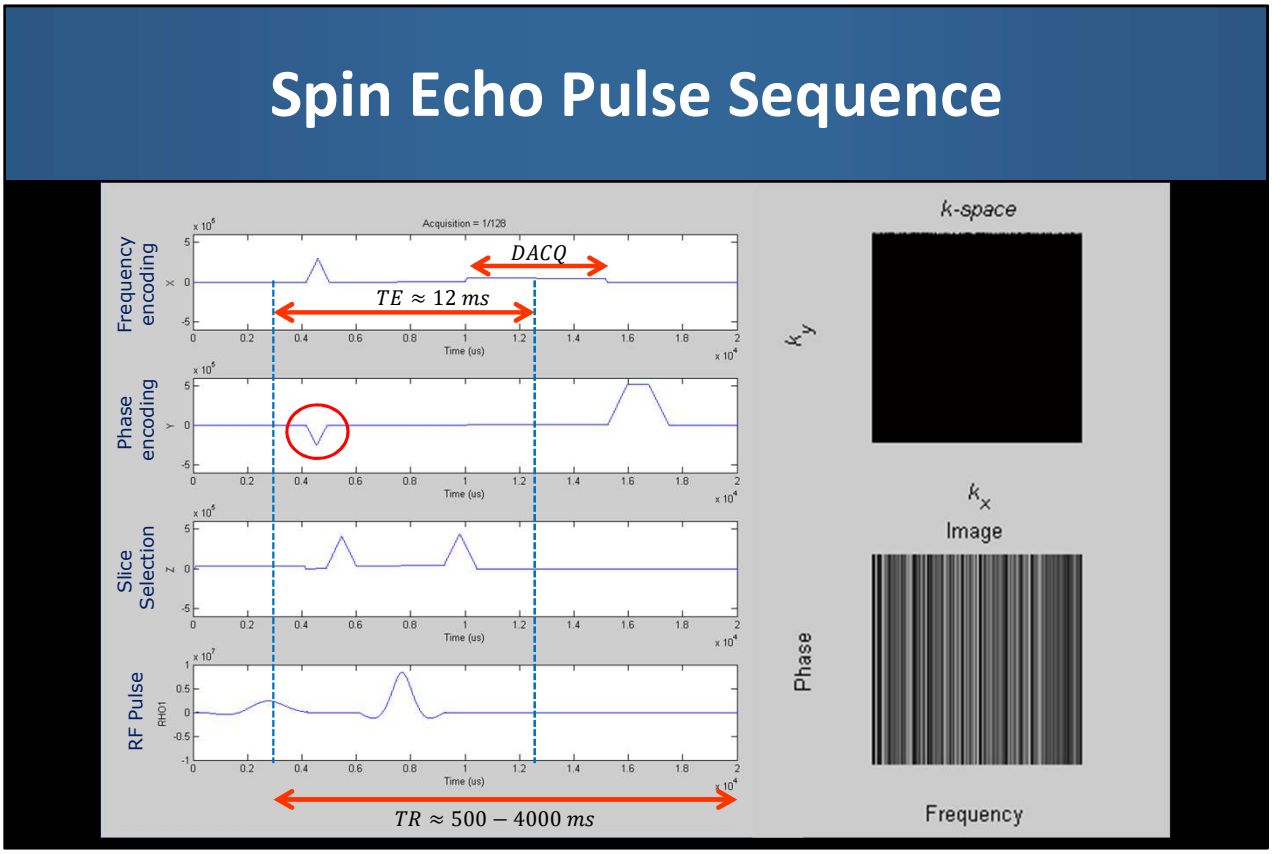

This movie shows a spin echo sequence being repeated 128 times. Note that all the gradients are the same for each repetition except for the phase encoding gradient (red circle) that is stepped ±64 times from maximum negative through to maximum positive. Each echo is placed in the appropriate position in *k*-space and in this example I have performed a Fourier transform of the partially filled k-space to show the developing appearance of the image. In standard MRI the image is not reconstructed until all of *k*-space is filled. This pulse sequence shows the first 20ms of a spin echo sequence. The actual TR, to allow for T_1 recovery and hence create a T1-weighted image, is 500ms.Therefore the actual acquisition time for this image is 500ms*128 = 64s.

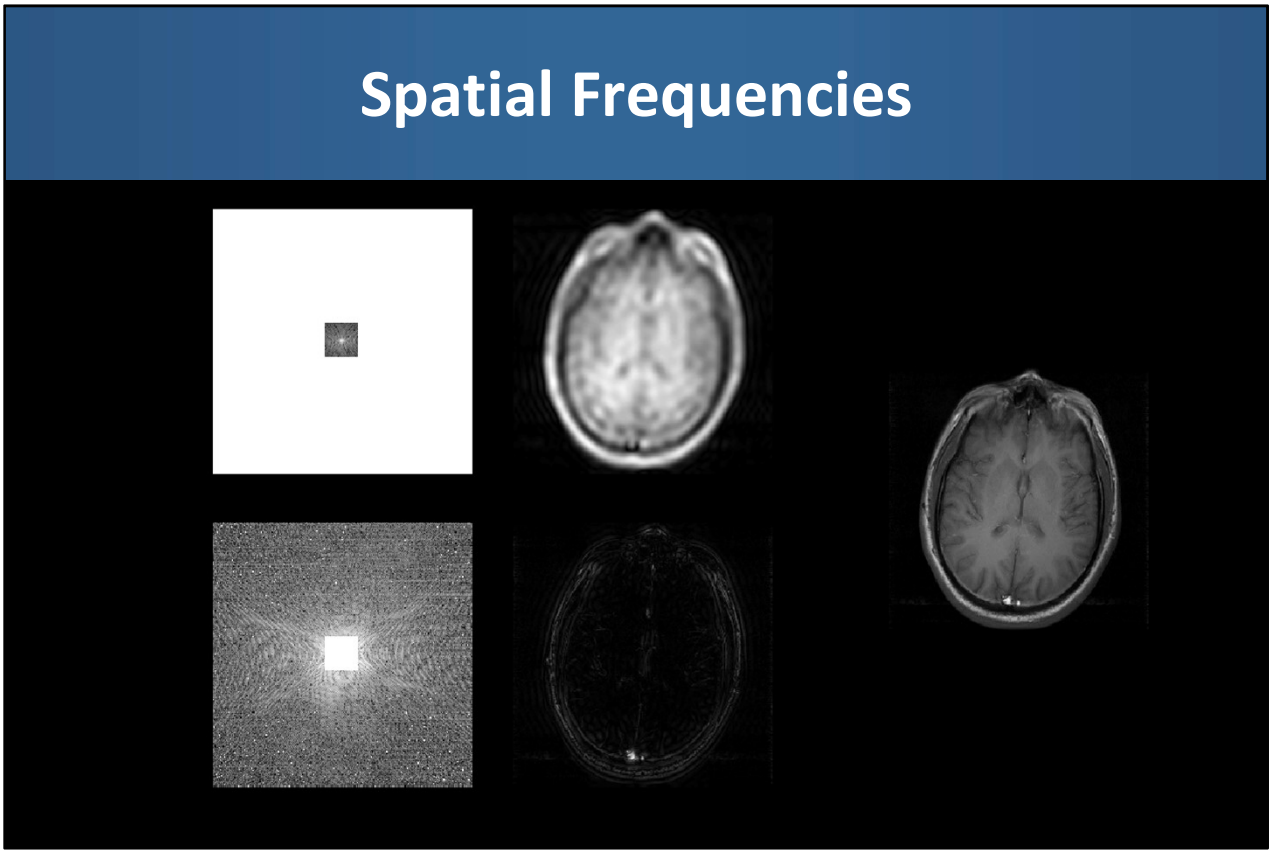

k-space is the spatial frequency representation of the image. If we just reconstruct data from the centre of *k*-space then you get a high SNR image but with very poor spatial resolution. Conversely reconstructing the periphery of *k*-space results in an image showing the high spatial frequencies, i.e. edges in the image but no bulk contrast. The full *k*-space gives a reasonable image.

Multi-slice Imaging

$$Scan\ Time = TR \cdot \mathrm{N_y} \cdot \mathrm{NSA}$$

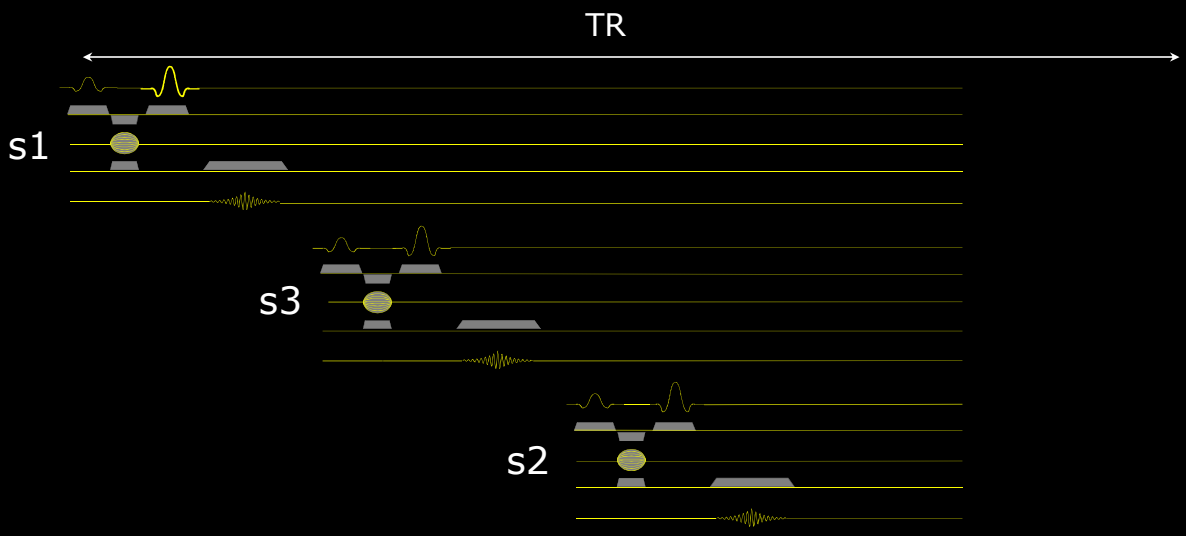

Since TR is usually much longer than TR there is substantial dead-time in a pulse sequence whilst we wait for T_1 recovery. The minimum acquisition time is given by $\mathrm{TR} \cdot \mathrm{N_y} \cdot \mathrm{NSA}$, where NSA is the number of signal averages. Signal averaging is a commonly used method to improve the SNR in an image, since the signal is coherent and the noise should be incoherent the SNR will improve proportional to $\sqrt{NSA.}$ During the recovery period other slices can be excited and acquired, simply by repeating the acquisition and changing the excitation frequency. Slices are usually acquired in odd then even order to avoid too much “cross-talk” between adjacent slices due to imperfections in the slice profile.

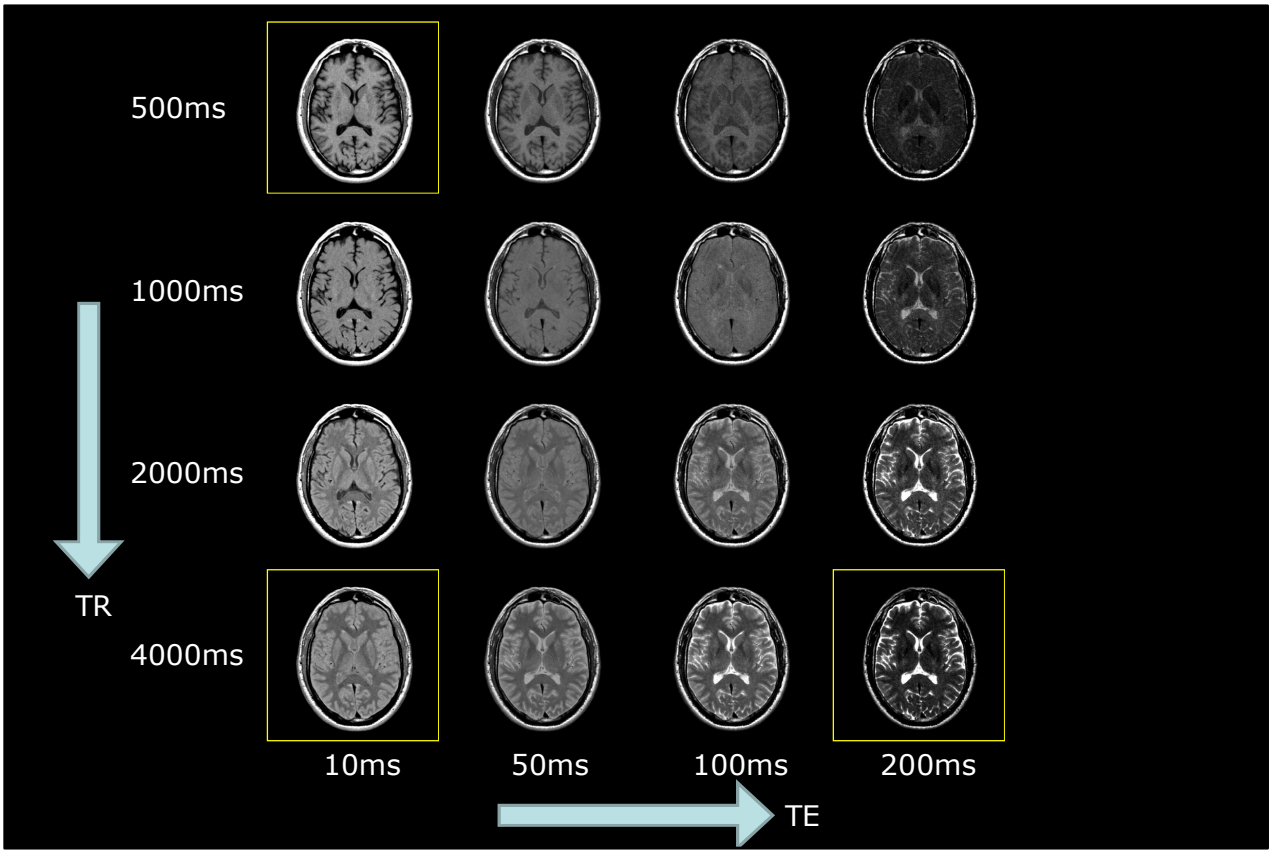

A refresher on the effects of TE and TR in a spin echo sequence.

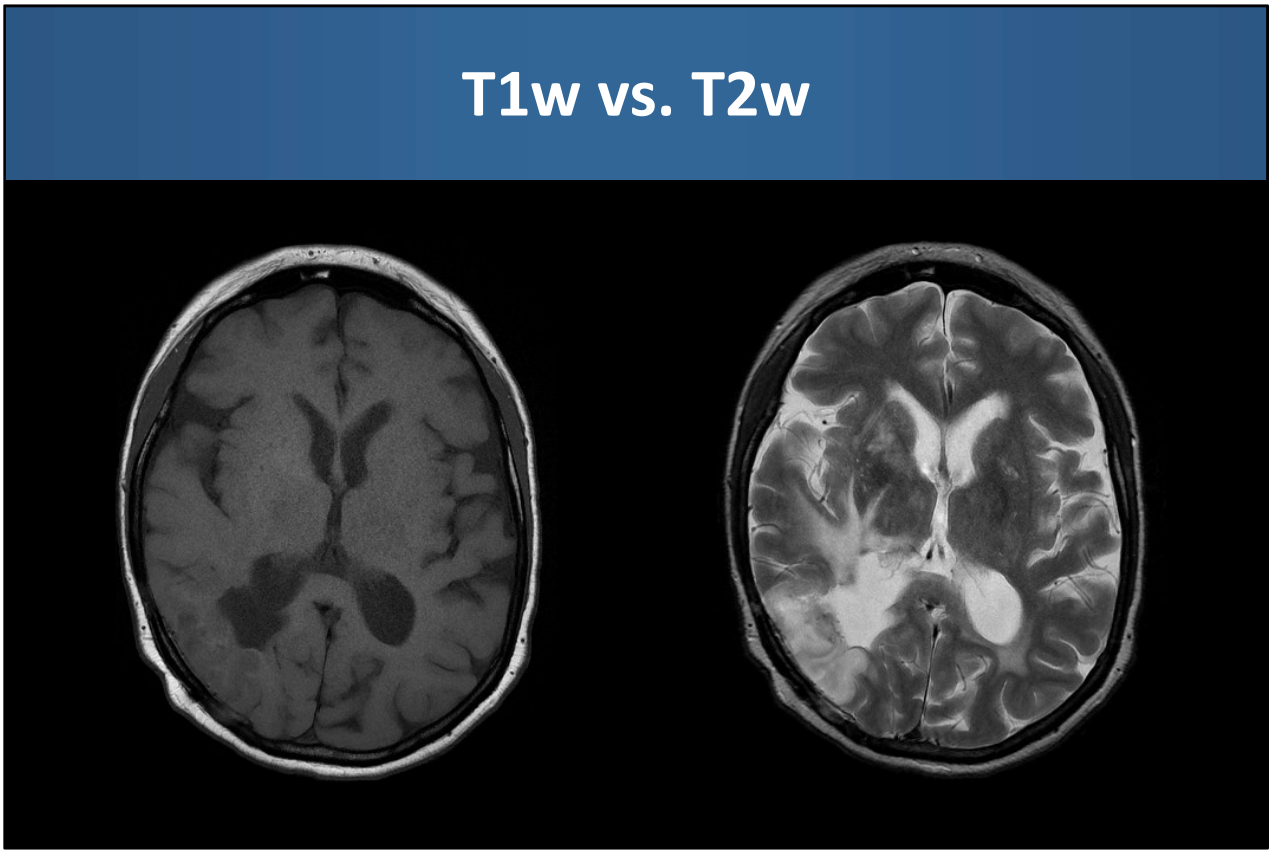

A comparison of a T1w and T2w images (matched locations) in a patient with a brain tumour. The T1w image doesn’t demonstrate much image contrast although the asymmetry of the left and right sides of the brain can be clearly seen. The tumour is seen as a hyperintense signal on the T2w image.

Inversion Recovery Spin Echo

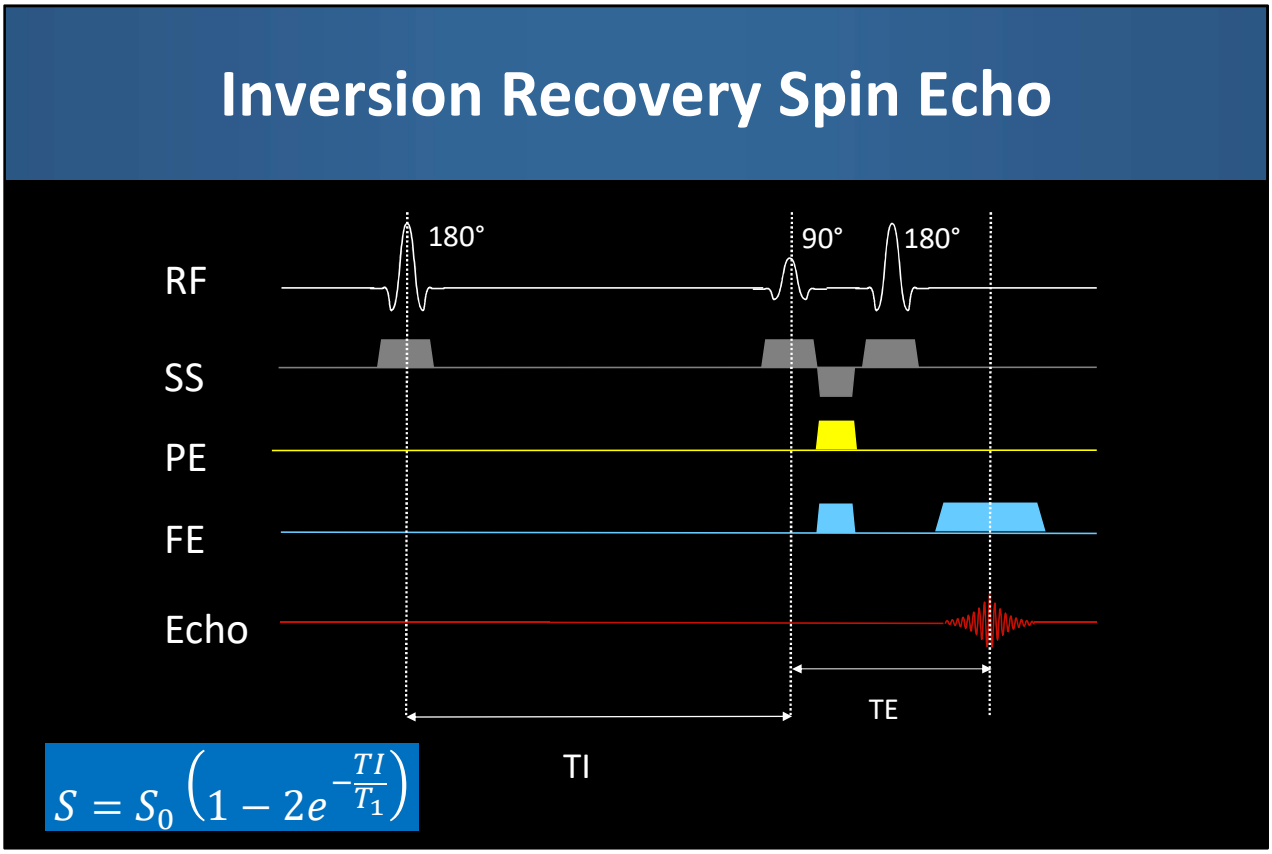

An alternative image contrast can be achieved by preceding the spin echo acquisition with an 180° pulse that inverts the z-magnetisation. We then wait for a time period known as the inversion time (TI) before playing out the spin echo, or more usually the fast spin echo readout.

Inversion Recovery - Real

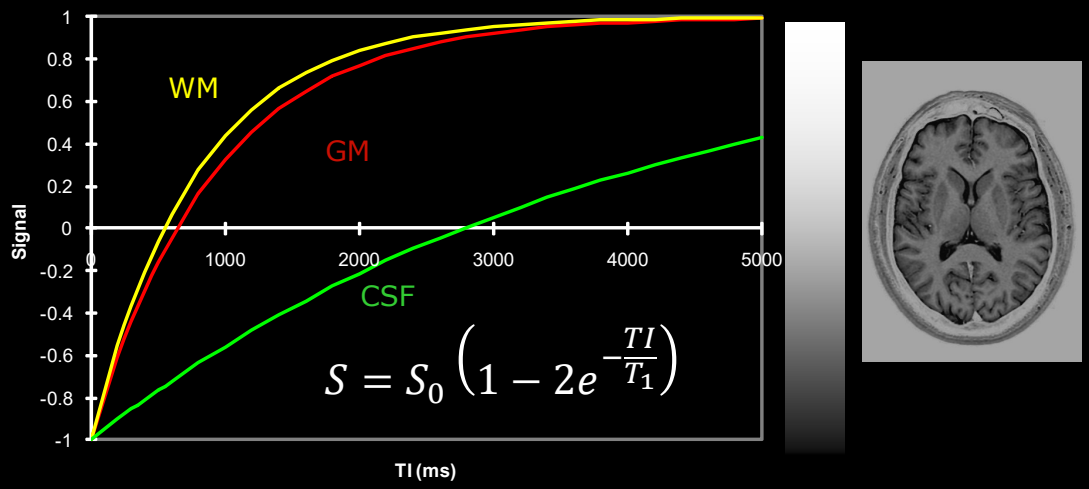

The use of an inversion pulse effectively doubles the dynamic range of the data. In this image the full signed data is achieved using a TI of 160ms. Note that zero signal (surrounding air) is represented as mid-gray.

Inversion Recovery - Magnitude

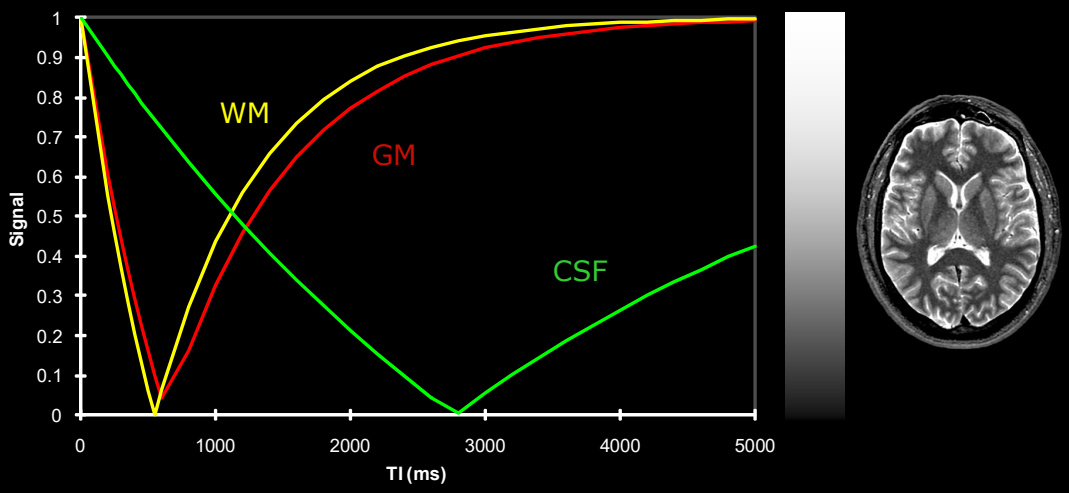

Same data as the previous slide using a TI of 160ms. However the signal magnitude has been reconstructed. Note that zero signal (surrounding air) is represented as black.

FLuid Attenuated Inversion Recovery (FLAIR) (TI≈2700ms)

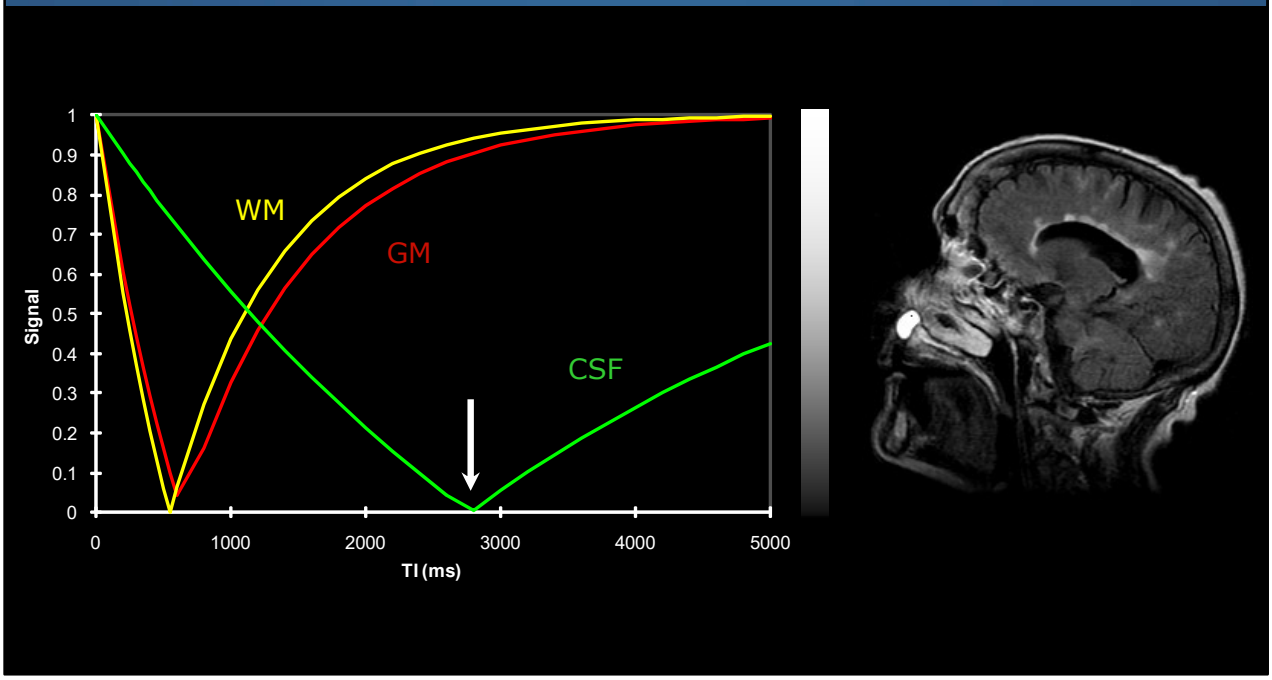

This is an IR sequence with a TI of approximately 2700ms. In this magnitude reconstruction the signal from CSF is nulled, providing the indication for the name of the sequence as FLuid Attenuated Inversion Recovery (FLAIR). This is a T2w image in which you can see signal hyperintensity indicative of multiple sclerosis around the ventricle. Normally these changes would be difficult to see on a conventional T2w images since there would be very high signal from the CSF in the ventricle. By knowing the T_1 of the CSF it is possible to effectively null the signal from CSF improving visualisation

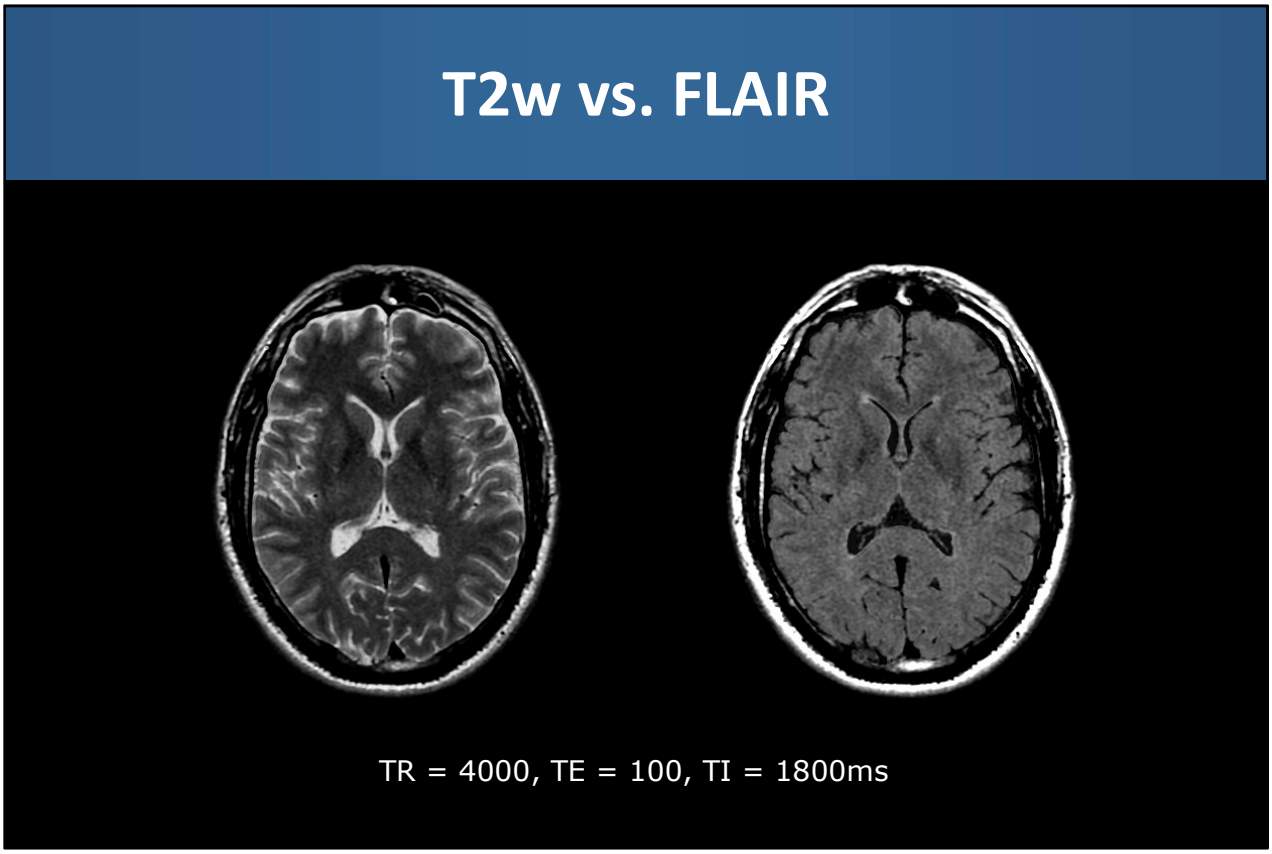

T2w image with and without IR pulse that effectively nulls the CSF in the image on the right.

Gradient Echo

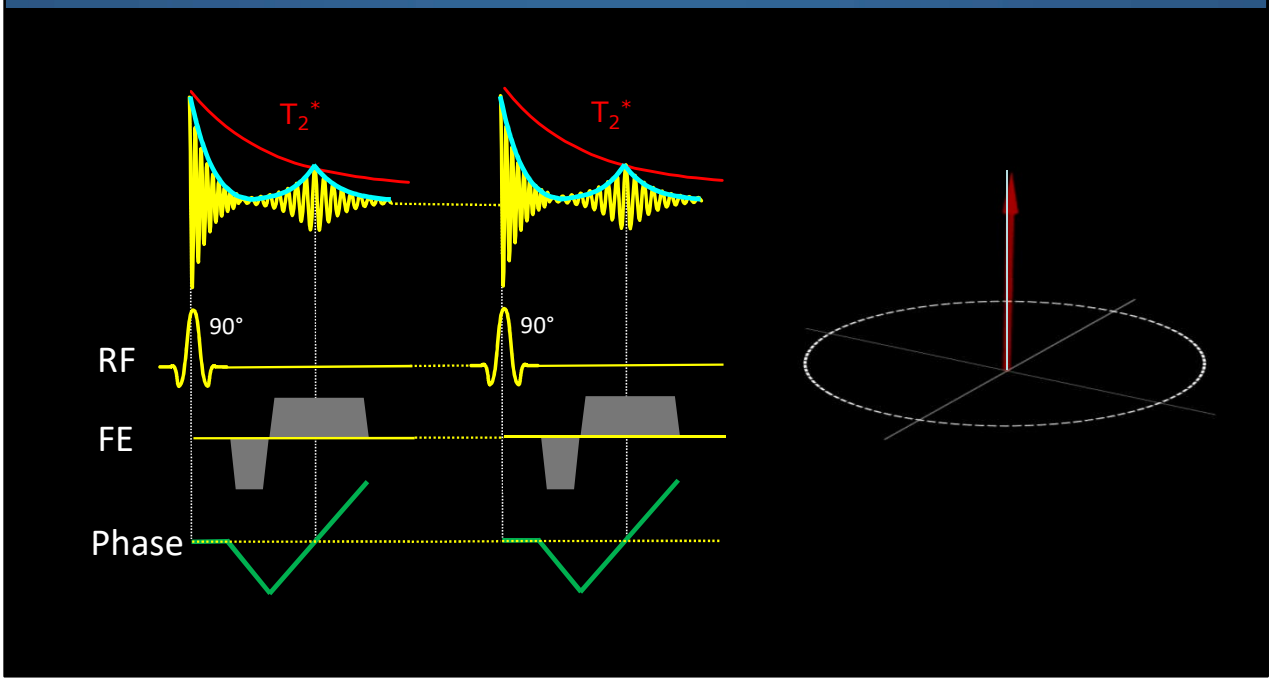

An alternative pulse sequence to spin echo is the gradient echo. This sequence does not use a 180° refocusing pulse but forcibly creates an echo through the use of the frequency encoding gradient. A negative gradient is applied that forcibly dephases the signal (note that this dephasing is in addition to the T_2^* dephasing already discussed). The polarity is then reversed and the spins rephase forming an echo. Since there is no 180° refocusing pulse the echo forms under the T_2^* envelope, rather than a T_2 envelope. A gradient echo sequence has the advantage of increasing the sensitivity of the acquisition to tissue susceptibility differences that may be enhanced in some pathologies, e.g. iron deposition. The absence of a 180° refocusing pulse means that the TE can also be made shorter.

Partial Flip Angle Excitation

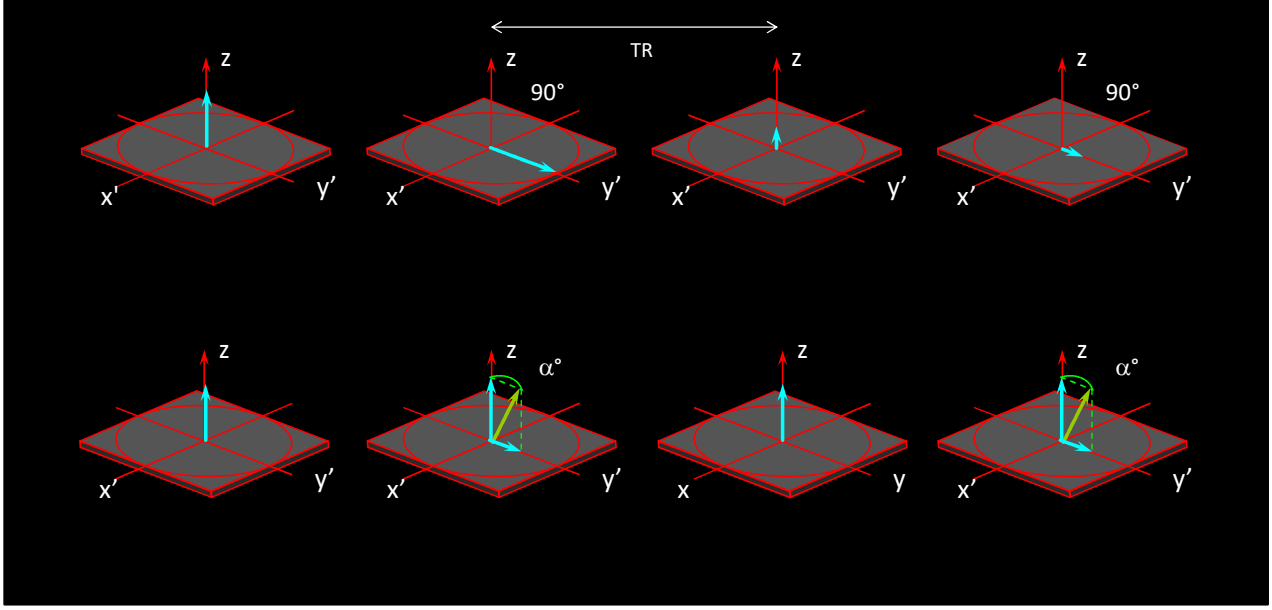

Gradient echo imaging is also often used with a short TR to reduce acquisition time. This necessitates the use of a reduced excitation flip angle to avoid signal saturation. In the top row if we use a 90° excitation with a short TR then there will be limited T1 recovery during the short TR and the available transverse magnetisation will be extremely small on subsequent excitations. Alternately on the bottom row if we tip the magnetisation by α° then as well as a component of magnetisation in the transverse plane a substantial component will remain in the longitudinal direction.

Gradient Echo Signal Behaviour

$$S \propto M_0 sin(\alpha) \left(\frac{1 - e^{-\frac{TR}{T_1}}}{1 - cos(\alpha) \cdot e^{-\frac{TR}{T_1}}} \right) e^{-\frac{TE}{T_2^*}}$$

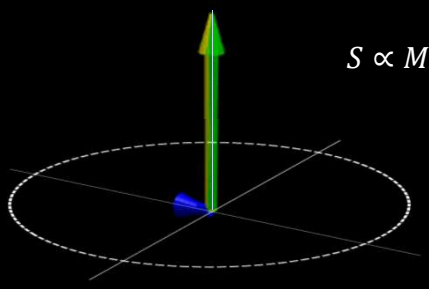

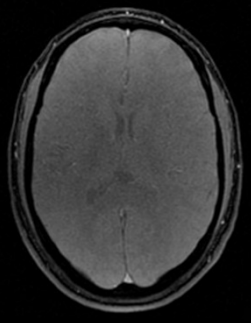

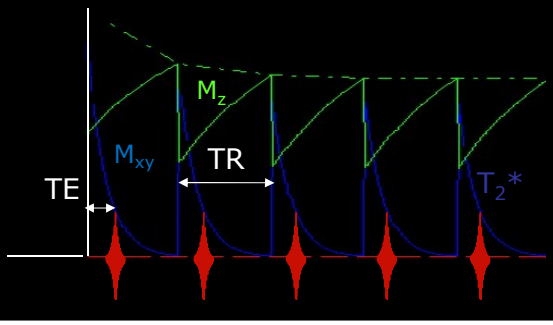

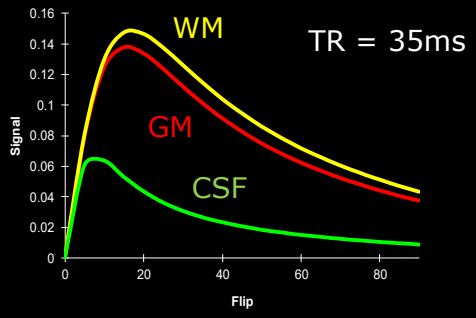

Here we can see the effect of a reduced flip angle excitation. Note that the signal behaviour is now a function of TE, TR and flip angle as shown in the slightly more complicated signal equation. The images how the effect of increasing the flip angle from 10°-90°. Note the changing contrast and decreasing SNR as the flip angle is increased.

Gradient Echo vs. Spin Echo

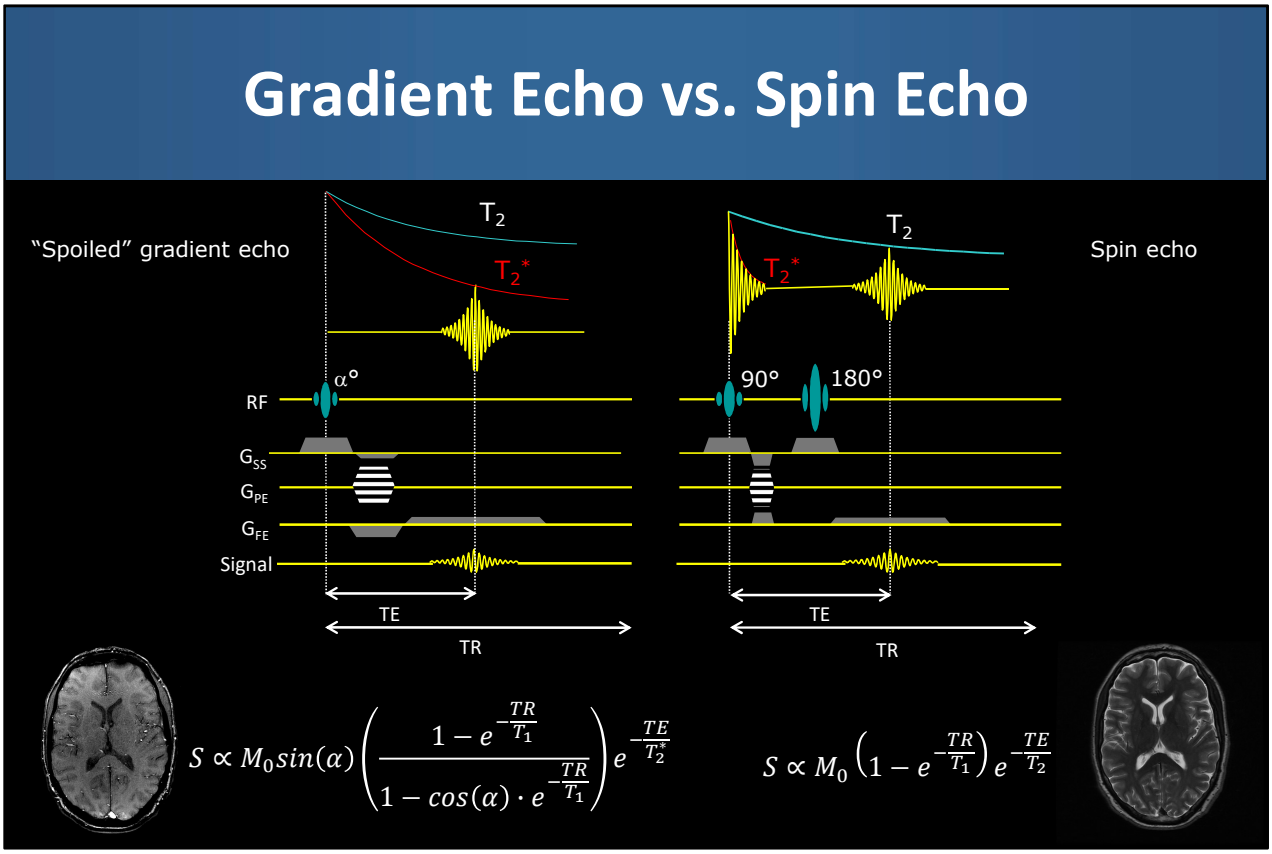

This slide show a comparison of the signals obtained from a gradient echo and spin echo pulse sequence. Since a gradient echo sequence does not contain a 180° refocusing pulse the signal is, depending upon the TE, T2*-weighted, rather than T2-weighted as in a spin echo sequence. Furthermore the contrast in a gradient echo sequence is also a function of the excitation flip angle α°. There are various types of gradient echo sequence, this diagram shows a "spoiled" gradient echo which primarily has a T1-weighted appearance since TE is usually very short so that the T2*-weighting is mimimised.

Basic Pulse Sequences

Spin echo

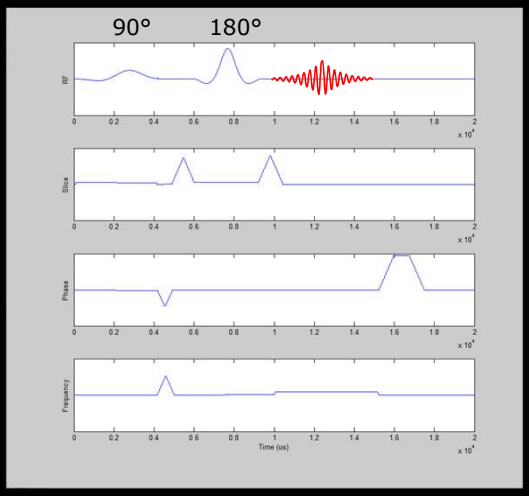

Gradient echo

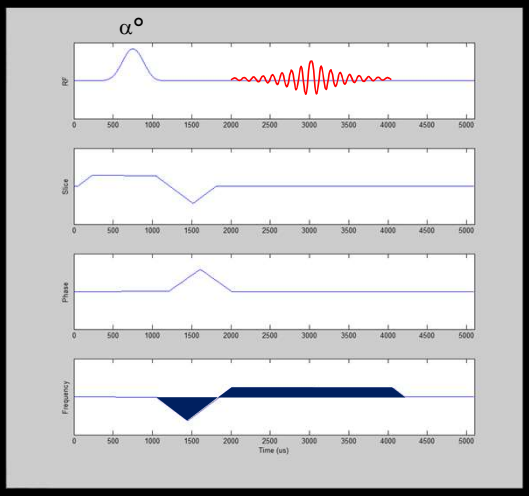

There are a wide range of pulse sequence available in MRI. This slide shows the two most basic sequences; the spin echo which we have already discussed and a gradient echo. A gradient echo does not have a 180° refocusing pulse and the echo is formed by a gradient reversal on the frequency encoding axis (shown in blue). In addition a $\alpha° < 90°$ excitation pulse is used so that only a component of the transverse magnetisation is tipped into the transverse plane. This allows gradient echo images to be acquired with a much shorter TE and TR than spin echo images, however the contrast can be more complex.

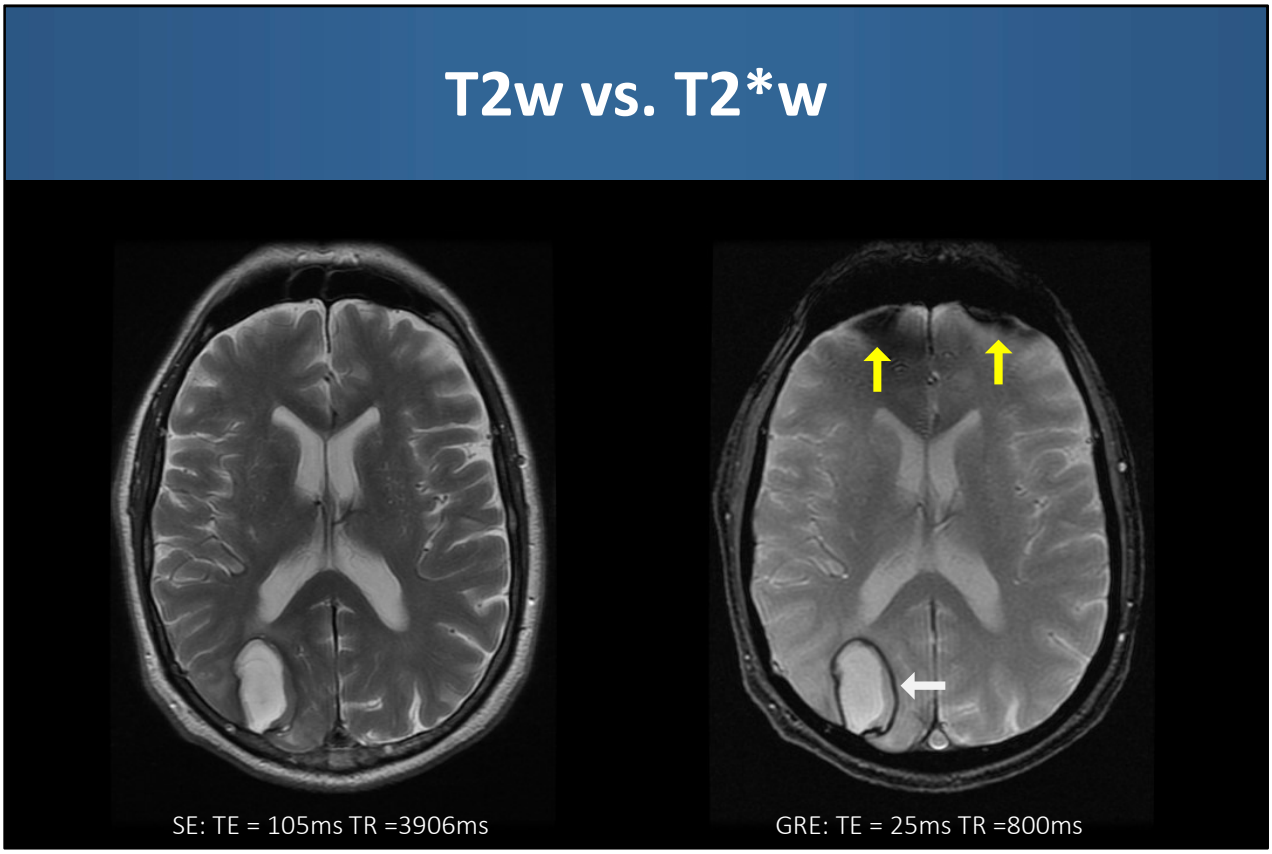

A T2w spin echo acquisition together with a T2*w gradient echo acquisition of a patient with a resolving haematoma. Note the intense black outline of the haematoma on the gradient echo image (white arrow). This is due to the susceptibility caused by the iron in the blood breakdown products. The refocusing pulse in the spin echo acquisition reduces this effect. Note also the signal loss at the top of the gradient echo image (yellow arrow). This is due to differences in the magnetic susceptibility of tissue and air in the prefrontal sinuses just below this slice. This artefacts is not seen in the spin echo image.

Signal from Fat

- Nuclear shielding gives rise to chemical shifts of 0.9 to 5.3ppm
- Most abundant resonance is methylene (CH_2) at 3.4ppm below water
- Triglycerides are relatively large molecules so they have a short T_1 of around 270ms at 1.5T
  - Hyperintense on T1w

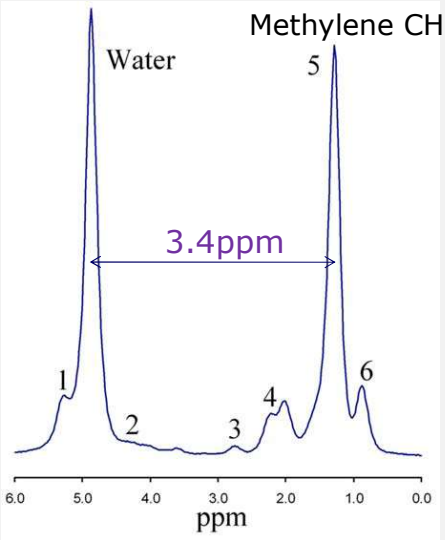

Essentially the protons in fat precess 3.4ppm slower than water due to magnetic shielding of the orbital electrons. So at 1.5T this results in a frequency difference of 64MHz * 3.4ppm = 220Hz

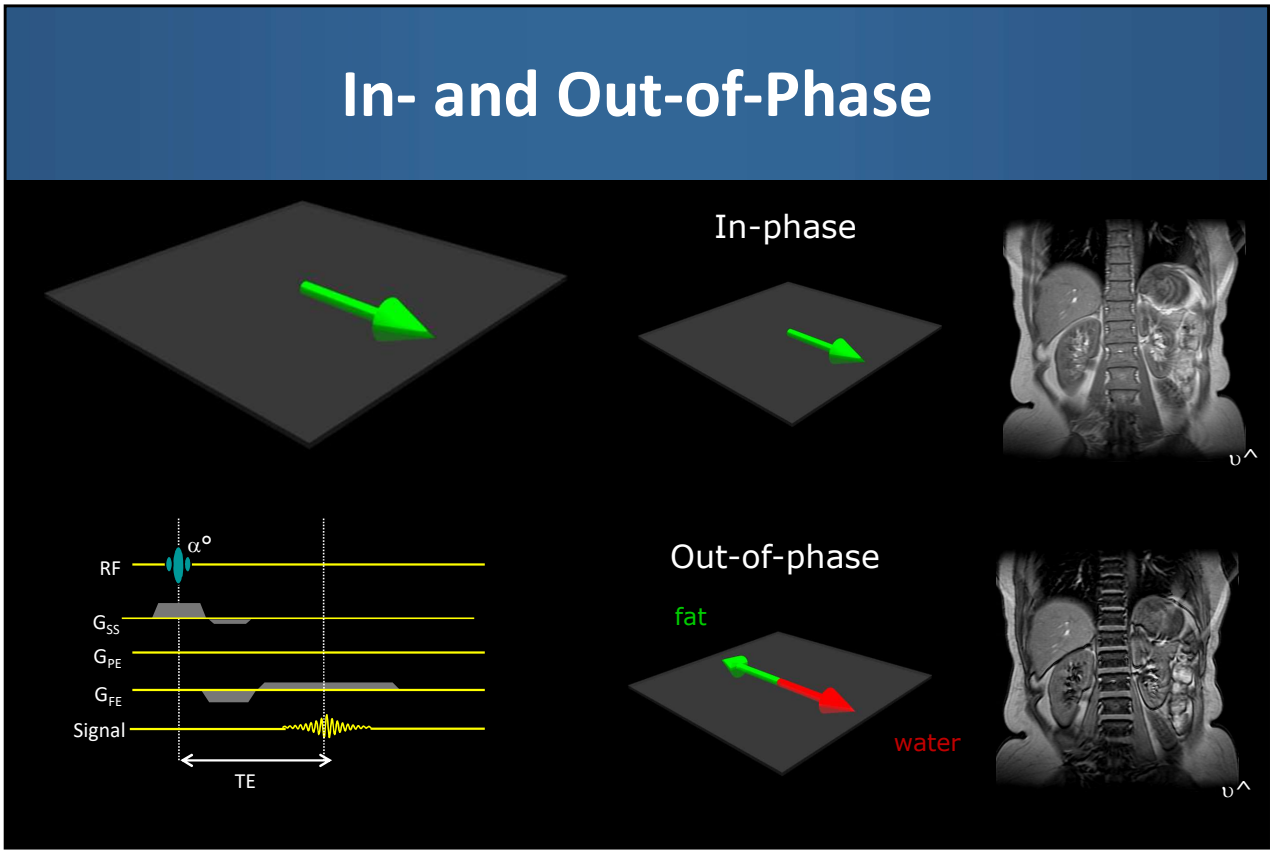

This frequency difference also results in water and fat periodically coming in and out of phase in a gradient echo acquisition. Depending upon the choice of TE the spins can be either in-phase or out-of-phase. At an out-of-phase TE any voxels containing equal amounts of water and fat will result in cancelling of the signal. This is often seen as a black outline at water/fat interfaces, e.g. around abdominal organs. The 180° refocusing pulse in a spin echo sequence means that water and fat are always in phase at the centre of the echo and this phenomenon is not seen.

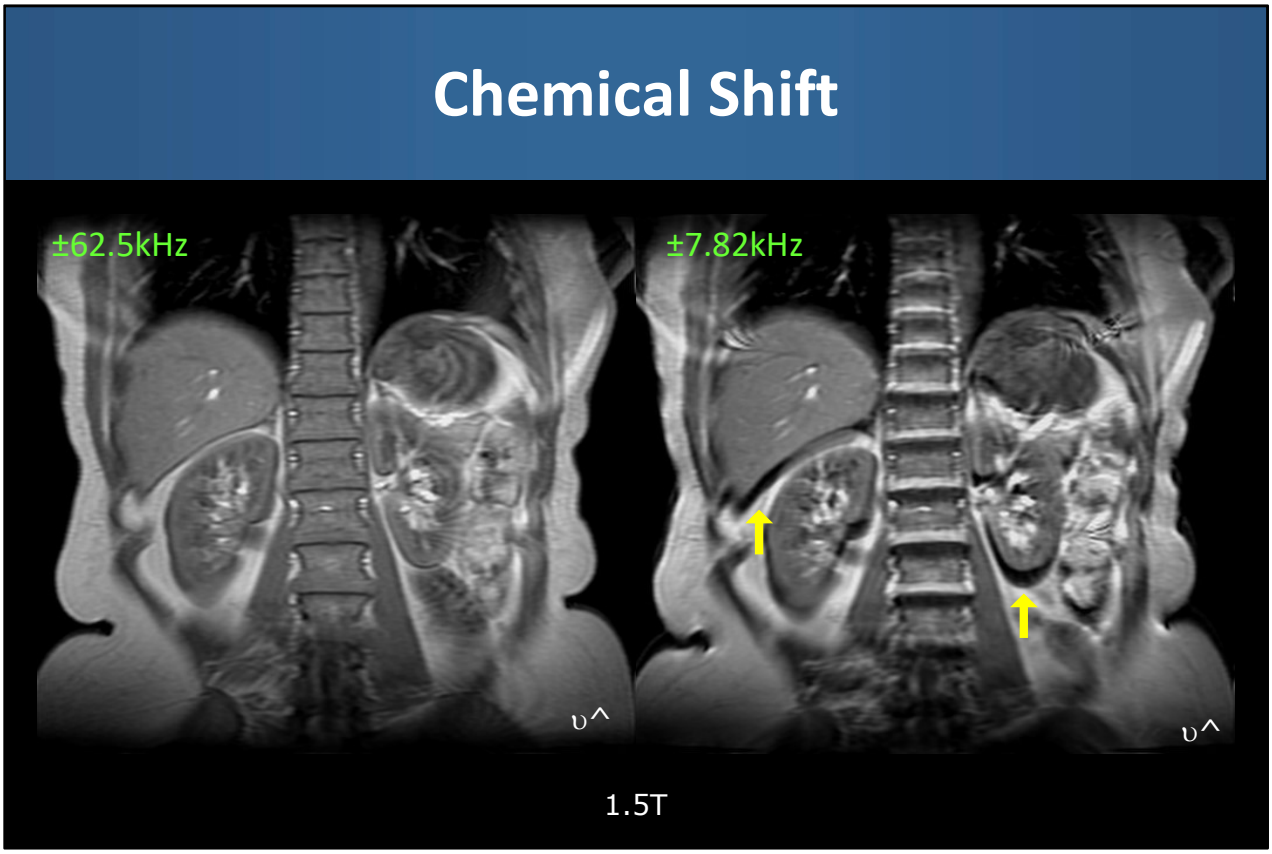

The precessional frequency difference does give rise to a chemical shift misregistration artefact in the frequency encoding direction of all spin warp acquisitions (yellow arrows). The chemical shift in pixels is proportional to the frequency encoding gradient amplitude and hence is dependent upon the receiver bandwidth and the number of points sampled in the frequency encoding direction. Knowledge of the field-of-view allows you to calculate the chemical shift in mm.

CHEmical Shift Selective (CHESS) Fat Saturation

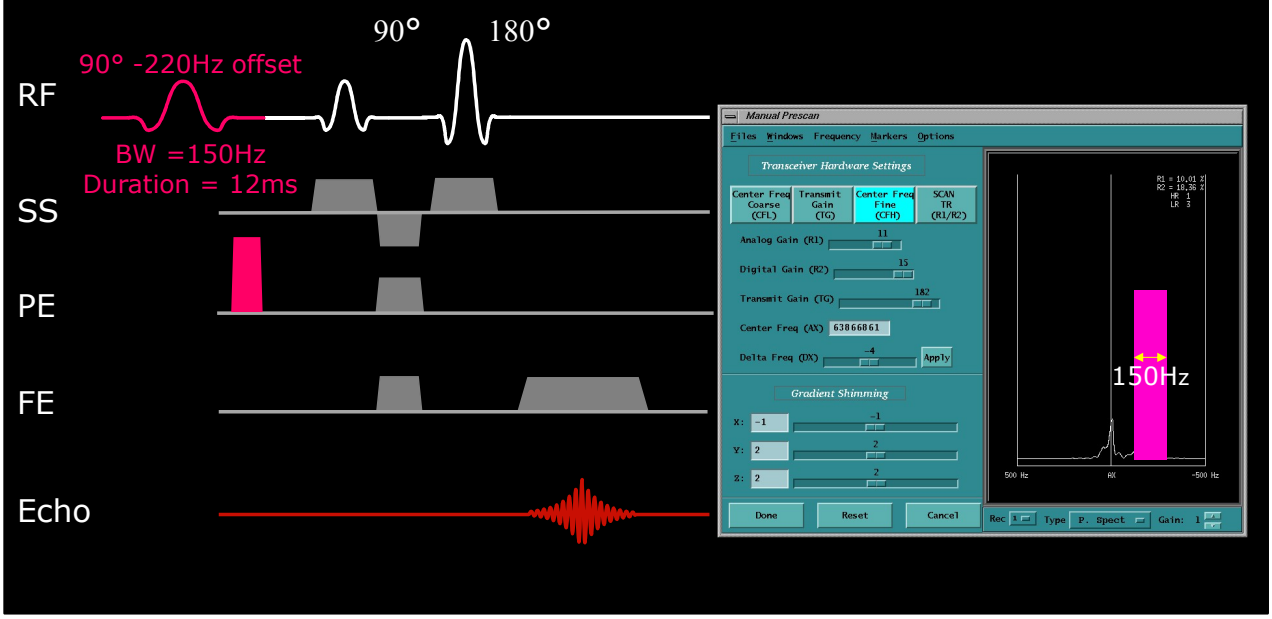

A common method to suppress the bright signal from fat, typically in T1w images is the use of a chemical shift selective fat saturation pulse. A relatively long duration pulse, i.e., having a narrow bandwidth is applied just prior to the imaging sequence. The frequency of the pulse is offset from the Larmor frequency by the desired chemical shift for the given field strength. This pulse will tip the fat magnetisation into the transverse plane where it is dephased by a spoiler gradient, effectively reducing the signal from fat. This method is dependent on a good B_0 field uniformity to ensure the fat signal is properly saturated.

CHESS Fat Saturation

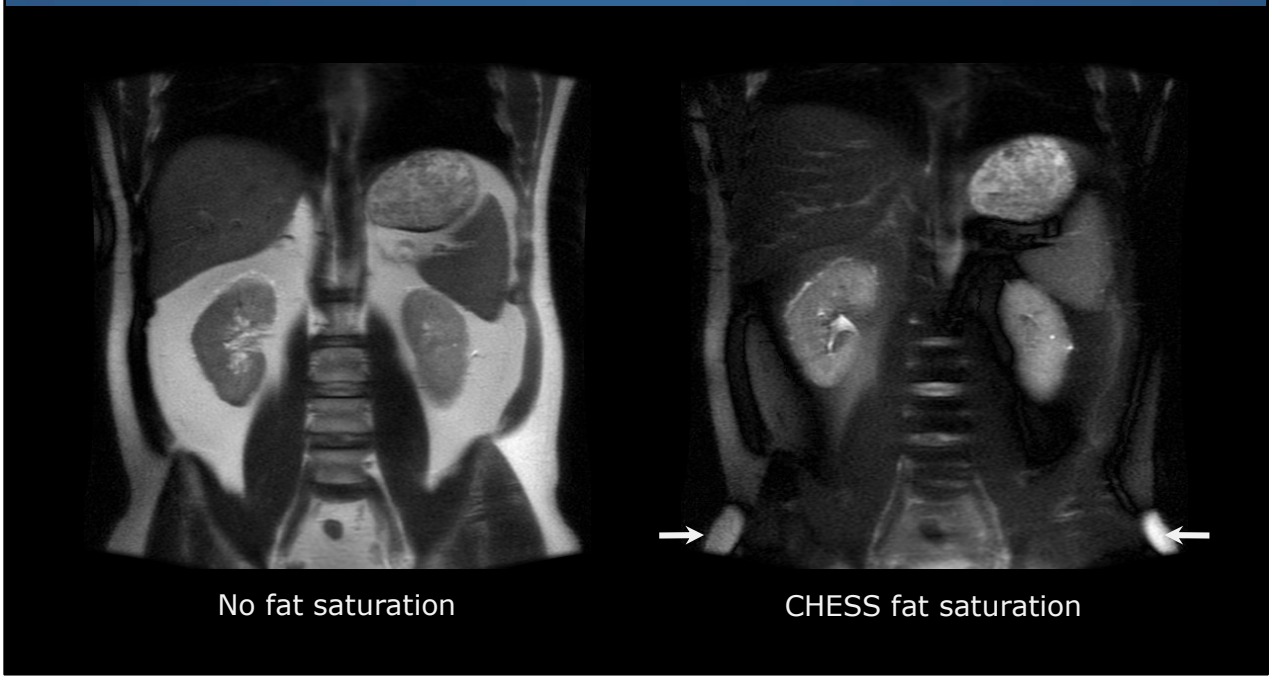

A coronal T1w acquisition through the abdomen with and without fat saturation. Note the saturation of the intrabdominal fat (signal hyperintense on the left image). Note the failure of the fat saturation in the extreme corners of the image (white arrows) where the B_0 field uniformity means the spins are outside the fat saturation pulse bandwidth.

Short τ (TI) Inversion Recovery (STIR) (TI≈190ms)

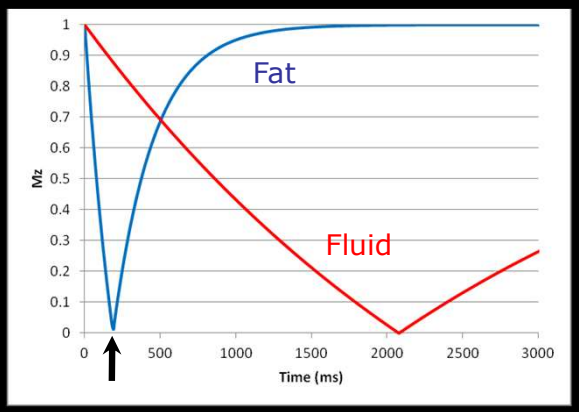

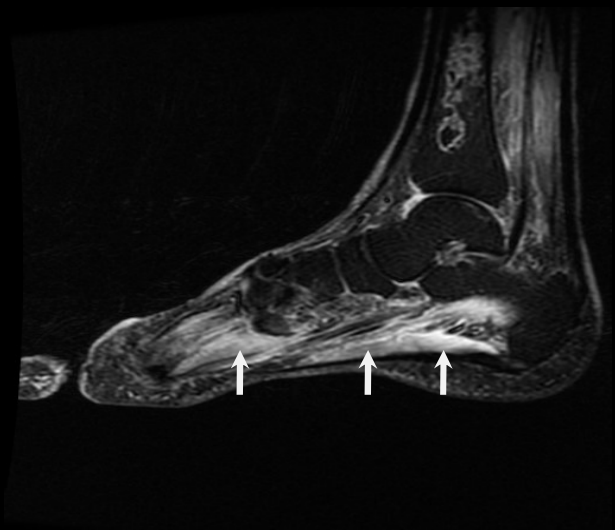

This is an IR sequence with a TI of approximately 190ms. In this magnitude reconstruction the signal from fat is nulled, providing the indication for the name of the sequence as Short τ (TI) Inversion Recovery (STIR). This method is sometimes preferred to chemical shift selective (CHESS) fat suppression as the anatomy of the ankle makes it sometimes very difficult to obtain a uniform fat suppression due to magnetic field nonuniformity. Note that due to the magnitude reconstruction, the signal from fluid (white arrow) is high. This sometimes leads people to erroneously call these images T2w, i.e., fluid is bright. However, this bright signal is entirely a consequence of the reconstruction method.

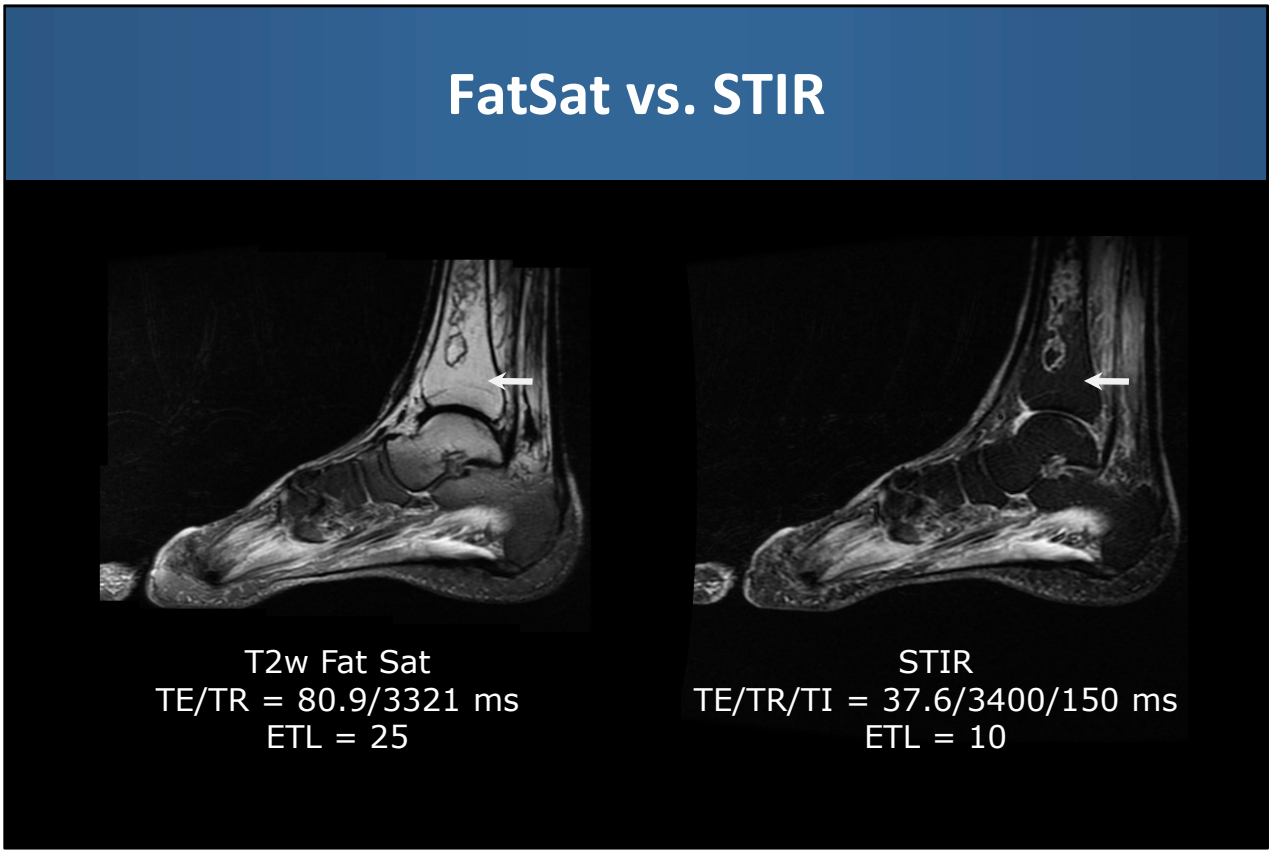

A comparison of CHESS and STIR in the ankle. Note the poor fat saturation uniformity in the bone marrow with the CHESS image compared to the STIR (white arrow).

Hardware Overview

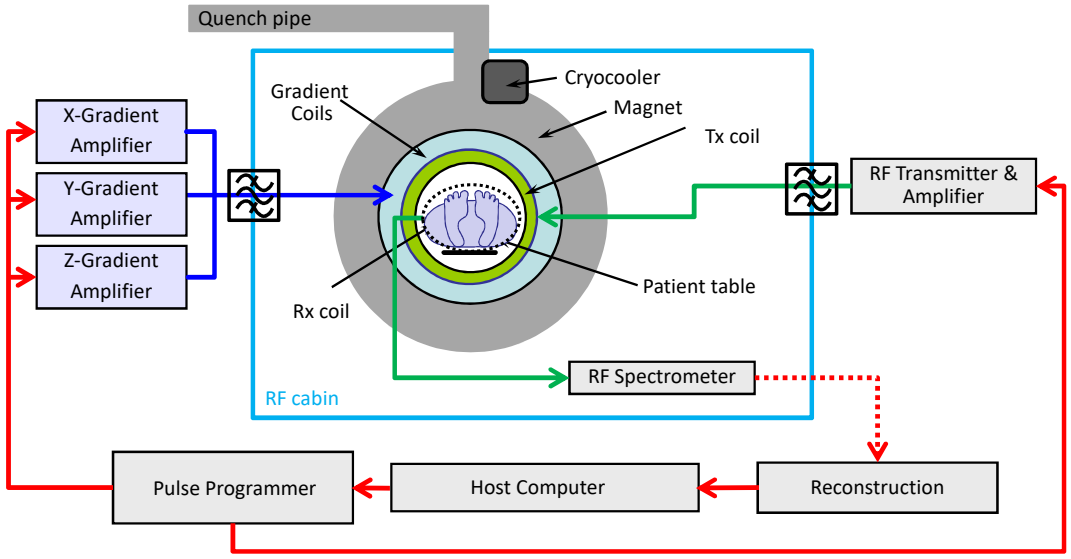

The diagram provides an overview of an entire MR system. The red lines represent digital signals, whilst the green lines represent the analogue RF transmit/receive signals and the blue lines the analogue gradient waveforms. The dotted red line is fibre-optic.

Types of Magnet

- Field strengths
  - Low field < 0.6T
  - Mid-field ~ 1.5T
  - High field ~ 3.0T
  - Ultrahigh field ≥ 7T
- Technologies
  - Permanent magnets
    - Neodymium Iron Boron
  - Iron-cored electromagnets
    - Copper
  - Superconducting magnets
    - Niobium Titanium (T_c = 10K)
    - Magnesium Diboride (T_c = 39K)

The 0.4T magnet uses permanent magnet pole pieces. The 0.6T electromagnet is an iron-cored electromagnet that weights over 100T. The 0.5T MgB_2 magnet is cryogen free using two Gifford-McMahon cryocoolers operating at 20K to mechanically keep the system operational. The 7.0T system uses Niobium Titanium windings at 4.2K

B_0 Dependency

Physical Parameter	**B_0 Dependence (approx.)**
Signal-to-noise ratio (SNR)	Linear: $SNR \propto B_0$
Frequency offset	Linear: $\Delta f \propto B_0$
Chemical shift in Hz (CS)	Linear: $CS \propto B_0$
Power deposition (SAR)	Quadratic: $SAR \propto B_0^2$
RF wavelength	Inverse: $\lambda \propto 1/B_0$
T_1 relaxation time	Increases: $T_1 \propto \alpha B_0^{\beta}$

A brief over view of the dependencies on static magnetic field strength

Superconducting Magnet

Generates strong, highly uniform and stable static magnetic field (B_0)

- 1.5T to 11.7T and above
- Steel cryostat containing approx. 2000L liquid helium at 4.2K (-270°C)
- Cryocooler minimises helium boil-off
- Actively shielded
- ΔB_0 (t) < 1ppm (40cm DSV)
- ΔB_0(x,y,z) < 0.01ppm/hour

- 60km of superconducting Niobium titanium (NbTi) filaments in a copper matrix
- I = 600A E = 15MJ

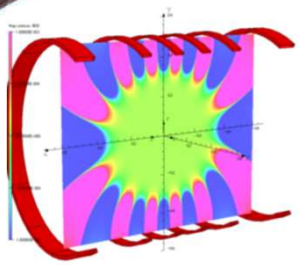

$\pm 1000 ppm$

This is a cross section through a typical 3T whole body MRI scanner. The system has to generate an extremely uniform and stable magnetic field. A 3T system typically has approximately 60km of superconducting NbTi filaments in a copper matrix. The windings are housed in a steel cryostat where they are immersed in a bath of liquid helium at 4.2K at which temperature the NbTi windings are superconducting. On energising the magnet approximately 600A is injected into the windings. Boil-off of the expensive helium is reduced through a cryocooler which mechanically cools the internal radiation shields. A second set of windings outside of the main magnet windings has current circulating in the opposite direction to reduce the fringe field, this is known as active shielding.

Gradient Coils

- Generate strong, linear, magnetic field variations in the z-direction, $\frac{\partial B_z}{\partial x}, \frac{\partial B_z}{\partial y}, \frac{\partial B_z}{\partial z}$ superimposed on B_0 that can be rapidly switched
  - max. amplitude, e.g., 50mT/m
  - min. rise time, e.g., 250μs
  - slew rate, e.g., 200T/m/s

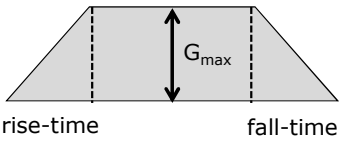

Performance specs.

- Linearity
- Eddy currents
- Heat dissipation

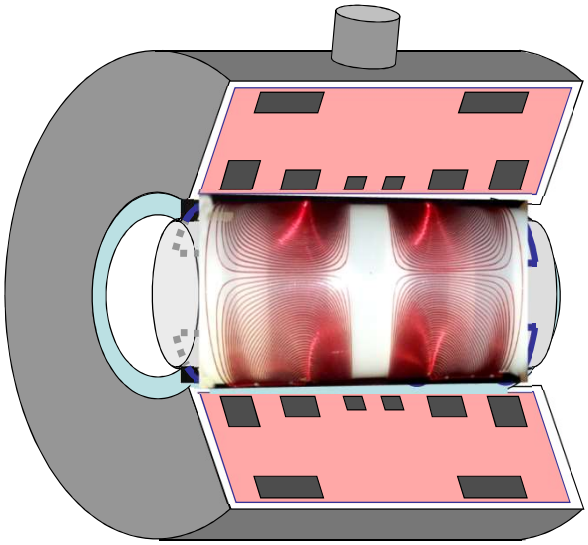

Inside the so-called room temperature bore of the magnet cryostat are positioned the gradient coils. These create the linear variations in magnetic field required for spatial localisation. The gradients must create variations along the z-direction. The z-gradient is created using a Maxwell-pair design , whilst the x and y gradients are created using a quadrupolar Golay style design. The gradients require high power amplifiers, e.g. 1.6KV @ 650A = 1MW to rapidly switch the gradients on and hold their amplitude across the bore radius. The gradient coils can generate in excess of 25KW of heat so they, and the amplifiers, are generally water cooled.

Spatial Localisation: Gradients

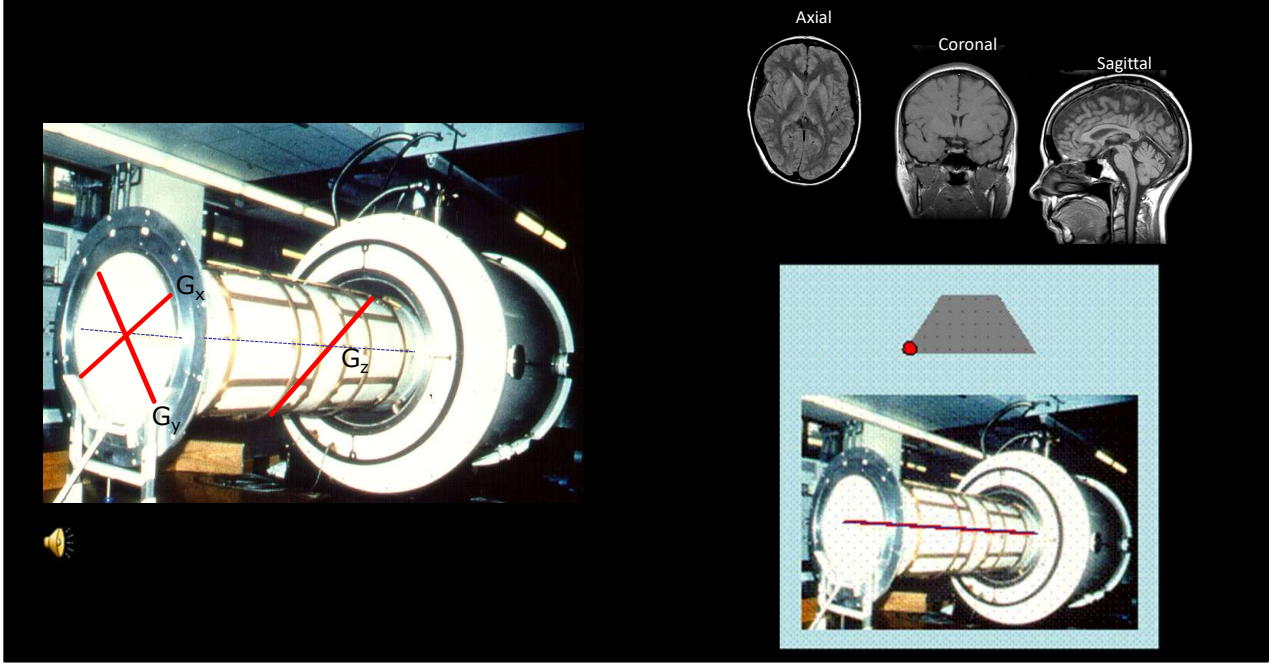

The physical G_x, G_y and G_z gradients are mapped to the logical slice select, phase encoding and frequency encoding gradients. This enables images to be obtained in any orthogonal plane or a combination of two or three allow imaging in a single or double oblique plane. The gradients physically flex when they are pulsed, like a loudspeaker, resulting in the characteristic knocking noise associated with MRI.

Eddy Currents

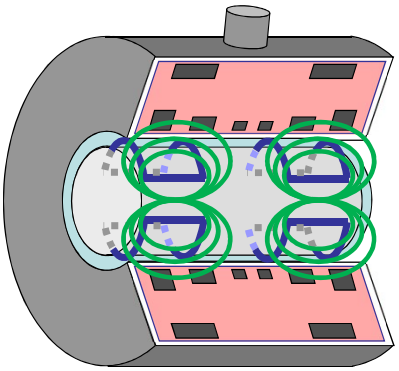

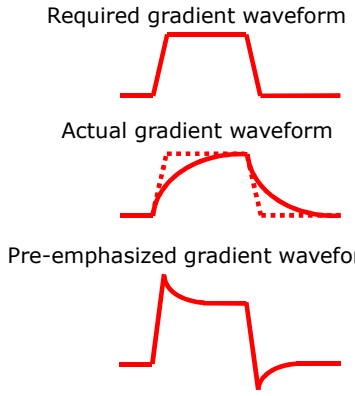

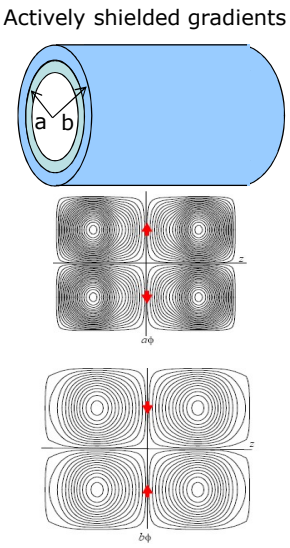

The rapid switching of the gradients induces eddy currents in nearby conducting components of the magnet cryostat. These persist for varying durations depending on the resistivity of the metal involved. The field generated by the eddy currents combines with the intended gradient field to create waveform distortions, which can result in image artifacts and signal loss.

All modern MR systems use active shielding on the gradients, very similar technology to the active shielding of the magnet coil itself. Additional “secondary” or “shield” coils surround the primary gradient coils and are driven with the opposite gradient waveform. This cancels the gradient field outside the shield coils, magnetically isolating the gradients from the cryostat so that eddy currents cannot be induced. The shield coils make the entire gradient assembly larger, reducing the free space available inside the bore, and also require more power to generate a given gradient amplitude. However, without the active shields, it is necessary to have a larger separation between the gradients and the first metal wall of the cryostat.

Although active shielded gradients induce less eddy currents, they are not perfect. The remaining effects can be minimized by *pre-emphasizing* the gradient waveforms so that, when combined with the eddy current field, the resultant is close to the ideal gradient waveform. Pre-emphasis uses extra electronic circuits that add additional voltages, with adjustable amplitudes and time constants, to the gradient driving waveform.

Gradient Non-linearity

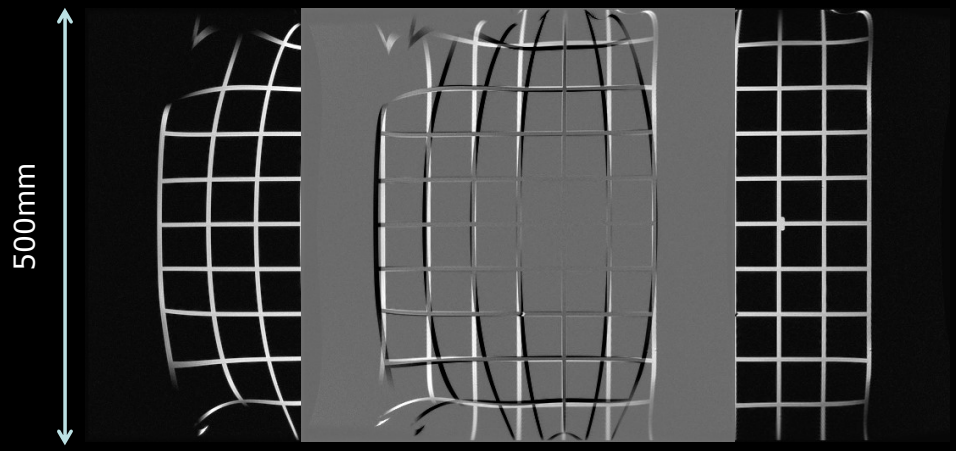

Before correction

After correction

Linear variation in the gradient field is required for accurate spatial encoding, however the gradient coils have a finite length and diameter and so they produce non-linear fields close to their edges. Linearity usually decreases fairly rapidly towards the edge of the imaging volume. The consequence of nonlinearity on an image is misplaced signal and geometric distortion. Most manufacturers make use of computer algorithms that warp the images after reconstruction to compensate for the gradient nonlinearities.

Gradient Amplifiers

- High power amplifiers are required to generate gradient pulses
- Amplifier power 1-3MW
- Gradients and amplifiers need to dissipate 25-75kW heat
- Amplifiers and gradient coils are water cooled

MGH "Connectome" gradient system
G_{max} = 300 mT/m

10,800 amps
@ 2,000V
≈22 MegaWatts

NIH Bluepr

Los Angeles class nuclear submarine
(27 MegaWatts)

Wald, Washington DC Sept. 2014 A.A. Martinos Center, MGH

https://sites.udel.edu/uhf-nmr-workshop/files/2015/08/Wald-22egclw.pdf

Gradient amplifiers operate at audio frequencies. The requirement for high gradient amplitudes means that the amplifier must be capable of producing large electrical currents through the coils. Furthermore, the requirement for short switching times means that this current must be rapidly increased from zero to the maximum and then back down. Of course, whenever you change the current flowing through a coil a 'back-emf' is generated. This is a voltage which tries to prevent the current rise in the coil; the faster the current changes, the stronger the back-emf becomes. The amplifier therefore needs to generate a sufficient driving voltage to overcome this back-emf.

Vertical Field System Gradients

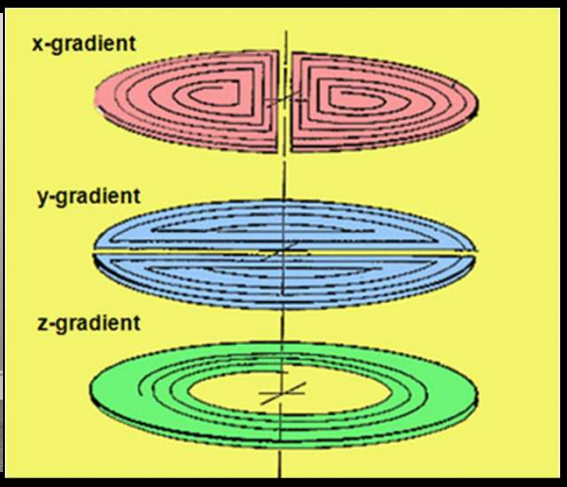

http://mri-q.com/open-scanner-gradients.html

Vertical field or “open” MR systems require specialised planar gradient coils. The inner arcs of the coils are primarily responsible for producing the desired gradient. By rotating these coils in plane by 90º either *x*- or *y*-gradient fields can be produced

RF Transmit Coils

- Generate time-varying magnetic fields (B_1) at the required frequency (ω)
- Typ. 25kW RF amplifier
- Coils
  - LC circuits tuned to the Larmor frequency (ω_0)
  - Impedance matched (50Ω)
  - Large diameter transmit coils to maximise excitation uniformity (flip angle)
  - Separate close fitting multi-element receiver coils to maximise detection sensitivity (mV)

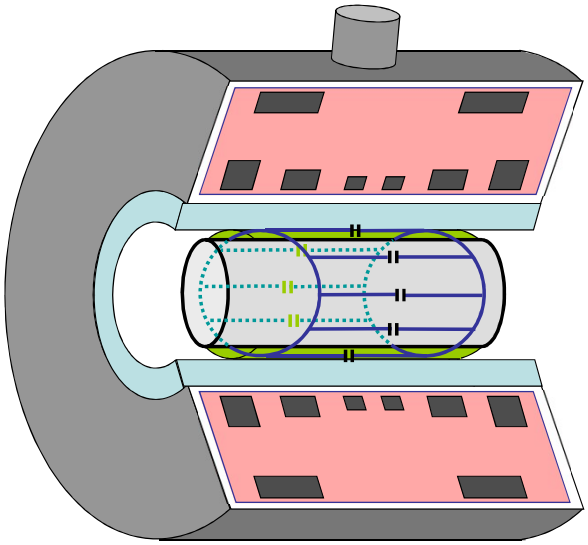

The purpose of the RF transmit coil is to create the circularly polarised time-varying B_1 field at right angles to B_0. A large diameter birdcage "body" coil is generally used since this creates the most spatially uniform B_1 field. The coil is a resonant circuit tuned to the Larmor frequency for the given field strength and impedance matched to the RF power amplifier.

RF Transmission

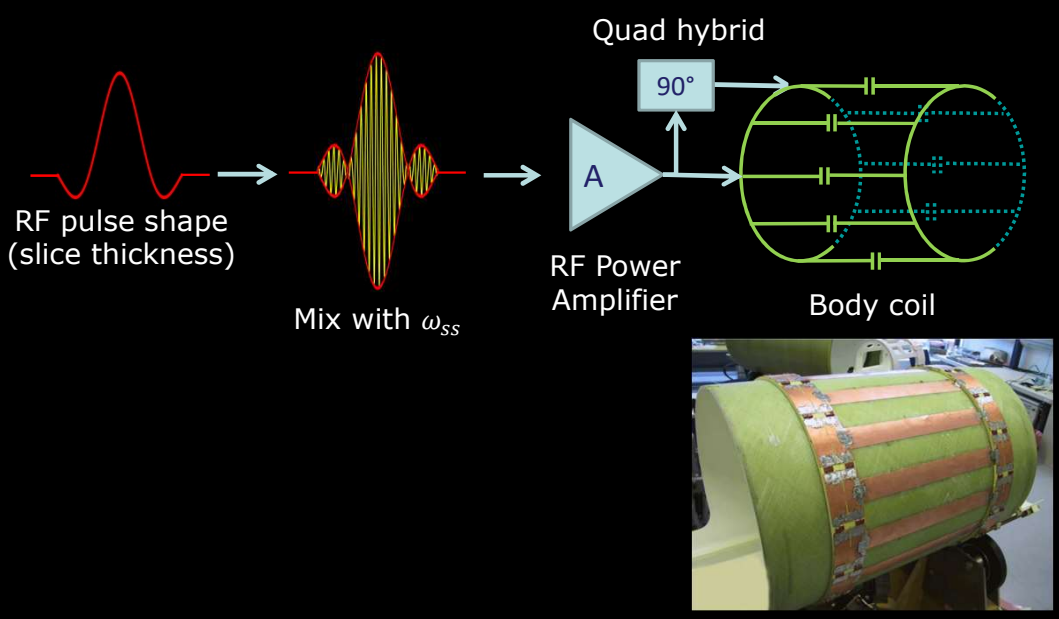

RF transmission involves mixing the digitally generated RF pulse envelope (which dictates the bandwidth of the excitation pulse) with the slice select frequency. This analogue waveform is amplified and applied in quadrature to the birdcage body coil in order to generate a circularly polarised RF that rotates in the same sense as the precessing nuclear magnetisation.

The main transmitting coil is usually the body coil, which surrounds the entire patient. This is usually built into the scanner bore and is not generally visible. Since this coil is large it has a very uniform transmission field, but this also means that it is not particularly sensitive if used as a receiver coil. In some systems other coils, e.g. head or knee, may also be used for transmission, in which case less power is required to flip the magnetization, but excitation uniformity may be sacrificed.

Types of RF Transmit Coil

RF coil design depends upon the orientation of B_0 compared to the subject

Vertical field magnet
- solenoid coils

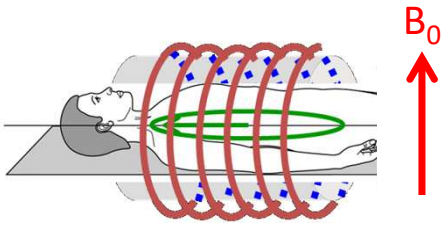

Horizontal field magnet
- birdcage coil

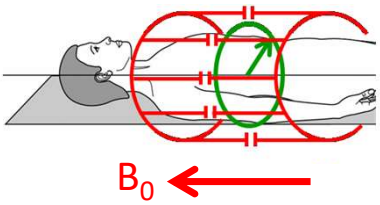

Vertical or horizontal field systems can use simple solenoids to create B_1 since B_0 is orthogonal. In superconducting magnets where the field is horizontal the coils need to be of the birdcage design.

So when we start the scanner the electromagnetic fields generated by the RF pulses excites the mercury vapour inside the fluorescent tube and the tube glows. As the amplitude of the RF pulse increases the light gets brighter.

RF Receive Coils

Example multi-channel coils

- Head
- Neck
- Spine
- Knee
- Foot/ankle
- Wrist
- Shoulder
- Cardiac
- Breast
- Torso
- Abdominal
- Endo-rectal
- Flexible

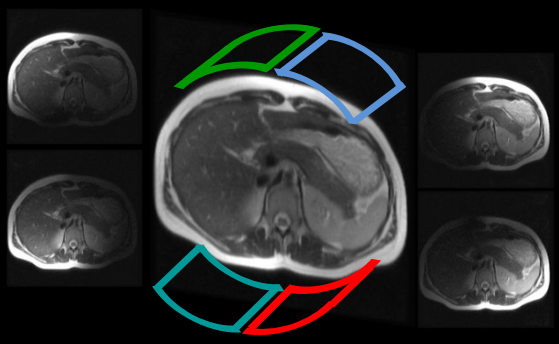

Sum-of-squares combination

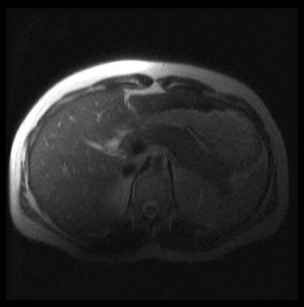

Individual coil images

Receiver coils generally comprise arrays of smaller individual coils or elements. The smaller the coil the better the signal-to-noise ratio , however the each individual coil element only has a limited depth penetration Therefore array of coils are used to achieve the desired coverage. The coils are electronically decoupled from each other so that they don't just appear as a single "large" coil. The images from individual coils are independently reconstructed and then summed together to create the final image.

Coil Basics

- Coils are resonant tuned circuits
- A coil has a depth sensitivity approx. equal to its diameter
- Arrays are combinations of individual coils that cover a large area/volume but do not interact
- Array geometries are optimised for parallel imaging

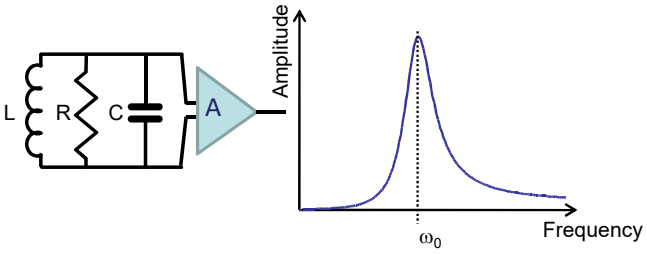

Original phased array design

Parallel imaging optimised array

Both transmit and receive coils are tuned circuits. The majority of receive coils in modern systems consist of multiple elements, each acting independently. These coils are formally known as “phased array” coils, but since they are now so common, we often just use the word “coil”.

These coils need to be designed very carefully so that the individual elements do not interact with each other, a phenomenon known as coupling which reduces SNR in the images. One way of effectively ‘decoupling’ one element from its neighbors is to geometrically overlap the coils in a particular way. Each element is connected to an entirely separate preamplifier and receiver which has the advantage that the noise in each receiver is completely different, i.e. uncorrelated, resulting in a higher SNR in the final image. However recent developments in very low impedance preamplifiers built into coils makes the designs much more flexible. Developments such as parallel imaging used to accelerate MRI acquisitions require different spatial sensitivities for the individual coils.

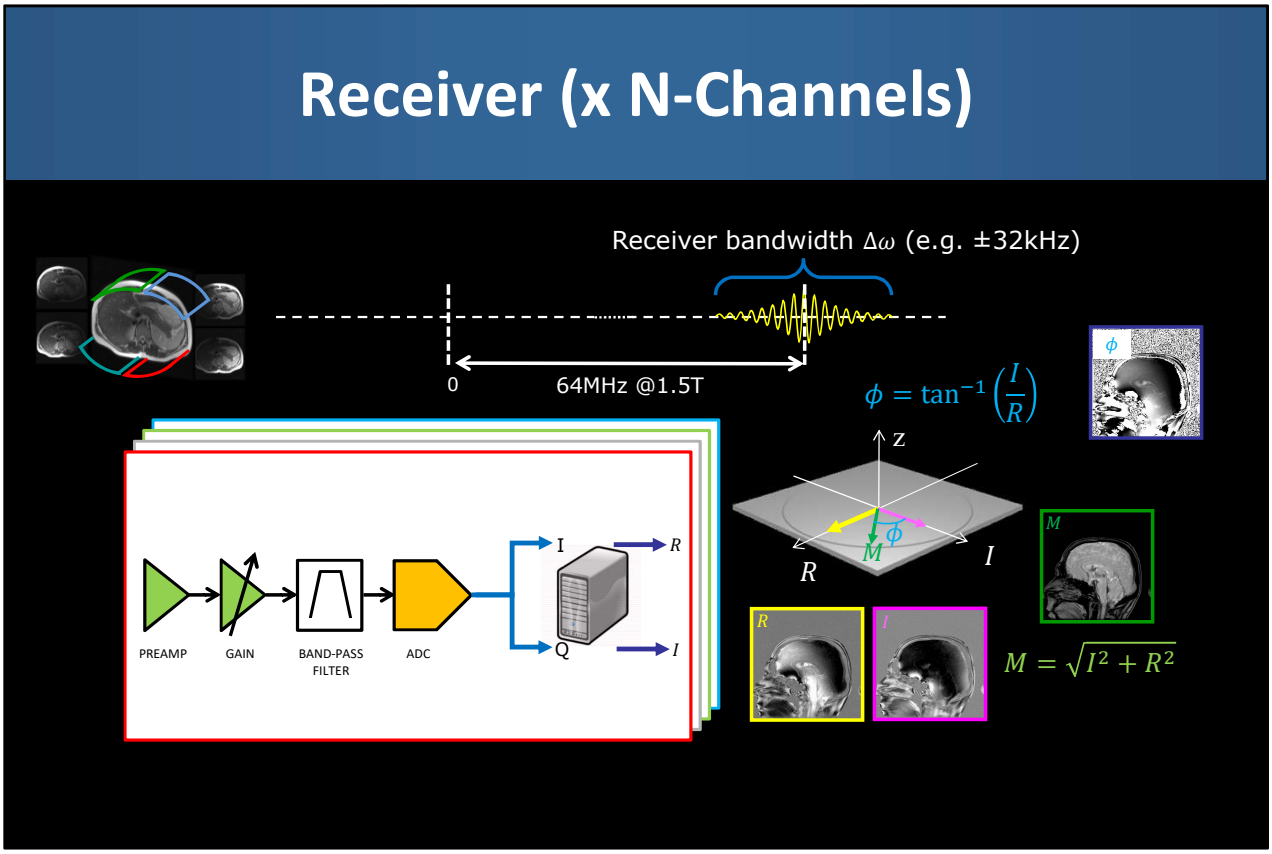

The MR signal only contains a narrow frequency range of interest Δω, embedded in or carried by the Larmor frequency ω_0 (with an offset due to the frequency encoding) Mathematically this is shown as $\cos(\omega_0 + \omega_{FE} \pm \Delta\omega)$. In earlier MR systems, it was not possible to digitize directly at the Larmor frequency, so the MR signal had to be demodulated down to a lower frequency (e.g. 125 kHz) before converting to a digital signal. However, analog-to-digital converters are much faster now and all modern system now use direct digital receivers. These ADCs operate at very high frequencies, 10s of MHz, and allow 16 or 32 bit digitization. This also has the advantage of minimizing image artifacts caused by drift in the older analog receiver circuitry. Each coil element is connected to its own receiver. Since the signals are detected in quadrature the reconstructed MR data is complex. We primarily reconstruct magnitude images but we can also use gradients to manipulate the phase of the MR signal which can be used to encode information such as the velocity of blood flow.

Signal-to-noise Ratio (SNR)

$$SNR \propto B_0 \cdot \frac{\Delta x \cdot \Delta y \cdot \Delta z \cdot \sqrt{N_x \cdot N_y \cdot NSA}}{\sqrt{RBW}}$$

Remember that some parameters are interdependent e.g. changing the matrix size will change the acquisition time as well as the pixel size

Some SNR relationships in MRI

Reconstruction

- Role:
  - Manage raw data
  - Reconstruct images
  - Inline post processing
- Performance specifications:
  - Raw data capacity
  - Reconstruction algorithms
  - Reconstruction speed
  - Post processing methods

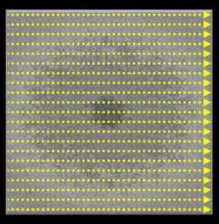

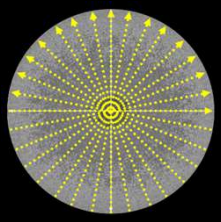

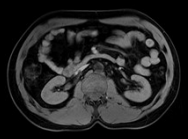

Future Hardware Developments

- Magnets
  - Low cryogen volumes, e.g. 10L (no quench pipe)
- Gradients
  - Higher performance with wider bore
  - Head-only systems
- RF
  - Higher channel counts
  - Lighter more flexible coils
  - Integrated high-order shims
  - On-coil digitisation
- Reconstruction
  - More sophisticated acquisition and hence reconstruction algorithms
  - Memory size and speed improvements
- Combined/hybrid modalities
  - PET/MR
  - MR-Linac

Michael Colombini

- Born 1995 Croton-on-Hudson NY
- 2001 suffers a "nasty fall" at home
- CT shows benign brain tumour
- Tumour resected
- Post-op MRI requested
- Michael sedated, taken into MRI scanner
- Sats start dropping ...

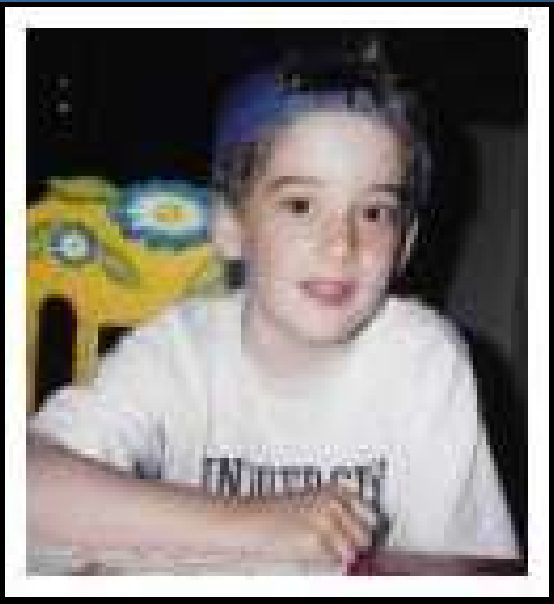

This was a sentinel event in the world of MR safety

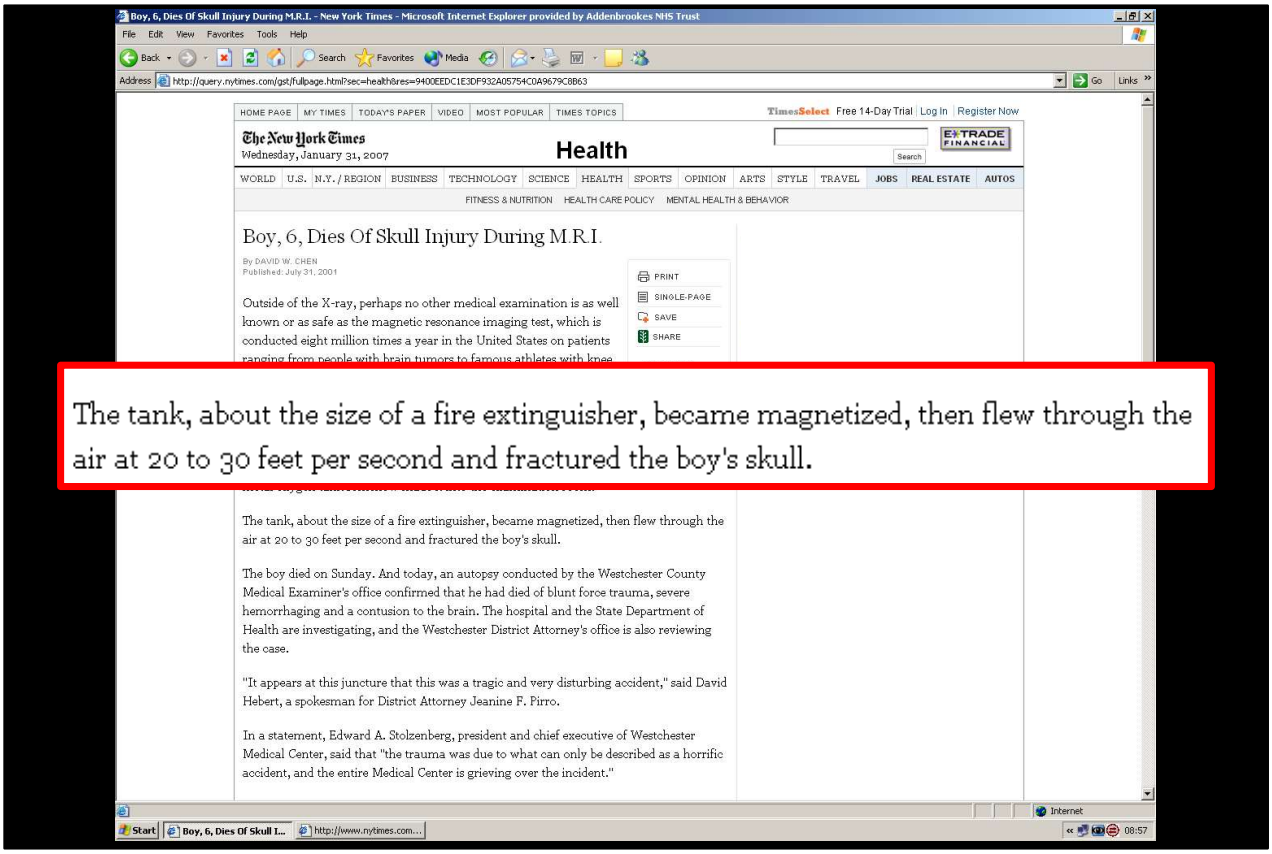
Boy, 6, Dies Of Skull Injury During M.R.I. - New York Times - Microsoft Internet Explorer provided by Addenbrookes NHS Trust
http://query.nytimes.com/gst/fullpage.html?sec=health&res=9400EEDC1E3DF932A05754C0A9679C8B63
HOME PAGE | MY TIMES | TODAY'S PAPER | VIDEO | MOST POPULAR | TIMES TOPICS
TimesSelect Free 14-Day Trial | Log In | Register Now
The New York Times
Wednesday, January 31, 2007
Health
Search
E*TRADE FINANCIAL
WORLD | U.S. | N.Y. / REGION | BUSINESS | TECHNOLOGY | SCIENCE | HEALTH | SPORTS | OPINION | ARTS | STYLE | TRAVEL | JOBS | REAL ESTATE | AUTOS
FITNESS & NUTRITION | HEALTH CARE POLICY | MENTAL HEALTH & BEHAVIOR
Boy, 6, Dies Of Skull Injury During M.R.I.
By DAVID W. CHEN
Published: July 31, 2001
PRINT
SINGLE-PAGE
SAVE
SHARE
Outside of the X-ray, perhaps no other medical examination is as well known or as safe as the magnetic resonance imaging test, which is conducted eight million times a year in the United States on patients ranging from people with brain tumors to famous athletes with knee
The tank, about the size of a fire extinguisher, became magnetized, then flew through the air at 20 to 30 feet per second and fractured the boy's skull.
The tank, about the size of a fire extinguisher, became magnetized, then flew through the air at 20 to 30 feet per second and fractured the boy's skull.
The boy died on Sunday. And today, an autopsy conducted by the Westchester County Medical Examiner's office confirmed that he had died of blunt force trauma, severe hemorrhaging and a contusion to the brain. The hospital and the State Department of Health are investigating, and the Westchester District Attorney's office is also reviewing the case.
"It appears at this juncture that this was a tragic and very disturbing accident," said David Hebert, a spokesman for District Attorney Jeanine F. Pirro.
In a statement, Edward A. Stolzenberg, president and chief executive of Westchester Medical Center, said that "the trauma was due to what can only be described as a horrific accident, and the entire Medical Center is grieving over the incident."
Internet
Start
Boy, 6, Dies Of Skull I...
http://www.nytimes.com...
08:57

Oxygen Cylinder

September 2010

$2.9 Million Settlement Closes Colombini MRI Death Case

This week the settlement documents were released — closing the chapter on the lawsuit that arose from the seminal event in MRI safety, the 2001 oxygen tank fatality of then-six-year-old Michael Colombini.

Nearly nine years after the accident, the lawsuit was settled for $2.9 million, a settlement that was likely both diminished by, and made possible by, a pre-trial motion which excused GE Healthcare as a defendant to the suit.

B_0 Spatial Gradient

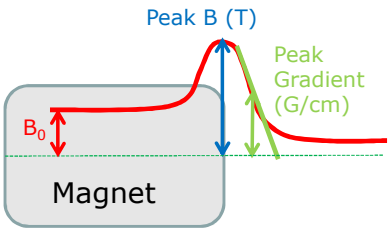

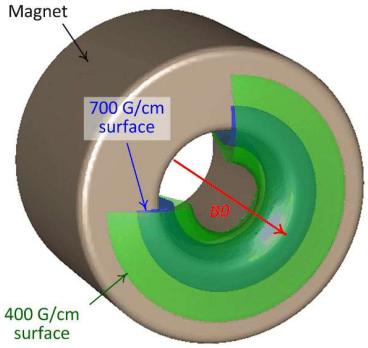

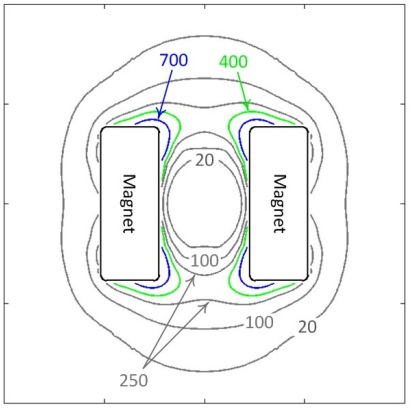

100 G/cm = 1.0 T/m

$$F \propto \chi V B \frac{dB}{dz}$$

In this example, there is no path into the magnet that does not pass through the "entry SG" contour of 250 G/cm (2.5 T/m)

Due to the active shielding of an MRI scanner the fringe field falls off very rapidly. The translational force (F) on a magnetically unsaturated object of volume (V) with magnetic susceptibility (χ) is proportional to the product of the static field (B) and its spatial gradient (dB/dz). Once the object is fully magnetized the force is simply proportional to the spatial gradient (dB/dz). Therefore it is the spatial gradient that dictates the safety of certain MRI conditional devices/implants going into the magnet

B_0 Spatial Gradients

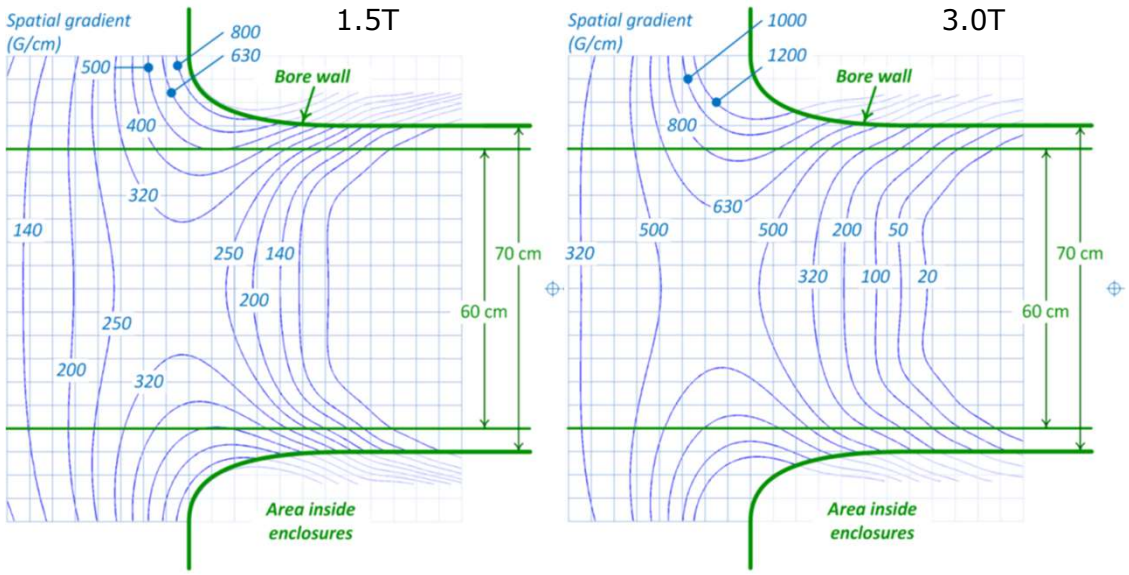

The SG approximately doubles for 3T compared to 1.5T

Note that the spatial gradient (SG) is approximately double for a 3T compared to a 1.5T. Therefore certain devices/implants may only be MR Conditional at 1.5T and NOT 3.0T

B_0 Fringe Field

- Restricted access to 0.5mT/5G field contour
- UK MHRA
  - MR Environment
- ACR
  - Zone III

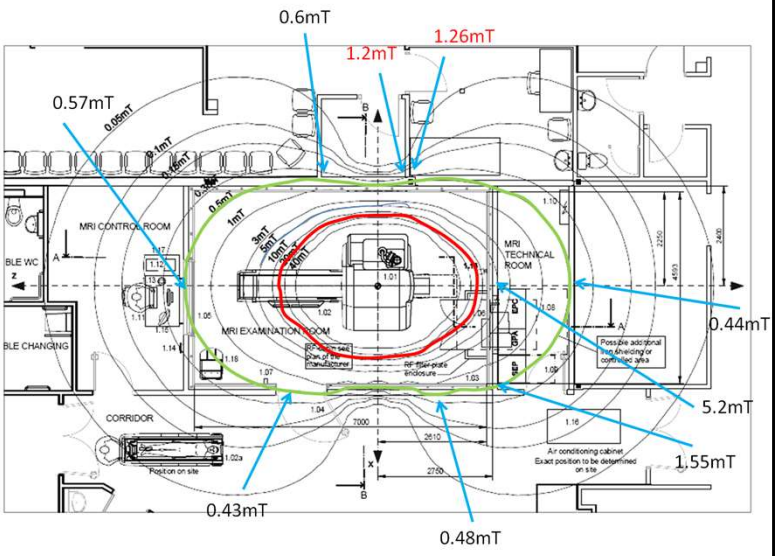

All MRI facilities have to restrict access to the “MR Environment”. This is usually enclosed within an MR Controlled Access Area. The guidelines for Clinical MRI in the UK are produced by the Medicines and Healthcare products Regulatory Agency (MHRA). In the US this is given by the American College of Radiology (ACR) zoning system.

Quench

- A superconducting magnet holds around 2,000 litres of liquid helium (-270°C)
- If the magnet ceases to be superconducting the huge energy stored (15MJ) is converted into heat
- The liquid helium is vaporised with a 754:1 expansion ratio (1.5M litres)
- The very cold gas is vented to the outside through the quench pipe
- In a double fault situation the gas could theoretically fill the magnet room
- Risk of cold contact burn, asphyxia and explosion risk from liquified oxygen

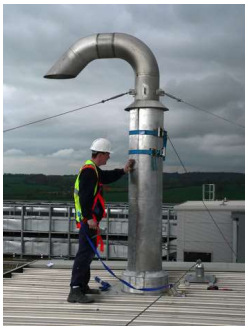

Gradients

- 100 times weaker than the static magnetic field
- Switch about 0-10kHz
- Peripheral nerve stimulation
  - From tingling sensation to painful muscle spasm
  - Avoid creating large loops
- Acoustic noise
  - Can exceed 100dBA
  - Hearing protection recommended

Radiofrequency Magnetic Fields

- 10,000 times weaker than the static magnetic field
- Switch about 60-130MHz
- Main effect is tissue heating, like a microwave oven or mobile phone
- Mobile phone: 2W
- Microwave: 1,000W
- MRI: 30,000W

- Whilst tissue heating is strictly controlled, anything electrically conducting can heat up

Specific Absorption Rate (SAR)

- Faraday's law gives $EMF \propto \frac{dB}{dt}$
- Electric fields produced in conducting tissues will drive electric currents and result in tissue heating
- For a volume conductor with induced current density $\mathbf{J}$ and induced electric field $\mathbf{E}$ the power is given by $P = \mathbf{J} \cdot \mathbf{E} = \sigma E^2$, where σ is the conductivity (Sm^{-1})
- The specific absorption rate (SAR) (Wkg^{-1}) is defined as $SAR = \frac{\sigma|E|^2}{\rho}$, where ρ is the tissue density
- Integrating over a spherical volume of radius R

$$\mathrm{SAR} = \int_{r=0}^{R}\int_{\theta=0}^{\pi}\int_{\phi=0}^{2\pi} \frac{\sigma|E|^2}{\rho} r\, dr d\theta d\phi$$

$$\mathrm{SAR} = \frac{\pi\sigma\omega_o^2 B_1^2 R^5}{15}$$

- Assuming uniform conductivity!
- Importantly,
  - SAR increases with B_0^2 i.e. static field strength squared
  - SAR increases with B_1^2 i.e. flip angle squared
  - SAR increases with patient size

Less than 1% of the energy dissipated is used to tip the nuclei. The vast majority produces nothing but undesirable heating

RF Exposure Limits (IEC 60601-2-33)

	Whole body SAR	Partial body SAR	Head SAR	Local SAR (a)		
Body Region →	whole body	exposed body part	head	head	trunk	extremities
Operating Mode ↓	(W/kg)	(W/kg)	(W/kg)	(W/kg)	(W/kg)	(W/kg)
Normal	2	2 - 10 (b)	3.2	10 (c)	10	20
1st Level Controlled	4	4 - 10 (b)	3.2	20 (c)	20	40
2nd Level Controlled	>4	>(4 - 10) (b)	>3.2	>20 (c)	>20	>40
Short duration SAR	The SAR limit over any 10 s period shall not exceed two times the stated values					

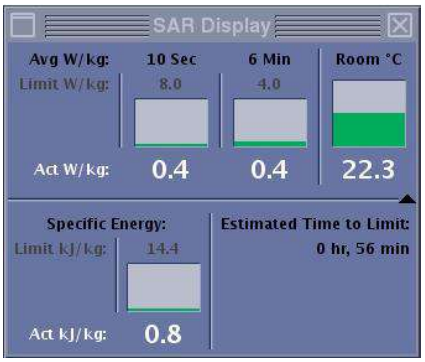

The SAR is averaged over a 6 minute period

Manufacturers empirically determine the energy absorbed within the subject.
For example, a 1ms hard 180° RF pulse has a B_1 of 11.7μT

IECG 60601-2-33 (BS EN 60601-2-33) is part of a series of international standards on medical electrical equipment, covering basic safety and essential performance for both equipment and systems. This latest update to Part 2-33 outlines guidelines relating specifically to Magnetic Resonance (MR) equipment, i.e., *Particular requirements for the safety of magnetic resonance equipment for medical diagnosis.* It complements BS EN 60601-1.

From the introduction, "The standard addresses technical aspects of the medical diagnostic MR SYSTEM and the MR EQUIPMENT therein, related to safety of PATIENTS examined with this system and personnel involved with its operation. Where limits of exposure of PATIENTS and medical staff are stated, these limits do not imply that such levels of exposure can be assumed to be acceptable for the population at large. Rather the implication is that the limits provide for the PATIENT a sensible balance between risk and benefit and for the medical staff a balanced risk, given their responsibility for the wellbeing of the PATIENT."

Metallic Microfibre Clothing

Published March 1, 2012 as 10.3174/ajnr.A2827

TECHNICAL NOTE

Invisible Metallic Microfiber in Clothing Presents Unrecognized MRI Risk for Cutaneous Burn

J.A. Pietryga
M.A. Fonder
J.M. Rogg
D.L. North
L.G. Bercovitch

SUMMARY: We report a case of a thermal burn that occurred during MR imaging likely caused by invisible silver-embedded microfibers in the fabric of an undershirt. As the prevalence of fabric containing nondetectable metallic microfiber increases in athletic and "tech" clothing, the importance of having patients change into safe facility-provided garments before MR imaging is emphasized.

ABBREVIATIONS: ACR = American College of Radiology; SAR = specific absorption rate; SMF = silver microfiber

Fig 1. A linear erythematous blistering eruption is noted on the patient's right flank minutes after completion of the MR imaging of her brain and spine.

MHRA Incident Reports

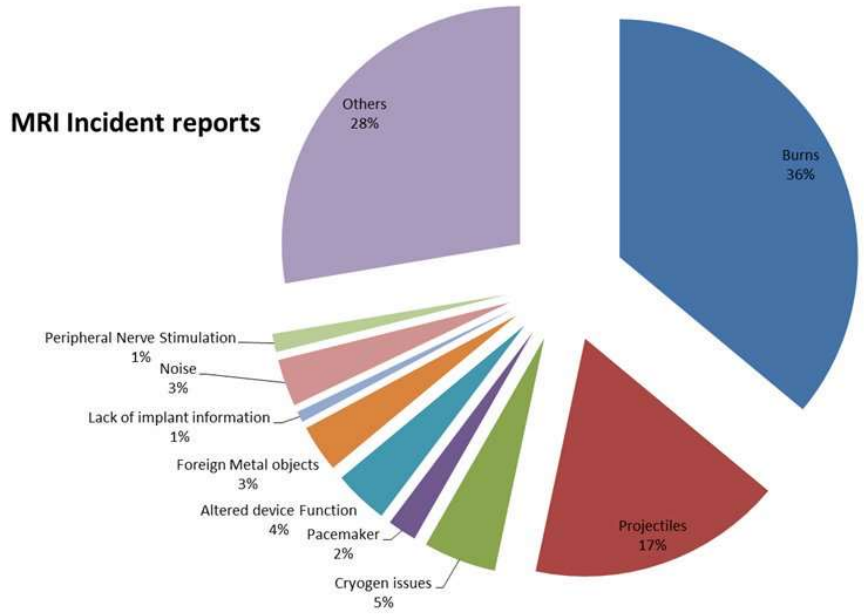

The majority of MRI incidents in the UK and worldwide are burns.

Safety Questionnaire

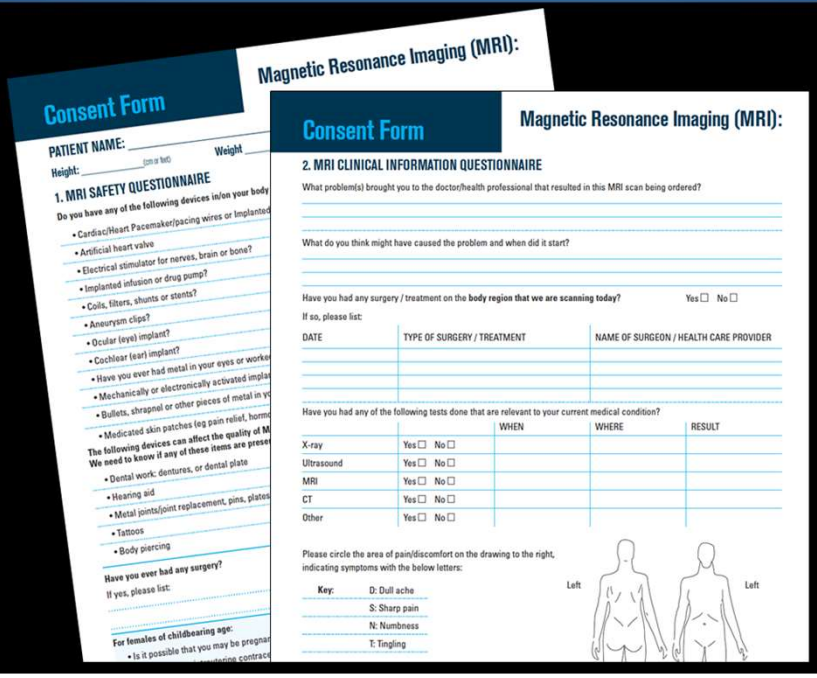

Consent Form

Magnetic Resonance Imaging (MRI):

PATIENT NAME:

Height: (cm or feet) Weight

1. MRI SAFETY QUESTIONNAIRE

Do you have any of the following devices in/on your body

- Cardiac/Heart Pacemaker/pacing wires or Implanted
- Artificial heart valve
- Electrical stimulator for nerves, brain or bone?
- Implanted infusion or drug pump?
- Coils, filters, shunts or stents?
- Aneurysm clips?
- Ocular (eye) implant?
- Cochlear (ear) implant?
- Have you ever had metal in your eyes or worke
- Mechanically or electronically activated implar
- Bullets, shrapnel or other pieces of metal in yo
- Medicated skin patches (eg pain relief, hormo

The following devices can affect the quality of M
We need to know if any of these items are prese

- Dental work: dentures, or dental plate
- Hearing aid
- Metal joints/joint replacement, pins, plates
- Tattoos
- Body piercing

Have you ever had any surgery?

If yes, please list:

For females of childbearing age:

- Is it possible that you may be pregnar

Consent Form

Magnetic Resonance Imaging (MRI):

2. MRI CLINICAL INFORMATION QUESTIONNAIRE

What problem(s) brought you to the doctor/health professional that resulted in this MRI scan being ordered?

What do you think might have caused the problem and when did it start?

Have you had any surgery / treatment on the **body region that we are scanning today?** Yes☐ No☐

If so, please list:

DATE	TYPE OF SURGERY / TREATMENT	NAME OF SURGEON / HEALTH CARE PROVIDER

Have you had any of the following tests done that are relevant to your current medical condition?

		WHEN	WHERE	RESULT
X-ray	Yes☐ No☐			
Ultrasound	Yes☐ No☐			
MRI	Yes☐ No☐			
CT	Yes☐ No☐			
Other	Yes☐ No☐			

Please circle the area of pain/discomfort on the drawing to the right, indicating symptoms with the below letters:

Key: D: Dull ache
S: Sharp pain
N: Numbness
T: Tingling

Left Left

RF Wavelength at 1.5T

$$\lambda = \frac{c}{f \cdot \sqrt{\varepsilon_r}}$$

$$\frac{3\text{x}10^8}{64\text{x}10^6 \cdot \sqrt{81}} = 52\text{cm}$$

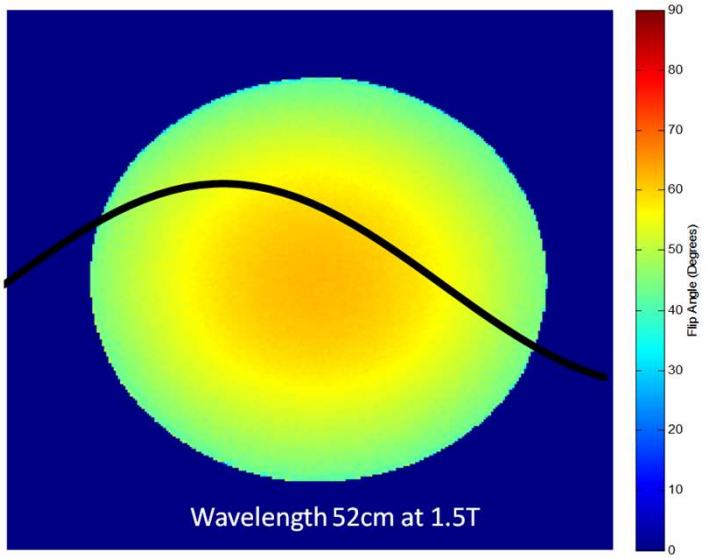

ε_r is the relative dielectric constant = 81 in water

This is a flip angle, i.e. B_1 map, in a uniform conducting phantom. At 1.5T the RF wavelength in water is about 52cm, so slightly larger than the average patient.

RF Wavelength at 3T

$$\lambda = \frac{c}{f \cdot \sqrt{\varepsilon_r}}$$

$$\frac{3\text{x}10^8}{128\text{x}10^6 \cdot \sqrt{81}} = 26\text{cm}$$

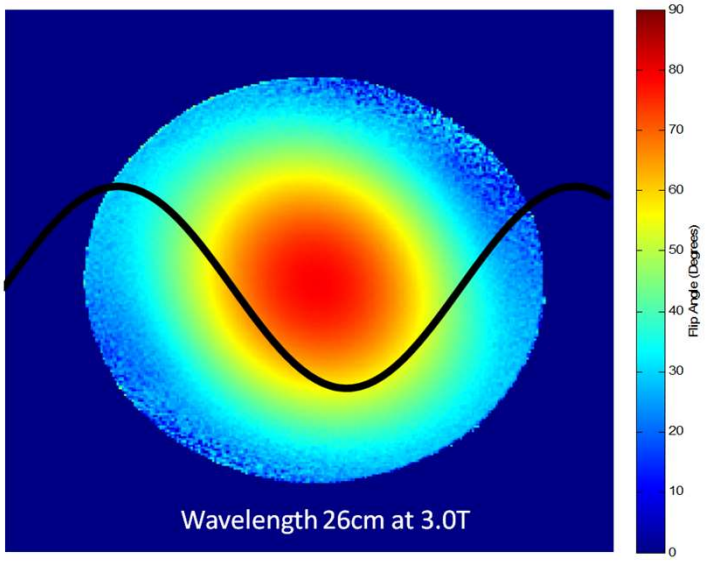

ε_r is the relative dielectric constant = 81 in water

This is a flip angle, i.e. B_1 map, in a uniform conducting phantom. At 3.0T the RF wavelength in water is about 26cm, so smaller than the average patient. This results in so-called dielectric standing waves and B_1 transmit field non-uniformity

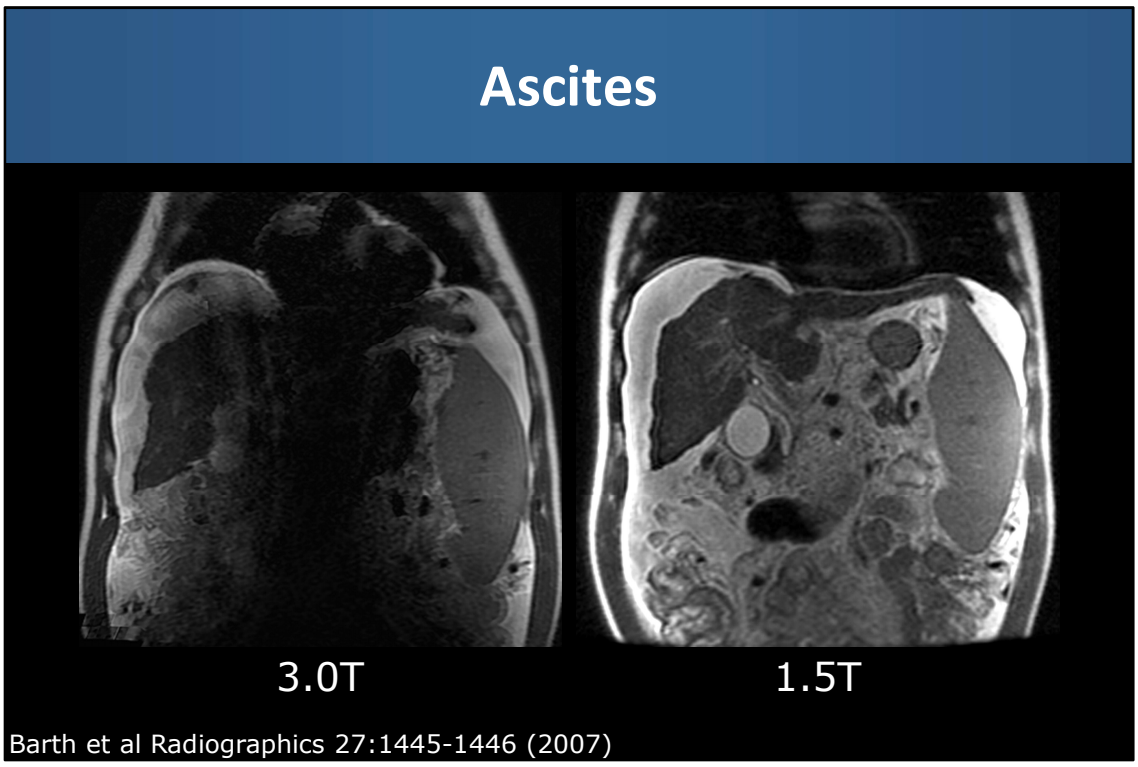

Ascites are fluid collections within the abdomen. Since the fluid is conducting this affects the B_1 uniformity especially at 3T causing signal drop-outs

Gadolinium Based Contrast Agent (GBCA)

- Chelate of Gadolinium (Gd^{3+})
- Seven unpaired electrons in outer shell
- 2,000x larger magnetic moment than proton
- Increases T_1 (and T_2 relaxation) of nearby water molecules
- Demonstrates T1w hyper-enhancement of perfused lesions

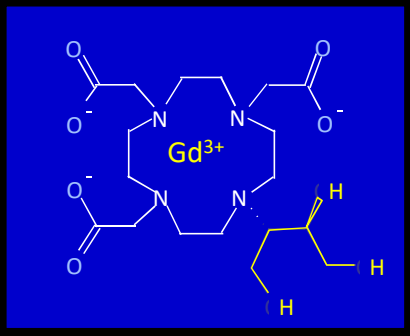

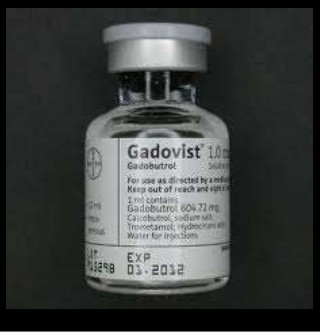

Contrast Agent Relaxation

$$(1/T_1)_{post} = [Gd]\ R_1 + (1/T_1)_{pre}$$

$$(1/T_2)_{post} = [Gd]\ R_2 + (1/T_2)_{pre}$$

[Gd] is the concentration (mM L^{-1})

R_1 and R_2 are the T_1 and T_2 relaxivities of the contrast agent (L mM^{-1} s^{-1})

[N.B. These are dependent upon B_0, temperature, surrounding material, e.g. water, plasma, blood]

Pre and Post Contrast T1w

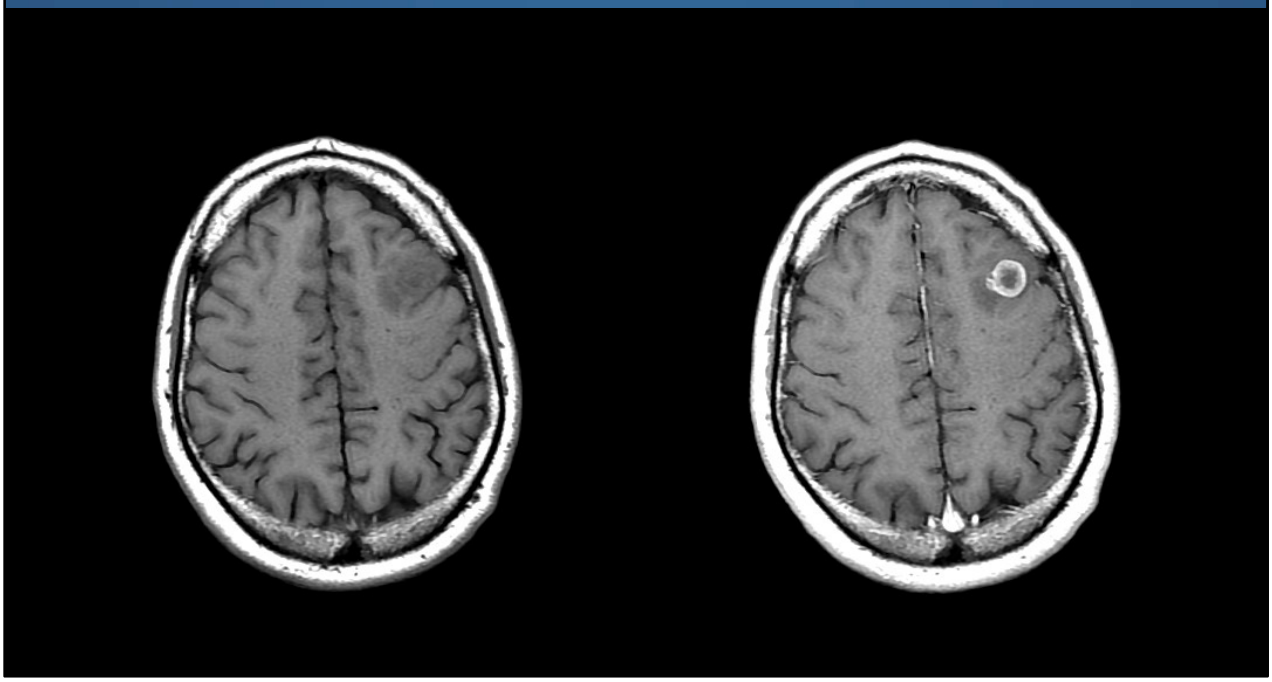

Diffusion Weighted Imaging (DWI)

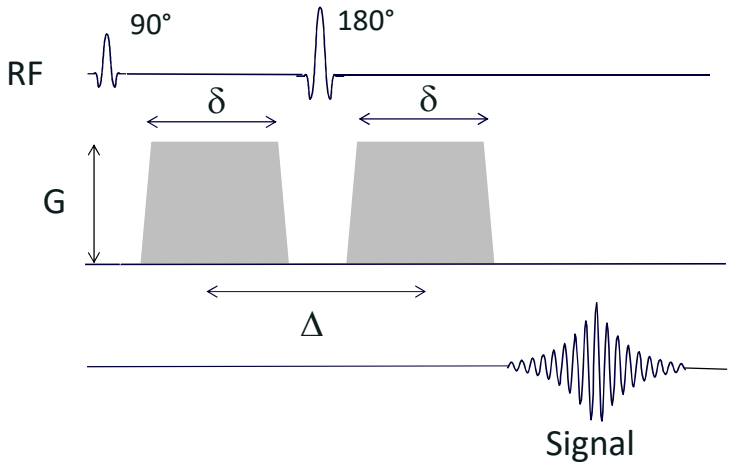

$$S = S_0 e^{-\left(\gamma^2 G^2 \delta^2 \left(\Delta - \frac{\delta}{3}\right)\right) D}$$

$$S = S_0 e^{-bD}$$

D is the intrinsic apparent diffusion coefficient (ADC)

b is the gradient factor in s mm^{-2}

The MR signal is naturally sensitive to molecular diffusion as we saw in the description of the Bloch equations. This diffusion weighted spin echo sequence increases the sensitivity to diffusion by the incorporation of additional diffusion sensitizing gradients either side of the refocusing pulse. The amplitude (G), duration (δ) and spacing (Δ) affects the diffusion sensitivity and is expressed as the b-value. In the simplest case of a diffusion gradient applied along a single gradient direction the effect of diffusion on the transverse magnetization is to add an extra exponential decay term e^{-bD} in addition to that due to normal T_2 decay.

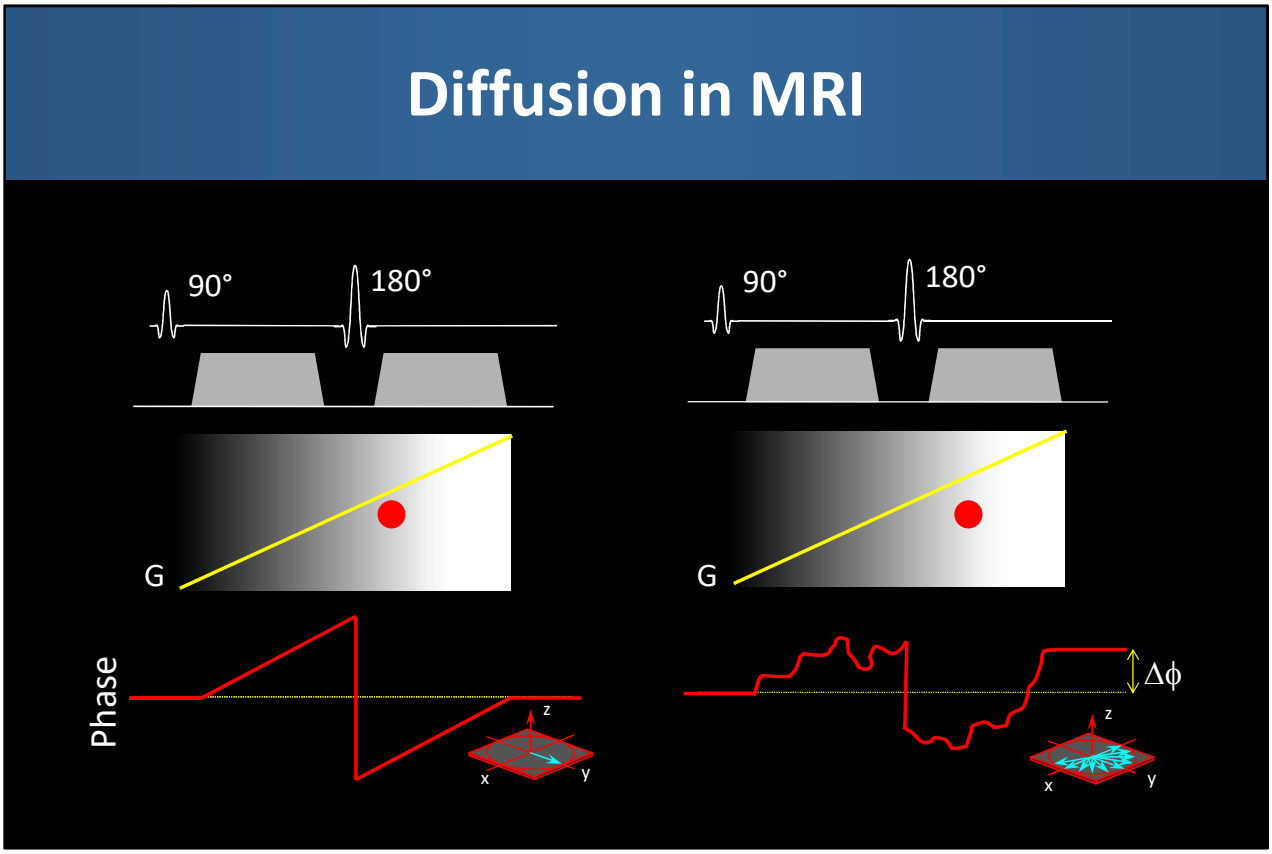

During the application of the first diffusion gradient pulse the spins (the red circle here) accumulates a phase shift which depends upon the position and motion during the application of the gradient. The 180° refocusing pulse inverts the phase of the spins and the second gradient lobe then induces another phase shift. If the spins are stationary then the phase shifts due to the two gradient pulse will be equal resulting in a zero net phase shift after the pulses. However, if the spins have changed position during Δ then the phase shifts will not be equal and the final echo amplitude will be attenuated.

Diffusion Weighted EPI

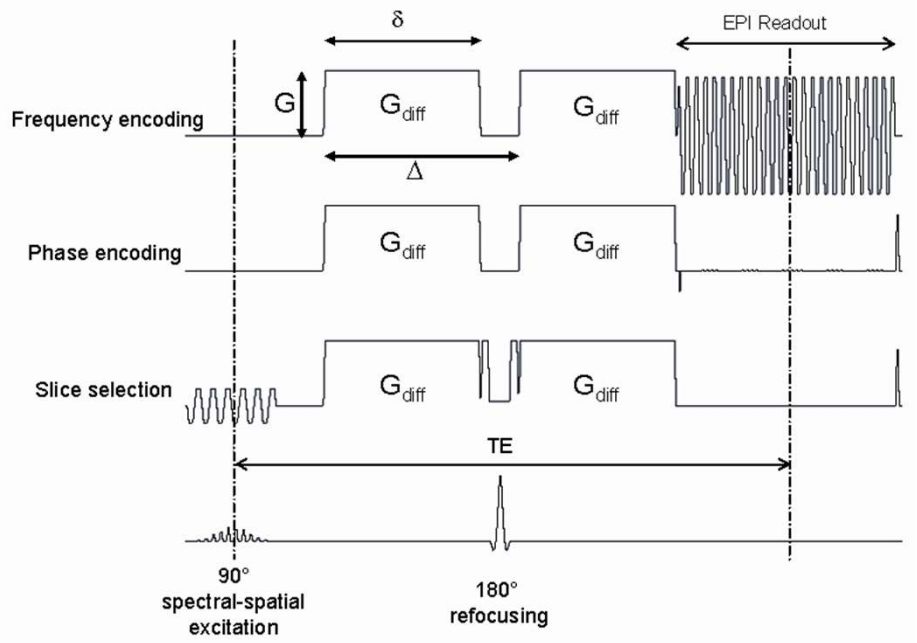

$$S = S_0 e^{-\left(\gamma^2 G^2 \delta^2 \left(\Delta - \frac{\delta}{3}\right)\right) D}$$

$$S = S_0 e^{-bD}$$

Average water displacement (at 37°) during a 50ms period is approx 30μm

Since we are trying to sensitise the DW sequence to molecular diffusion the methods will also be prone to motion artefacts due to macroscopic motion of the head or pulsation of the brain. Therefore most DWI methods employ at ultrafast acquisition method known as echo-planar imaging (EPI) to acquire the entire image in under 100ms. This diagram shows an actual diffusion-weighted spin echo planar imaging sequence. The diffusion gradients may not necessarily be applied on all three axes simultaneously.

Gradient Echo EPI

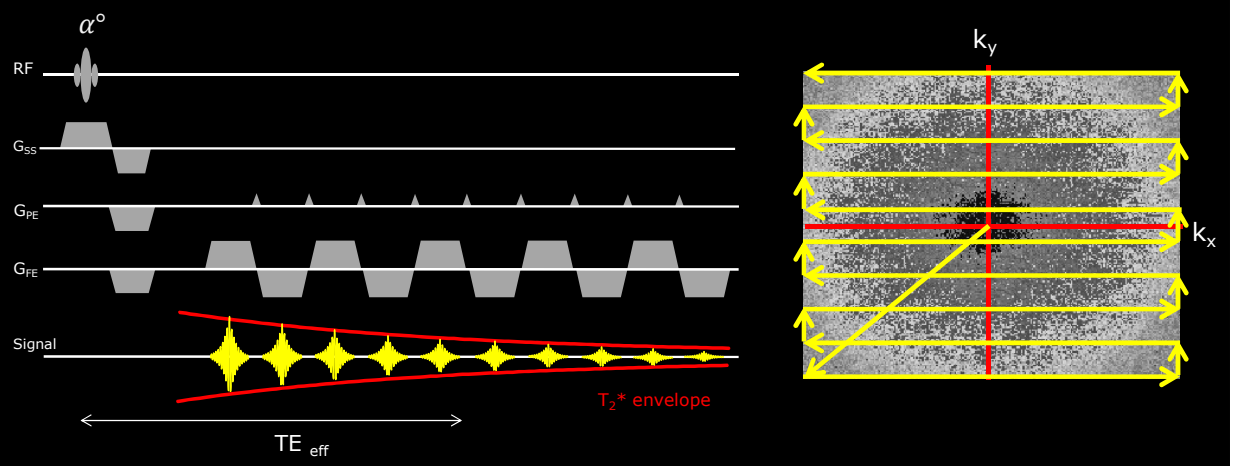

Although this is a gradient echo EPI sequence, i.e. the readout is immediately following an α° RF pulse and not a 90°-180° spin echo EPI – the echo-planar readout trajectory is the same in both cases. The animation demonstrates the raster style k-space trajectory. The phase encoding gradient is blipped to move up one k-space line whilst the frequency encoding gradient alternates in polarity so the echoes are alternately readout forward and backward.

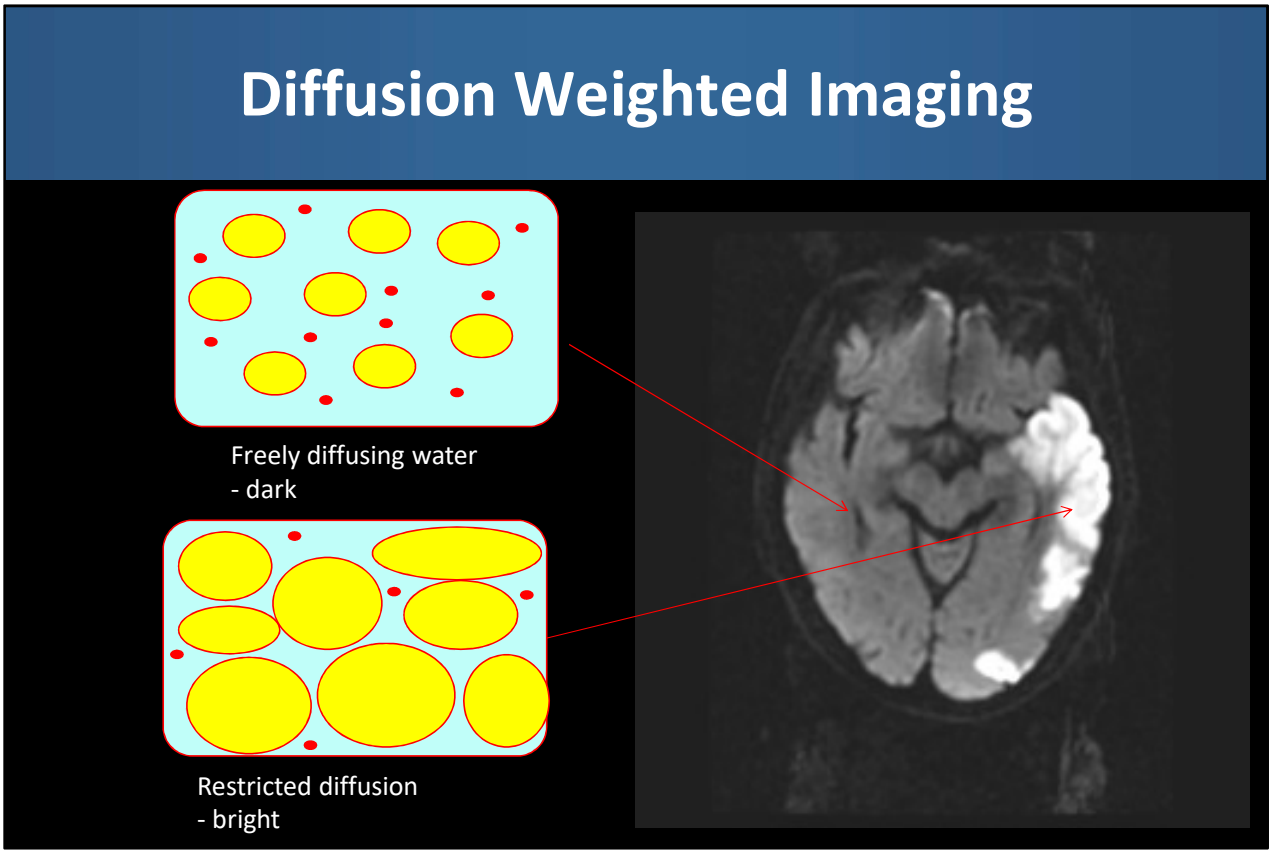

This is a classical application of DWI in showing an ischaemic stroke. Following the stroke the cells in the affected region swell reducing the distance that the water molecules can diffuse. In the ischemic region (relative signal hyperintensity) the restricted diffusion results in less phase dispersion and hence the echo amplitude is less attenuated than in normal tissue (relative signal hypointensity)

Quantitative Apparent Diffusion Coefficient (ADC)

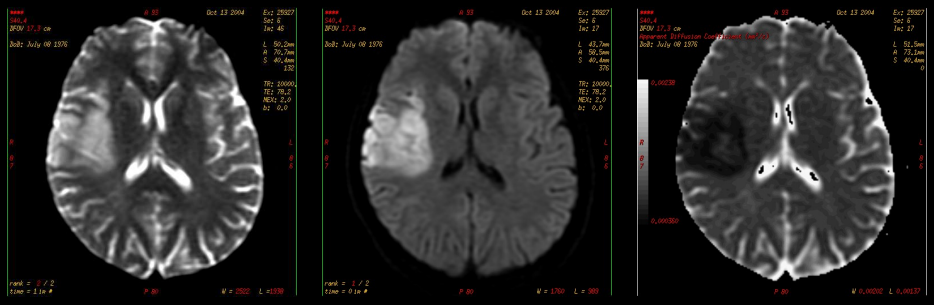

b=0 (T2 weighted) b=1000 ADC map

$$S_{(b=1000)} = S_{(b=0)} e^{-bD}$$

$$D = -\frac{\ln\left(S_{(b=100\ )}/S_{(b=0)}\right)}{b}$$

Is it possible to calculate an Apparent Diffusion Coefficient map from a simple two point DWI acquisition.

Tumour Microstructure: Diffusion

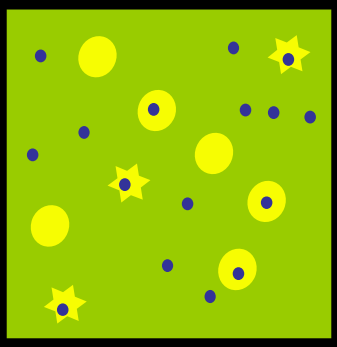

Low cellular density, defective membranes e.g. cystic/necrotic tissue, free diffusion
↓ DWI ↑ADC

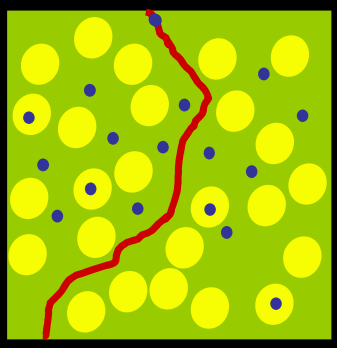

High cellular density, e.g. solid tumours, restricted diffusion
↑ DWI ↓ ADC

DWI is now extensively used in oncological imaging. Solid tumors can be characterized by their restricted diffusion

DWI in Oncology

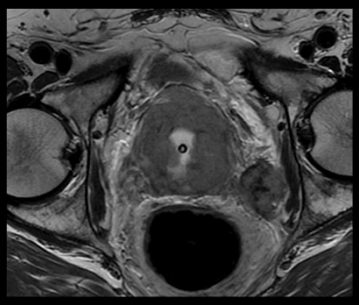

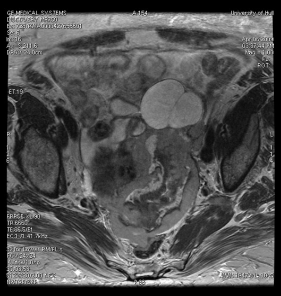

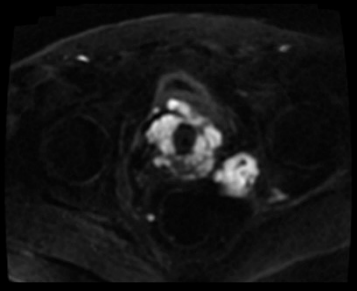

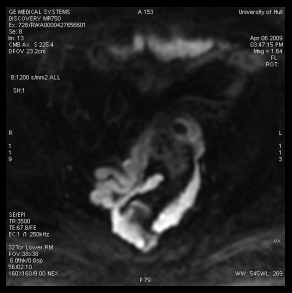

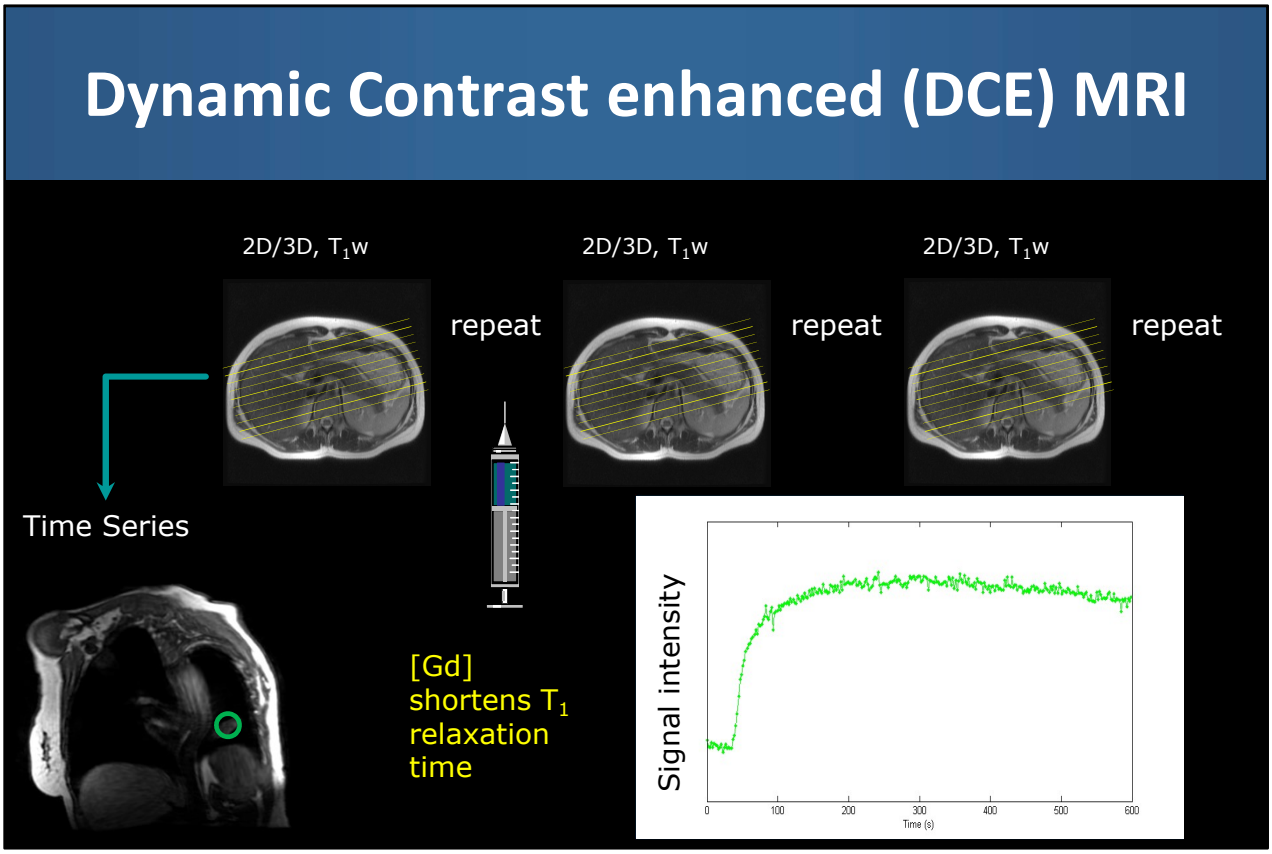

Tumours also often have immature, i.e. leaky, blood vessels. Dynamic contrast enhanced MRI is a method where by rapid, dynamic (repeated) T1w MRI acquisitions can be used with the bolus injection of a gadolinium-based contrast agent. The contrast agent leaks out of the blood vessels resulting in a transient increase in signal intensity within the tumour. The signal intensity change can be converted to a gadolinium concentration and the data fitted to a pharmacokinetic model that can provide quantitative images of the blood vessel permeability.

Quantitative DCE-MRI

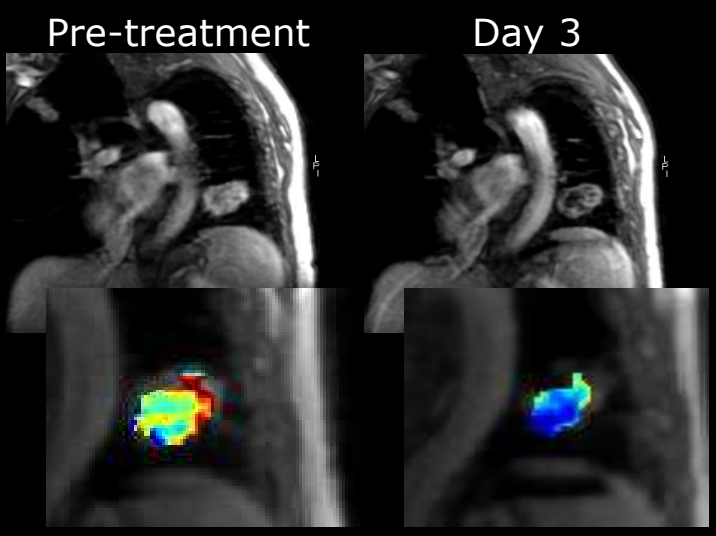

A tumour in the chest whose contrast agent uptake has been PK modelled. The images on the right shows the tumour three days after an anti-cancer drug (Avasatin) that disrupts the tumour blood supply. The quantitative reduction in the parameter K^{trans} shows that the vascular permeability has been affected. It might take months for the tumour size to reduce so DCE-MRI is a potential method to rapidly determine an early therapeutic response.

Functional MRI (fMRI)

- Increase in neuronal activity causes local vasodilatation
- This causes increased blood flow to region
- This results in an excess of oxyhaemoglobin beyond the metabolic need
- This reduces the fraction of paramagnetic deoxyhaemoglobin
- Manifest as an increase in spin coherence and therefore an increase in signal on T2*W imaging
- **B**lood **O**xygen **L**evel **D**ependent (BOLD) contrast

Blood Oxygenation

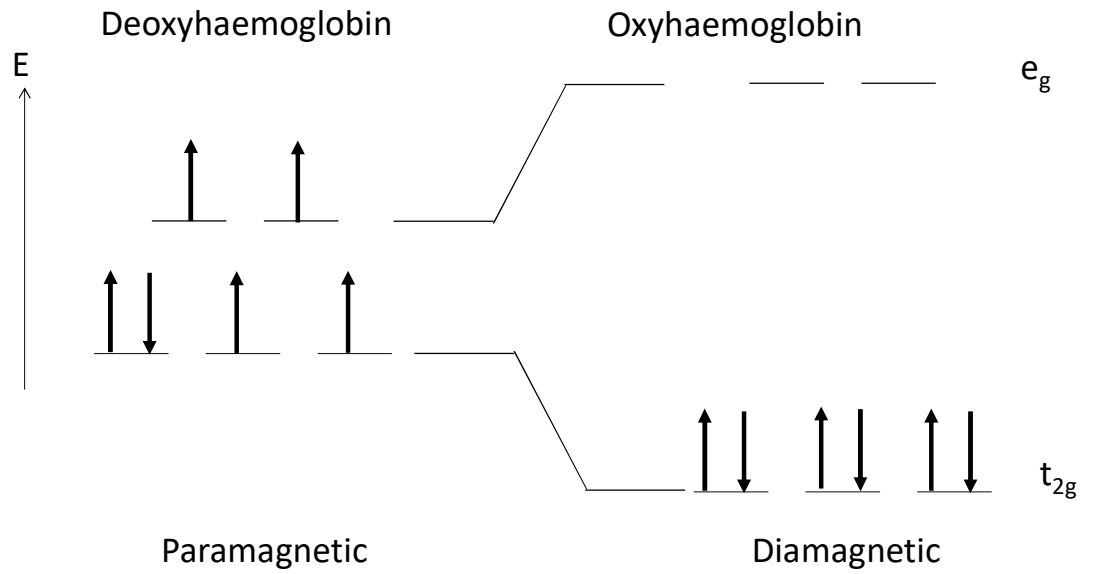

Deoxyhaemoglobin (Hb) is paramagnetic where as oxyhaemoglobin (HbO_2) is diamagnetic. Paramagnetism causes an shortening of the T_2^* relaxation time in comparison to diamagnetism. Activation of a brain area, e.g. the motor cortex results in a increase in HbO_2 above the metabolic need. There is therefore a surfeit of HbO_2 and hence an increase in signal intensity on T2*-weighted gradient echo.

Motor Strip Activation

- Bi-lateral finger tapping
- 10-second on-off (simple box-car) paradigm
- Axial slices high in cortex

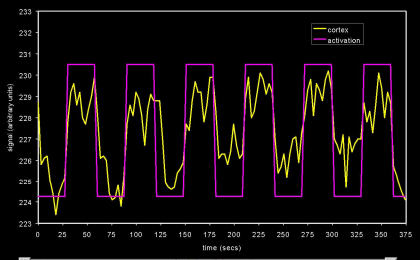

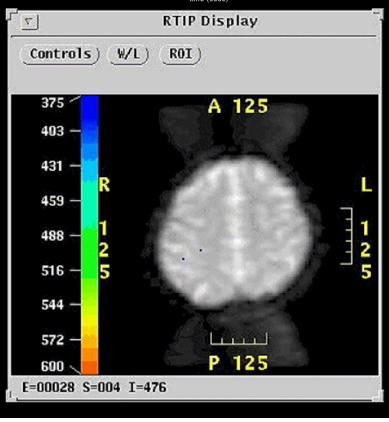

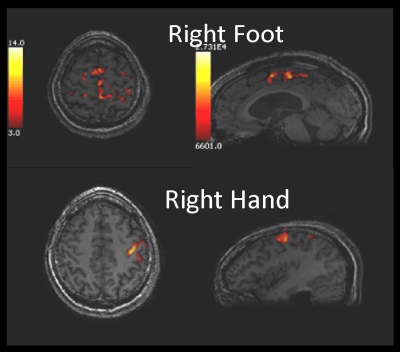

A simple box car paradigm of bilateral finger tapping causes transient changes in signal intensity on dynamic (repeated) T_2^* weighted gradient echo imaging. The level of statistical correlation of the temporal SI change with the activation paradigm is displayed as a colour overlay. In this particular application the position of the motor cortex can be localised. This could be used for example in the pre-surgical planning of tumours to see the tumours position with respect to the motor cortex

fMRI

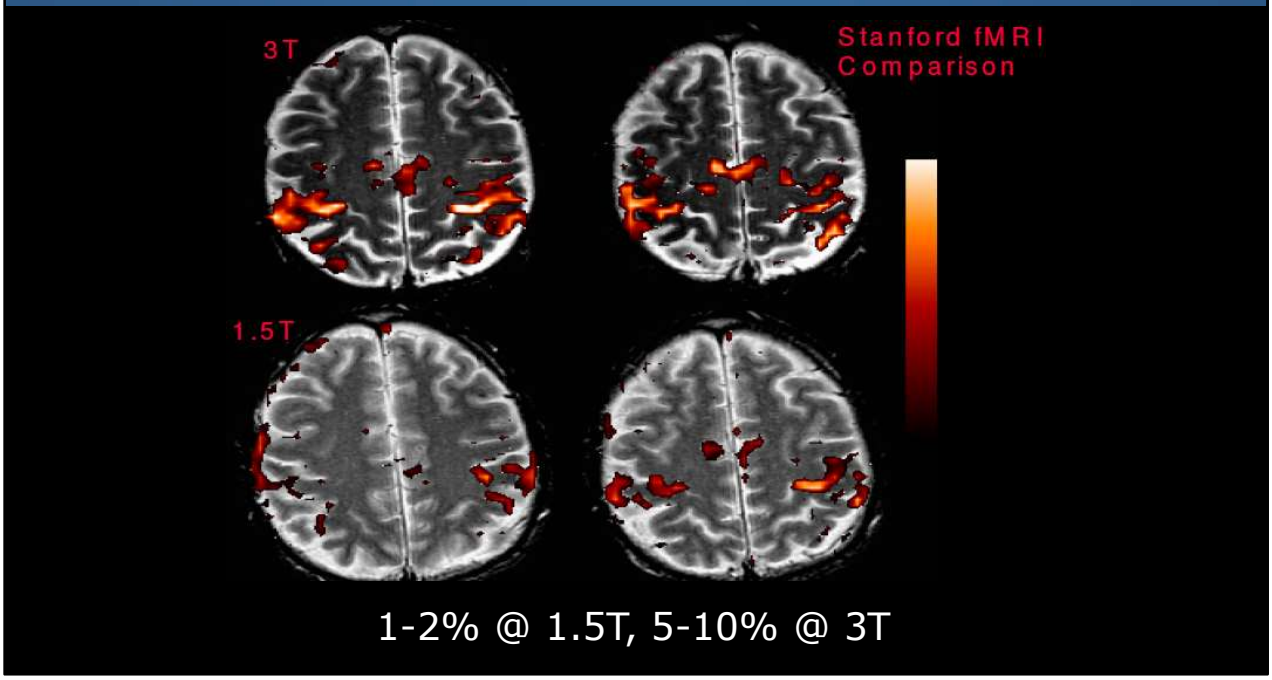

An advantage of 3T imaging is that the T2* effect is greater resulting in a greater sensitivity to the BOLD effect. This is part of the drive to even higher static magnetic field strengths, e.g. 7.0T and above

Learning Outcomes

- After these lectures you should be able to:
  - Explain how nuclear spin gives rise to magnetic resonance
  - Understand the principles of T_1, T_2 and T_2^* relaxation
  - Explain the principles of MR image formation
  - Describe the spin echo and gradient echo pulse sequences
  - Outline the basic components of an MRI system
  - Understand the safety issues related to MRI
  - Describe some advanced applications of MRI